Structural characterization of caseinolytic protease (ClpP) from *Klebsiella pneumonia.*

By

Sbahle Zuma (BSc Hons)

Submitted in fulfilment of the requirement for the degree of

Master of Science

in

Biochemistry

In the

College of Agriculture, Engineering and Sciences

at the

University of KwaZulu-Natal

Supervised by Dr. Thandeka Khoza

Preface

The experimental work described in this thesis was carried out in the School of Life Science, University of KwaZulu-Natal, Pietermaritzburg, from February 2022 to June 2023, under the supervision of Dr. Thandeka Khoza. The studies represent original work by the author and none of this work has been submitted for the award of any degree or examination at any university. All authors of data and any other information has been acknowledged accordingly by reference.

Student: Sbahle Naledi Zuma

Signature: [redacted]

Date: 13/06/2023

As the candidate's supervisor, I have approved this thesis for examination.

Supervisor: Dr. Thandeka Khoza

Signature: [redacted]

Declaration

I, **Sbahle Naledi Zuma**, declare that:

1. The research reported in this dissertation, except where otherwise indicated or acknowledged, is my original work.

2. This thesis has not been submitted in full or in part for any degree or examination to any other university.

3. This thesis does not contain other persons' data, pictures, graphs or other information, unless specifically acknowledged as being sourced from other persons.

4. This thesis does not contain other persons' writing, unless specifically acknowledged as being sourced from other researchers. Where other written sources have been quoted, then:

a. Their words have been re-written, but the general information attributed to them has been referenced.

b. Where their exact words have been used, their writing has been placed inside quotation marks, and referenced.

5. This dissertation does not contain text, graphics or tables copied and pasted from the Internet, unless specifically acknowledged, and the source being detailed in the dissertation and in the Reference sections.

Student Name: Sbahle Naledi Zuma

Signature: 

Date: 13 June 2023

Abstract

Klebsiella pneumonia (*K. pneumoniae*) is a non-motile bacterium that is characterized as an opportunistic pathogen known to cause hospital-acquired infections (HAI) in immunocompromised patients. It is part of a group of pathogens referred to as ESKAPE pathogens. Other pathogens that form a part of this group include; *Enterococcus faecium, Staphylococcus aureus, Klebsiella pneumoniae, Acinetobacter baumannii, Pseudomonas aeruginosa* and *Enterobacter*. These pathogens are known to "ESKAPE" the effect of antibiotics. Moreover, *Klebsiella pneumoniae* is amongst the top 8 most critical pathogens in hospitals therefore, this pathogen poses a great global concern and is life threatening in low- and middle-income countries. Caseinolytic proteases (ClpP) are thermostable proteins which play an important role in protein homeostasis by degrading aggregated and misfolded proteins and allows the pathogen to survive in different environmental conditions. To our knowledge, there are no studies which have focused on the diversity of *clpp* genes in the *Klebsiella* species as well the expression and purification *K. pneumoniae* (*Kp*) ClpP, to date. Therefore, this study aimed to address this knowledge gap. Bioinformatic analysis was used to investigate the diversity of ClpP in the *Klebsiella* species. ClpP was found to be present in all the investigated *Klebsiella* strains with each strain containing more than one ClpP and 17 different ClpP isoforms were identified across the species. Homology modelling of the hypothetical *Kp* ClpP structure and molecular dynamic simulations showed that this protein was mainly alpha helical, highly dynamic, stable and flexible. The gene encoding for *Kp* ClpP was cloned into a pColdI vector. This was followed by successful expression *Kp* ClpP with a band size of 25 kDa, this was slightly higher than the expected size of 21 kDa. Western blot and liquid chromatography mass spectrometry (LC-MS) analysis was used to confirm that the 25 kDa protein was indeed *Kp* ClpP. This protein was then purified to homogeneity using affinity chromatography.

Acknowledgements

I would like to thank the Almighty God for giving me this opportunity, for being with me throughout the difficult times, none would have been possible without you.

Secondly, I would like to give thanks to my supervisor Dr. Khoza for giving me the opportunity to do this project, her guidance, advice and support throughout the duration of my research work.

Appreciation to my lab colleagues for an enjoyable moment at the lab and for your comments as well as suggestions.

Special thanks to Tehrim and Nomfundo for support, assistance and great advice that allowed me to develop and tackle my research work.

I would like to express my sincere gratitude to Thandolwethu, Nomacusi, Sandile, TK, Sinethemba, Asanda and Nontokozo for the sleepless nights, working together, the great discussions and the fun times.

Last but not least I am deeply grateful for my family for the spiritual and emotional support, this project wouldn't have been possible without you.

Table of Contents

List of Figures

List of tables

List of abbreviations

Abbreviation	Full form
[θ]	Mean residue ellipticity
°C	Degrees Celsius
µg	Microgram
µl	Microliter
µM	Micromolar
3D	Three dimension
Å	Angstrom
ACCs	Acetyltransferases
AEC	Acyl-enzyme complex
AME	Aminoglycoside-modifying enzyme
AMR	Antimicrobial resistance
ANT	Aminoglycoside-2-O-nucleotidyltransferases
APH	Aminoglycoside O-phosphotransferase
ATP	Adenosine triphosphate
BTZ	Bortezomib
$CaCl_2$	Calcium chloride
CD	Circular dichroism
Clp	Caseinolytic
ClpP	Caseinolytic protease P
CPS	Capsular polysaccharide
cspA	Cold shock protein A
Cα	Carbon alpha
Da	Daltons
DNA	Deoxyribonucleic acid
DTT	Dithiothreitol
E. coli	*Escherichia coli*
ESBL	Extended spectrum beta-lactamases
ESKAPE	*Enterococcus faecium, Staphylococcus aureus,*
EXPASY	Expert Protein Analysis
FQs	Fluoroquinolones
HAI	Hospital acquired infections
HPLC	High performance liquid chromatography
Hsp	Heat shock protein
IAA	Iodoacetamide

IM	Inner membrane
IPTG	Isopropyl β-D-1-thiogalactopyranoside
iTOL	Tree of life
K. pneumoniae	*Klebsiella pneumoniae*
KCl	Potassium chloride
kDa	Kilo daltons
	Klebsiella p*neumoniae, Acinetobacter baumannii*,
Kp ClpP	*Klebsiella pneumonia* Clp
KPC	*Klebsiella pneumoniae* Carbapenemases
LC-MS	Liquid chromatography-mass spectrometry
Lcn2	Lipocalin 2
LPS	Lipopolysaccharide
M	Molar
M. tuberculosis	*Mycobacterium tuberculosis*
mA	Milliamps
MD	Molecular dynamics
MD-2	Myeloid differentiation factor 2
MDR	Multidrug resistance
MFP	Membrane fusion protein
$MgCl_2$	Magnesium chloride
Min	Minutes
mL	Milliliter
mM	Millimolar
mRNA	Messenger RNA
NaCl	Sodium chloride
NCBI	National Center for Biotechnology Information
Ni^+	Nickel ion
Nm	Nanometer
Ns	Nano seconds
OD	Optical density
OM	Outer membrane
PBP	Penicillin-binding proteins
PBS	Phosphate buffered saline
PCR	Polymerase Chain Reaction
PDB	Protein data bank
	Pseudomonas aeruginosa and Enterobacter
QMEAN	Qualitative Model Energy Analysis

Rg	Radius of gyration
RMSD	Root-mean square deviation
RMSF	Root-mean square fluctuation
RNA	Ribonucleic acid
RND	Resistance-nodulation-division
rpm	Revolution per minutes
S. aureus	*Staphylococcus aureus*
SDS-PAGE	Sodium dodecyl sulfate-polyacrylamide gel electrophoresis
sec	Seconds
TBS	Tris buffered saline
TEE	Translation enhancing element
TLR	Toll-like receptor
UTI/s	Urinary tract infection/s
V	Voltage
WHO	World Health Organisation
α	Alpha
β	Beta
γ	Gamma

Chapter 1: Introduction

1.1. Disease global burden and habitat

Antimicrobial resistance (AMR) is one of the top 10 global public health threats to human health and reports suggest that AMR may kill 10 million people a year by 2050 *(de Kraker et al*., 2016). Resistance towards antimicrobials occurs when antibiotics used to treat pathogens are no longer effective, meaning the pathogen has developed a mechanism which renders the drug ineffective (Chinemerem Nwobodo *et al*., 2022). Another complication to AMR, are persistent species which remain dormant during antibiotic treatment (Huemer *et al*., 2020, Vogwill *et al*., 2016). Upon completion of the antibiotic treatment regime, the pathogen resuscitates (Schrader *et al*., 2020). Subsequently, the World Health Organization (WHO) amongst other organizations advocates for research activities to be intensifying and coordinating to arrest the spread of AMR (Prestinaci *et al*., 2015).

In 2017, WHO published a priority pathogen list of bacterial species resistant to various classes of antibiotics This list consists of both Gram-negative and Gram-positive bacteria and further classifies the pathogens into three groups, depending on antimicrobial resistance (Table 1) (Tsakou *et al*., 2020). Also, in this list are selected members of the Enterobacteriaceae family such as *Klebsiella pneumoniae (K. pneumoniae)*, *Escherichia coli* (*E. coli*), *Serratia marcesens*, and *Proteus mirabilis* amongst other species and ESKAPE pathogens (Santajit and Indrawattana, 2016). ESKAPE pathogens are named such due to their ability to "ESKAPE" the action of well-known antibiotics (Mulani *et al*., 2019, Santajit and Indrawattana, 2016). This group of pathogens includes *Enterococcus faecium*, *Staphylococcus aureus (S. aureus), K. pneumoniae, Acinetobacter baumannii, Pseudomonas aeruginosa*, and the *Enterobacter* spp. (Mulani *et al*., 2019). Of interest in this study is *K. pneumoniae* which belongs to the *Klebsiella* genus and are part of the *Enterobacteriaceae* family.

Table 1: Antibiotic resistance of bacterial species identified as being part of the pathogen priority list by the WHO.

Bacterial species	Antibiotic resistance	Severity	Gram - / +
Acinetobacter baumannii	carbapenem-resistant	Critical	-
Pseudomonas aeruginosa	carbapenem-resistant	Critical	-
Enterobacteriaceae	Carbapenem-resistant, extended-spectrum β lactamase. (ESBL)-producing	Critical	-
Enterococcus faecium	vancomycin-resistant	High	+
Staphylococcus aureus	methicillin-resistant, vancomycin-intermediate and resistant	High	+
Helicobacter pylori	clarithromycin-resistant	High	-
Campylobacter spp	fluoroquinolone-resistant	High	-
Salmonellae	fluoroquinolone-resistant	High	-
Neisseria gonorrhoeae	cephalosporin-resistant, fluoroquinolone-resistant	High	-
Streptococcus pneumoniae	penicillin-non-susceptible	Medium	+
Haemophilus influenzae	ampicillin-resistant	Medium	-
Shigella spp.	fluoroquinolone-resistant	Medium	-

K. pneumoniae is highly ubiquitous in nature and is primarily found in the environment (e.g. plants, soil, and water surfaces) as well as on the mucosal surfaces of humans and animals (Martin and Bachman, 2018). They are characterized as Gram-negative, encapsulated, nonmotile bacterium and were initially known as Friedlander's bacterium when it was first identified in the 19th century (Paczosa and Mecsas, 2016). These species are amongst the leading causes of hospital-acquired infections (HAI) in immunocompromised patients with underlying conditions such as diabetes mellitus, and chronic pulmonary infections (Martin and Bachman, 2018). Moreover, urinary tract infection (UTIs), bloodstream infections, pneumonia and neonatal septicemia are additional infections detected in these Gram-negative species (Gonzalez-Ferrer *et al*., 2021, Ma *et al*., 2021, Paterson, 2006). Hospital-acquired infections are described as infections that were initially not present prior to the patient being admitted to the hospital thus, they pose a great global concern and are life threatening in low- and middle-income countries where healthcare resources are limiting (Maki and Zervos, 2021).

In the United States and Europe, the *Klebsiella* spp. are responsible for up to 8% of HAI and noted as among the top 8 most critical pathogens in hospitals (Podschun and Ullmann, 1998). The HAI trend is also alarming for low-income countries, for example in Bangladesh, it is reported that one in 20 patients admitted to the hospital for more than 3 days developed a hospital acquired respiratory infection with an incidence rate of 6.1 cases per 1000 patient days (Gurley *et al*., 2010). One of the contributing factors to increased nosocomial infections is the incorrect use of antibiotics leading to the emergence of pathogens that are resistant to a wide spectrum of antibiotics (Sequeira *et al*., 2020, Podschun and Ullmann, 1998). The

Centre for Disease Control and Prevention reported that 2.8 million people are infected by multidrug-resistant strains annually result in at least 35 000 deaths. Furthermore, it is predicted that deaths due to AMR will increase by up to 10 million per year by 2050 (Cassini *et al*., 2019). This concerning health risk associated with antimicrobial resistance and pathogens responsible for HAI has increased research efforts from the scientific community to develop new antimicrobial therapies, uncovering the mechanisms of antimicrobial resistances and identifying new drug targets in these pathogens.

K. pneumoniae are opportunistic pathogens that colonize the human microbiota and are found within the environment especially in healthcare settings (Argimón *et al*., 2021, Martin and Bachman, 2018, Podschun *et al*., 2001). Transmission of *K. pneumoniae* is through person-to-person contact and contaminated hospital medical devices such as endoscopes (Ito *et al*., 2015, Pomakova *et al*., 2012). Additionally, *K. pneumoniae* forms biofilms on medical devices, and this biofilm formation produces an extracellular matrix which protects the bacterium and renders chemical disinfectants ineffective (Ochońska *et al*., 2021). Consequently, *K. pneumoniae* is characterized as being the most critical and the second most frequent pathogen that causes infections in humans (Stewart *et al*., 2022, Effah *et al*., 2020). Also, up to 80% of nosocomial infections have been linked to pathogens that form biofilms on medical devices used in hospitals (Murphy *et al*., 2013).

1.2. Pathogenesis of *K. pneumoniae*

K. pneumoniae is a pathogenic bacterium which burdens the health care sector globally therefore, knowledge of virulence factors is key in fighting the emergence and spread of multidrug-resistant (MDR) bacterium. The virulence factors of *K. pneumoniae* contribute to its pathogenicity and allows the pathogen to circumvent host immune response to promote survival and growth within the host cell (Barawi *et al*., 2021, Podschun and Ullmann, 1998). Virulence factors include the capsule, lipopolysaccharide (LPS), siderophores, fimbriae and serum resistance (Barawi *et al*., 2021, Podschun and Ullmann, 1998).

1.2.1 Fimbriae

Host cell adherence is the first step to pathogenic invasion and it occurs through bacterial extracellular structures which bind to host cell receptors (Dowling *et al*., 2020). The attachment of *K. pneumoniae* to host cell receptors are mediated by prolonged organelles called fimbriae. There are two types of fimbriae namely Type 1 and Type 3 fimbriae (Wu and Fives-Taylor, 2001). Type 1 fimbriae are composed of thin, adhesive, thread-like appendages within the outer membrane along with repeating units of FimA subunits which promote the adhesion to mannose containing structures and are primarily present on species which have a potential to cause UTIs (Li *et al*., 2014, Vuotto *et al*., 2014, Schroll *et al*., 2010). Type 3 fimbriae are

composed of long appendages which act as attachment agents to stimulate biofilm formation on both biotic and abiotic surfaces (Li *et al*., 2014, Vuotto *et al*., 2014, Schroll *et al*., 2010). Thus, type 3 fimbriae are linked to biofilm formation and contribute to the spread and persistence of hospital-acquired infections (Li *et al*., 2014, Schroll *et al*., 2010).

1.2.2. Capsule

Pathogenic bacteria consist of a range of surface organelles that grant them the ability to outlast different host cell habitats during the course of infection (Pizarro-Cerdá and Cossart, 2006). These surface organelles, cover and subsequently camouflage the antigenic molecules to enhance bacterial survival (Wen and Zhang, 2015). Surface organelles include pili and capsule which are antigenic, thus triggering host immune response following pathogen attachment and invasion to the host cell (Finlay and McFadden, 2006, Guerina *et al*., 1983). The capsule is an outer membrane which is composed of tightly packed repeating units of polysaccharides with serotype-specific capsular polysaccharide (CPS) and is expressed by *K. pneumoniae*. The capsule shields the pathogen from immune recognition (Rendueles, 2020, Wen and Zhang, 2015). Primarily, the thickness of the capsule protects *K. pneumoniae* from phagocytosis (Rendueles, 2020, Doorduijn *et al*., 2016). The thick cellular capsule also known as K-antigen provides *K. pneumoniae* defence against macrophages through the lack of mannose repeating units (Lee *et al*., 2017). Moreover, the *K. pneumoniae* capsule preserves the bacterial cell from the host cell immune system by altering stimulation of cytokines (Panjaitan *et al*., 2021). Apart from this, the capsule has been reported to defend *K. pneumoniae* from antimicrobial peptides by attaching to these peptides and blocking interaction to the bacterial surface (Campos *et al*., 2004). This increases bacterial tolerance to drug administration and results in minimal response to the immune system (Rendueles, 2020).

1.2.3. Lipopolysaccharide

In addition to CPS, *K. pneumoniae* produces LPS which is present on the outermost membrane and primarily functions as a transporter of antibiotics, antimicrobial peptides and as a defender of any peptides exported into the cell (Chai *et al*., 2014). The LPS is made up of lipid A, oligosaccharide core, and O antigen as shown in Figure 1 (Zhu *et al*., 2021). Lipid A is made up of six acryl groups which stimulate the Toll-like receptor 4 (TLR4)/MD-2 complex and is responsible for initiating the activation of host innate immunity as well as inflammatory cascades (Bulati *et al*., 2021). Thus, *K. pneumoniae* modifies the Lipid A structure, this results in poor stimulation of TLR4/MD-2 and leads to bacterial evasion (Matsuura, 2013). The core oligosaccharide mainly connects Lipid A and the O antigen which is part of the outermost compartment of the LPS (Opoku-Temeng *et al.*, 2019). The O antigen contains a polymer of oligosaccharide repeating units and is linked to complement killing resistance, increased bacterial survival within the host cell as well as lethality (Hsieh *et al*., 2012, Clements *et al*.,

2007). Specifically, the O antigen binds to complement C3b which activates the complement-mediated killing mechanism and thus stimulates bacterial survival (Bulati *et al*., 2021).

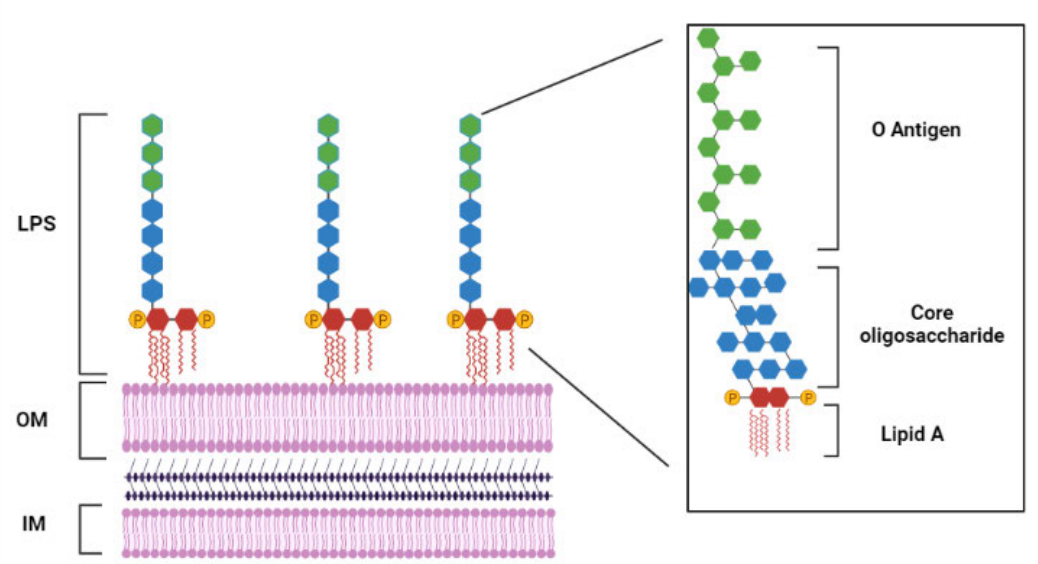

Figure 1: A schematic representation of the components of bacterial cell wall. LPS is made of O antigen which is linked to core oligosaccharide and lipid A which act as defensive barrier. Image generated using BoRender.

1.2.4. Siderophores

K. pneumoniae produces siderophores which scavenge iron from the host environment. Irons are essential in many cellular processes such as deoxyribonucleic acid (DNA) replication and oxygen metabolism (Holden *et al*., 2016, Holden and Bachman, 2015, Neilands, 1995). The siderophores produced by *K. pneumoniae* include aerobactin, enterobactin, salmochelin, and yersiniabactin which are located outside the extracellular space where they bind iron and transport them back into the bacterial cell. The pathogen then uses iron to influence host immunity by modifying iron homeostasis (Namikawa *et al*., 2022, Choby *et al*., 2020, Chakradhar, 2017). In response to bacterial invasion, the host cell produces lipocalin 2 (Lcn2) which interacts with pathogen siderophores to prevent the consumption of iron by pathogens and induces an inflammatory response. However, *K. pneumoniae* produces glycosylated enterobactin (Gly-Ent, salmochelin) or yersiniabactin to escape Lcn2 and thus maintains iron-scavenging activity (Behnsen and Raffatellu, 2016, Wilson *et al*., 2016, Bachman *et al*., 2012).

1.3. Mechanism of resistance

Resistance of *K. pneumoniae* to a number of antibiotics is enhanced by the ability of the pathogen to naturally develop mutations to antibiotics or through a transfer of resistance genes from one species to another (Navon-Venezia *et al*., 2017). Also, the pathogen may use biochemical mechanisms such as inactivation of antibiotics, drug site modification and the efflux system to evade the effects of antibiotics (Figure 2). These multifaced strategies for

antibiotic resistances has allowed *K. pneumoniae* to survive five major classes of antibiotics which inhibit functions such as cell wall synthesis, protein synthesis, and DNA synthesis (Table 2). Over the past few years (2002-2010), antibiotic resistance of *K. pneumoniae* against carbapenems has increased from 0.1% to 4.5% while resistance to third generation cephalosporins has increased from 5.3% to 11% (Kuehn, 2013). And this upward trend is of great concern in medicine especially in low-income countries where resources and access to health care may be limited.

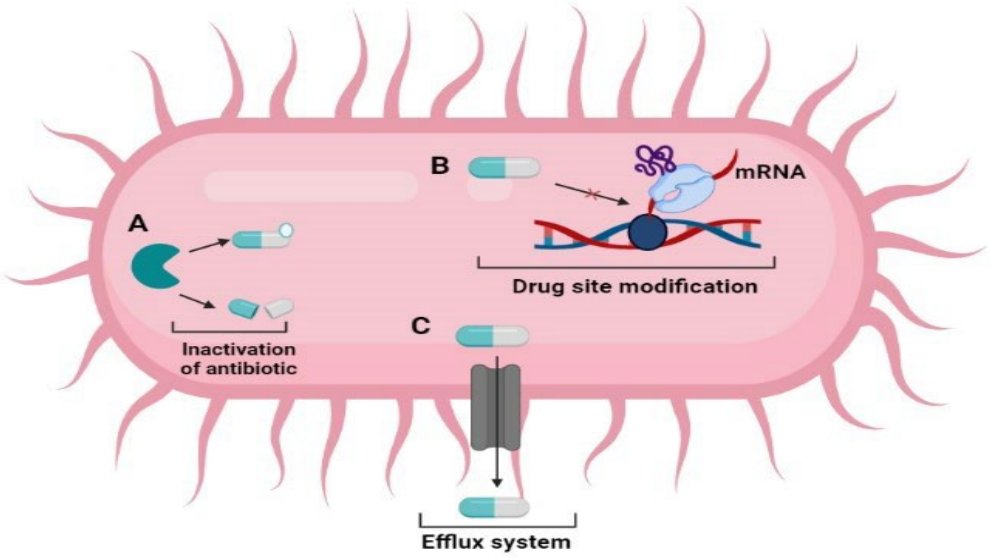

Figure 2: Multiple antibiotic resistance mechanisms. (A) Inactivation of antibiotics by alteration of antibiotic structure or degradation of functional group following antibiotic impaired functioning (Laws *et al*., 2019). (B) Drug site modification involves target modification through Ribonucleic acid (RNA) methylation resulting in reduced antibiotic binding (Kapoor *et a*l., 2017). (C) Efflux system activation responsible for export of antibiotics reducing their concentration within bacterial cell (Darby *et al*., 2022). Image was generated using BioRender.

Table 2: Biochemical mechanism of action of different classes of antibiotics to which *K. pneumoniae* is resistant.

Class of antibiotic	Examples	Mechanism of action	References
ß-LACTAMS	Carbepenem and Cephazolin	Inhibit synthesis of the bacterial cell wall.	(Effah *et al*., 2020)
Aminoglycosides	Amikacin	Inhibit the synthesis of bacterial proteins	(Effah *et a*l., 2020)
Sulfonamides	Co-trimoxazole	Prevent bacterial growth and multiplication.	(Sikarwar and Batra, 2023)
Tetracyclines	Limecycline	Inhibit bacterial protein synthesis	(Sikarwar and Batra, 2023)
Quinolones	Ciprofloxacin	Interfere with bacteria DNA replication and transcription.	(Effah *et al*., 2020)

Primarily *K. pneumoniae* is the first species from the *Klebsiella* genus that is mostly isolated in human clinical samples. Genomic studies have shown that antibiotic resistant of *K. pneumoniae* contains a wide range of chromosomally or plasmid-encoded genes encoding for β-lactam resistance genes (Oliveira *et al*., 2022). This finding is a concern given that β-lactam antibiotics, including penicillin derivatives, cephalosporins and carbapenems are commonly used for treatment bacterial infections (Oliveira *et al*., 2022, Pitout *et al*., 2015). The β-lactam antibiotics are a structurally diverse group of compounds that are characterised by a reactive four-membered β-lactam ring (azetidinone) which interferes with the synthesis of peptidoglycan, a core component of the bacterial cell wall thus inhibiting bacterial cell wall synthesis (Turner *et al*., 2022, Eiamphungporn *et al*., 2018). These β-lactam antibiotics and their derivatives, blocks the transpeptidation activity mediated by penicillin-binding proteins (PBP) during peptidoglycan synthesis thus weakening the bacterial cell wall causing the bacterial cell to be vulnerable to osmotic stress subsequently autolysis (Sethuvel *et al*., 2023, Nauta *et al*., 2021). To block the transpeptidation, the catalytic serine residue in the active site of PBP is acylated with reactive β-lactam core resulting in stable acyl–enzyme complex (AEC), preventing the PBP from catalysing transpeptidation (Mora-Ochomogo and Lohans, 2021).

To render β-lactam antibiotics ineffective, *K. pneumonia* produces an enzyme (β-lactamase) which inactivates β-lactam antibiotics and their derivatives (penicillins, cephalosporins, cephamycins, and carbapenems) (Aurilio *et al*., 2022, Pitout *et al*., 2015). One of the early discovered β-lactamase was penicillinase in the 1940s and now there are over 200 known β-lactamase including ESBLs (De Jesus *et al*., 2015). Lactamases are enzymes that inactivates β-lactam antibiotics via antibiotic chemical modification. This enzyme binds to β-lactam antibiotics forming a stable acyl-enzyme complex and the catalytic active serine residue in the active site of β-lactamase catalyse hydrolysis of β-lactam rings and therefore degrades the chemical structure responsible for antimicrobial activity (Khanna and Gerriets, 2021).

Lactamases are classified into four classes (A, B, C and D) based on their amino acid sequences (Table 3) (Tooke *et al*., 2019). The active site of each class is driven by an amino acid which bind to antibiotic supressing antibacterial effect thus class A, C and D contain serine active site while class B contain metal ion (zinc) (Hirvonen *et al*., 2019). ESBLs catalyse the hydrolysis of the β -lactam ring however they are active against broader range of antibiotics including a new class β-lactam antibiotics known as monobactam which consists of monocyclic β-lactam structure (Saxon *et al*., 1984). These ESBLs are a constantly evolving group of β-lactamases and more than 350 different natural ESBL variants have been classified into nine distinct structural and evolutionary families based upon their amino acid sequence comparisons (Gniadkowski, 2001). With such genetic diversity in ESBL, it is not surprising that ESBL producing *K. pneumoniae* are reported to be the most frequent pathogen leading to the

outbreak of nosocomial infections (Bouassida *et al*., 2016, Silva *et al*., 2006). Another factor that contributes to the global increase of antibiotic resistant strains of *K pneumoniae* is that these ESBL genes produced by this pathogen can be passed through transduction or transformation to other pathogens (Jiang *et al*., 2020).

Table 3: Different class of lactamases.

Class	Enzyme	Active site	References
A	Extended-spectrum β-lactamases *Klebsiella pneumoniae* carbapenemases	Serine β-lactams	(Bush and Bradford, 2019)
B	Metallo-β-lactamases	Metallo- β-lactams	(Oelschlaeger, 2021)
C	Celphalosporines	Serine β-lactams	(Munita and Arias, 2016)
D	Oxacillinases	Serine β-lactams	(Yoon and Jeong, 2021, Antunes and Fisher, 2014)

Clinical isolates of *K. pneumoniae* have been found to have genes encoding for aminoglycoside-modifying enzymes (AMEs). Aminoglycosides are antibiotics with a broad-spectrum activity against various Gram-positive and Gram-negative organisms. Furthermore, this class of antibiotics is potent for the *Enterobacteriaceae* family (Krause *et al*., 2016). Examples of the frequently used aminoglycosides include kanamycin, gentamicin and streptomycin and they exhibit their antimicrobial activity by inhibiting protein synthesis (Block and Blanchard, 2022, Serio *et al*., 2018). Genes encoding for AMEs are located on plasmids containing multiple resistance elements and are believed to be transferred via horizontal gene transfer (Pradier and Bedhomme, 2023). AMEs inactivate aminoglycosides via drug site modification (Nasiri *et al*., 2018, Labby and Garneau-Tsodikova, 2013). To date, there are over 100 AMEs known and are grouped into three groups namely acetyltransferases (AACs), aminoglycoside-2-O-nucleotidyltransferases (ANTs), and phosphotransferases (APHs) based on their mode of action (Figure 3). Moreover, alteration of antibiotic by the addition of an acetyl, adenyl or phosphoryl group to the aminoglycoside core scaffold catalysed decreases the binding affinity of the antibiotic to its ribosomal target resulting in the misreading of the genetic code and inhibition of translocation during protein synthesis (Krause *et al*., 2016). These events lead to the loss of antimicrobial activity of aminoglycosides (Zhang *et al*., 2021, Krause *et al*., 2016). Despite the production of AMEs, *K. pneumoniae* also uses aminoglycosides to modulate its outer cell membrane to reduce its susceptibility to antibiotics.

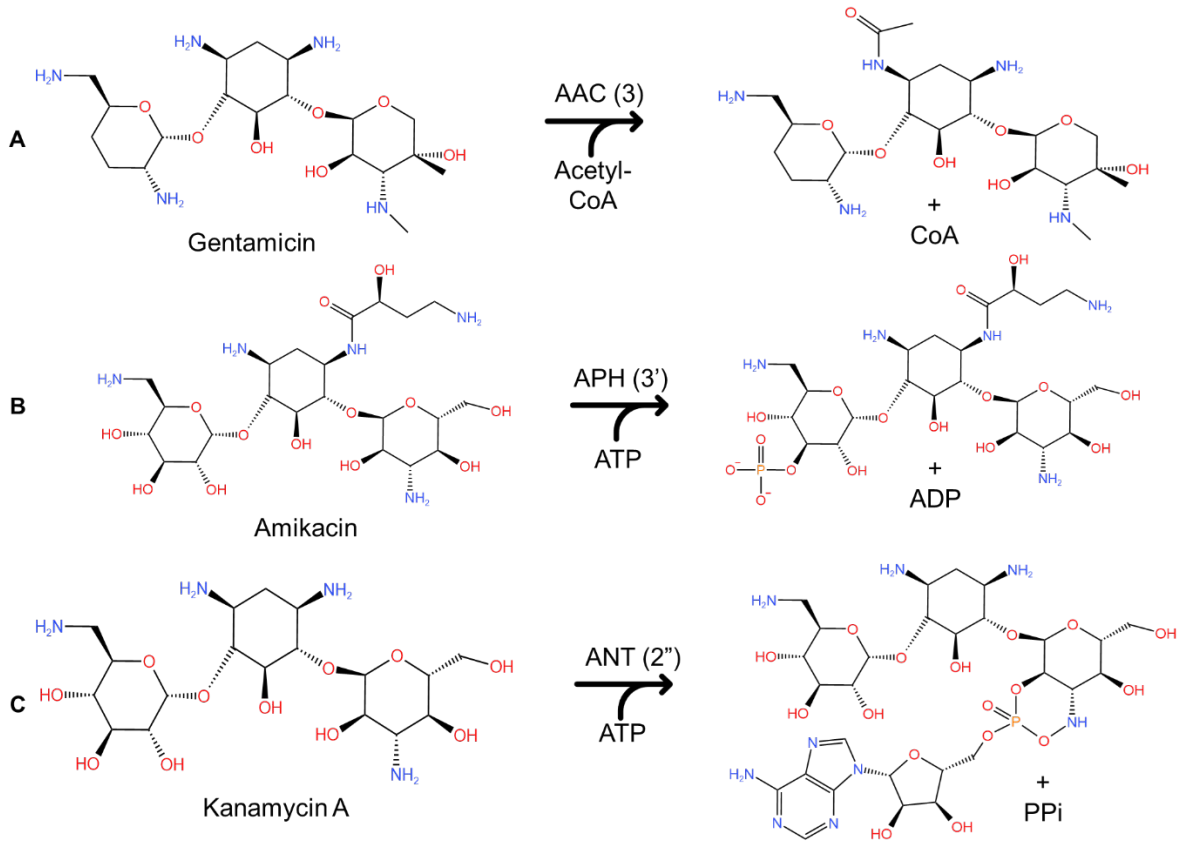

Figure 3: Structural modification of aminoglycosides by aminoglycoside-modifying enzymes. (A) Process of transfer of acetyl from acetyl coenzyme A by aminoglycoside acetyltransferase AAC (3) using Gentamicin as an example, (B) transfer of γ-phosphate from Adenosine triphosphate (ATP) by aminoglycoside phosphotransferase APH (3') using Amikacin as an example, (C) transfer of adenosine monophosphate from an ATP donor by aminoglycoside nucleotidyltransferase ANT (2") using Kanamycin A as an example. Image was adapted from Krause *et al*. (2016) and generated using KingDraw.

Another mechanism which *K. pneumoniae* uses to escape the effect of antibiotics is alterations or mutations on target enzymes and changes in drug entry and efflux (Pulzova *et al*., 2017). Clinical isolates of *K. pneumoniae* with resistance to fluoroquinolones (FQs) have been identified with mutation in key enzymes targeted by these antibiotics (Moya and Maicas, 2020). FQs are derivatives of quinolones (Figure 4), a synthetic antimicrobial compound with a broad spectrum of antimicrobial activity (Bush *et al*., 2020). Quinolones are used in medicine to treat a variety of infection caused by Gram-negative and Gram-positive. FQs kills bacteria by targeting bacterial DNA topoisomerases (Cheng *et al*., 2018). DNA topoisomerases are grouped into two classes namely type I (topoisomerases I, III and V) and type II (topoisomerases II, IV and VI) (Capranico *et al*., 2017). These enzymes play an essential role in bacterial DNA replication and transcription where type I and type II DNA topoisomerases catalyse transient single-or double-strand breaks respectively (Forterre and Gadelle, 2009). Additionally, FQs target DNA gyrases which are topoisomerase II and topoisomerase IV. DNA gyrase is unique in bacteria and archaea and is responsible for initiating DNA replication by introducing negative super helical twists in the bacterial DNA double-helix ahead of the

replication fork to separate daughter chromosomes to allow for binding of initiation proteins (Helgesen *et al*., 2021, Stracy *et al*., 2019, Reece and Maxwell, 1991). On the other hand, topoisomerase IV is responsible for the decatenation of interlinked chromosomes at the end each round of replication (Helgesen *et al*., 2021). Therefore, FQs exhibit their antimicrobial effect by binding to the enzyme-bound DNA complex (which could be DNA gyrase -bacterial DNA or topoisomerase IV-bacterial DNA) and induce conformational changes to inhibit the activity DNA gyrase or topoisomerase IV enzyme thus blocking DNA synthesis and causing cell death (Zhao *et al*., 1997). Sequence analysis of FQs resistant strains shows that *GyrA* subunit of DNA Gyrase enzyme which is known to bind to DNA for DNA gyrase activity consist of mutations in its DNA binding region (Redgrave *et al*., 2014, Jacoby, 2005). DNA GyrA topoisomerase IV and DNA gyrase mutations are present in various pathogens including *K pneumoniae* thus threatening the efficacy and effectiveness of FQs in clinical settings (Kareem *et al*., 2021). These mutations result in decreased affinity of FQs for the DNA gyrase- bacterial DNA complex as well as topoisomerase IV (Yakout and Ali, 2022).

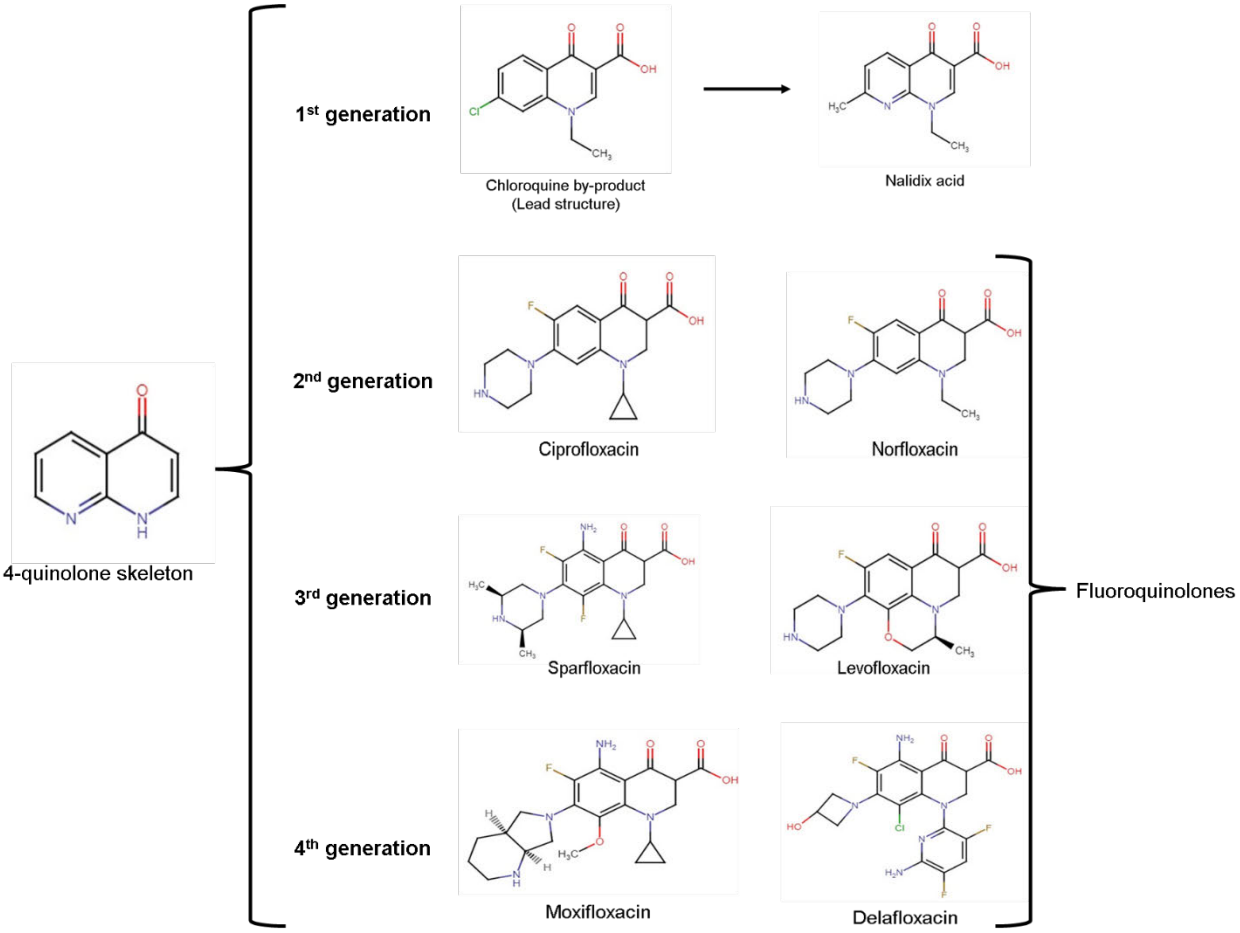

Figure 4: Different fluoroquinolones discovered. Chloroquine was the first quinolone to be discovered followed by nalidixic acid a by-product of chloroquine along with recently discovered fluoroquinolones. Image was adapted from Bush *et al*. (2020) and generated using King Draw.

Activation of the efflux system is also used by *K. pneumoniae* in FQ resistance (Dehnamaki *et al*., 2020, Maurya *et al*., 2019, Srinivasan *et al*., 2014). For FQs to be effective, they must cross the cell wall and cytoplasmic membrane in all bacteria, as well as the outer membrane of Gram-negative organisms (Cramariuc *et al*., 2012). Resistant strains express efflux systems such as AcrAB and OqxAB (Dehnamaki *et al*., 2020, Maurya *et al*., 2019, Srinivasan *et al*., 2014, Kim *et al*., 2009). The AcrAB and OqxAB efflux pumps are part of the resistance-nodulation-division (RND) family composed of a tripartite complex which spans the inner membrane (IM), periplasm and outer membrane (OM) (Huang *et al*., 2022). These membranes are responsible for the collection of compounds such as quinolones, chloramphenicol, tetracycline, trimethoprim, and β-lactams. These compounds are then transported to the periplasmic membrane fusion protein (MFP), to the OM pump and outside the cell (Klenotic *et al*., 2020, Petersson, 2017, Pakzad *et al*., 2013).

1.4. Proteases as an alternative antimicrobial drug target

Traditionally, antibiotics targets cell wall, protein and DNA/RNA synthesis and the alarming increase of multidrug-resistant bacterial strains suggests that new antimicrobial targets need to explored to combat the global crises of antibiotic resistance (Belete, 2019, Culp and Wright, 2017). One possible target are bacterial proteases which are protein degrading enzymes with diverse structure and function (Chanumolu *et al*., 2012). These proteins play a key role in the cell viability, stress response and pathogenicity (Table 4). Proteases can categorically be grouped as extracellular or intracellular proteases (Wandersman, 1989). The extracellular proteases are expressed as monomeric zymogens to prevent unregulated proteolytic activity (Müller *et al*., 2013, Neurath, 1986). The zymogens are activated via hydrolysis reaction or conformational changes that exposes their active site (Khan and James, 1998). These extracellular proteases are reported to have high substrate specificity for a specific protein or particular protein family (Zhou *et al*., 2020). Furthermore, extracellular proteases are key in pathogenicity virulence for example via degradation of host defence proteins (Lantz, 1997). The intracellular proteases on the other hand, form multi-trimeric structures with very little substrate specificity, subsequently their activity is tightly regulated (Choi *et al*., 2012).

Table 4: Diverse ClpP function in different species.

Type of organism	Function	Reference
E. coli	Metabolism, cell division, damage repair and protein regulation	(Sassetti *et al*., 2019)
Streptococcus pneumoniae	Oxidative stress	(Park *et al*., 2010)
S. aureus	Virulence	(Böttcher and Sieber, 2008)
Pseudomonas aeruginosa	Biofilm formation and mortality	(Fernández *et al*., 2012)
Bacillus subtilis	Protein homeostasis	(Illigmann *et al*., 2021)
Salmonella	Transcription factor regulation	(Bhandari *et al*., 2018)
Listeria monocytogenes	Regulate phagosome evasion	(Frees *et al*., 2003)
Salmonella typhimurium	Regulate iron systems	(Farrand *et al*., 2013)
Plasmodium falciparum	Control apicoplast development	(Rathore *et al*., 2010)

Caseinolytic protease P (ClpP) is one of intracellular proteases that expressed are in prokaryotic systems and are essential for the maintenance protein homeostasis (MorenoCinos *et al*., 2019). When bacteria are exposed to stressful conditions such as oxidative stress, osmotic shock, heavy metal toxicity, changes in hydrostatic pressure, heat or cold shock and the presence of drugs or antibiotics this results in a negative shift in protein homeostasis (Khodaparast *et al*., 2021a). And such a shift is detrimental to cell viability given that all biological activities in a cell are mediated by proteins. It therefore seems reasonable for ClpP to be targeted for antimicrobial drug development. Also, studies have reported models of ClpP

gene knock out pathogens are unable to cause infection and these was attributed to decreased activity of proteases (Aljghami *et al*., 2022, Malik and Brötz-Oesterhelt, 2017).

1.5. Caseinolytic protease P (ClpP)

ClpP was first discovered in *E. coli* as an additional proteolytic enzyme to protease La, a defensive machinery towards abnormal conditions (Hwang *et al*., 1987, Katayama-Fujimura *et al*., 1987). Proteolytic enzymes have four main groups categorized based on their catalytic sites residues (Rawlings *et al*., 2011). The four groups are serine, cysteine, aspartic, metallo proteases (Figure 5). Additional two groups namely threonine and glutamate have been discovered which consists of threonine and glutamate on catalytic active site respectively (Ward *et al*., 2009, Powers *et al*., 2002). ClpP is a serine protease which is expressed in the cell mitochondria of both prokaryotes such as *E. coli*, *Neisseria Meningitidis*, *S. aureus*, *Mycobacterium tuberculosis* (*M. tuberculosis*) as well as eukaryotes (Kahne and Darwin, 2021, Voos, 2013, Maurizi *et al*., 1990). Genome mining studies have shown that some species such as *E. coli* contains one ClpP isoform whereas others such as *M. tuberculosis* have multiple isoforms (Bhandari *et al*., 2018, Akopian *et al*., 2012). For the ClpP to be functional it assembles into tetradecameric structure containing a chamber where proteolysis occurs. For organism such as *M. tuberculosis* which contains two isoforms (ClpP1 and ClpP2), these tetradecameric structure consists of both isoforms (Illigmann *et al*., 2021).

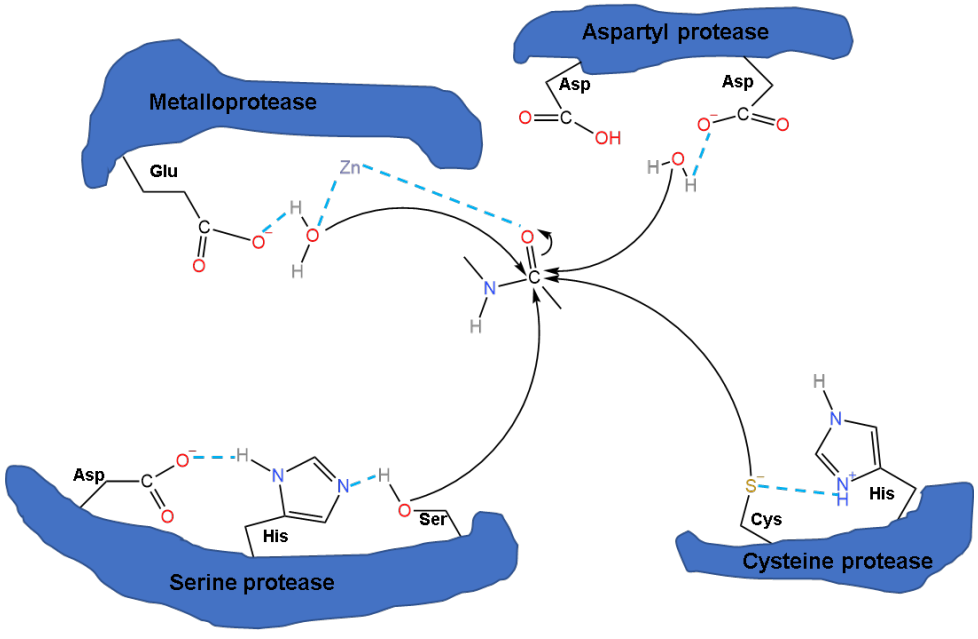

Figure 5: Different protease enzymes classified according to their catalytic site to hydrolyse peptides bonds. The serine and cysteine nucleophilic attack is mediated by proton with drawing group attached to either serine or cysteine's while water acts as a nucleophile for aspartyl proteases and metalloproteases (Neitzel, 2010). Dotted lines represent the interactions at the catalytic active site.

1.6. Structure of ClpP

ClpP in *E. coli* is approximately 21.5 kDa and folds predominantly into alpha helical structure (Mabanglo *et al*., 2019). This protein consists of three subdomains namely N-terminal, the core domain (also called globular head), and the handle region (Figure 6). The N-terminal forms an ordered loop structure which is very conserved across different ClpP in prokaryotic genomes (Mabanglo and Houry, 2022). For ClpP to be conformationally active, 14 monomeric ClpP units assemble to form heptameric rings containing a barrel shape like structure encompassing the proteolytic active site (Yu and Houry, 2007). Aligned with ClpP being a serine protease, the active site consists of Ser-His-Asp catalytic triad (Nouri *et al*., 2020, Moreno-Cinos *et al*., 2019). The ClpP heptameric structure, is formed by the ClpP monomeric units binding to each other via core domain through hydrophobic interactions and hydrogen bonding network (Nouri *et al*., 2020) (Figure 7). Also located in the core domain is oligomerization sensor that is essential for the stability of the heptameric structure. ClpP can adopt different conformations which includes an extended, compact and compressed state (Felix *et al*., 2019, Kimber *et al*., 2010). In the extended state handle domains within heptameric rings are interlocked, in the compact state the handle domain is unstructured and in the compressed state the long helix is interrupted at the centre (Ye *et al*., 2013).

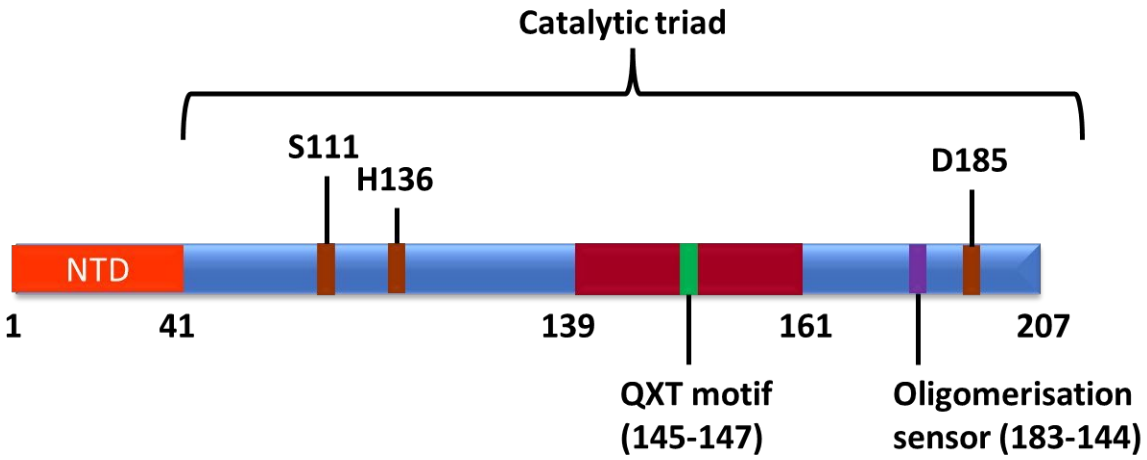

Figure 6: genome organization of *E. coli* ClpP. *E. coli* ClpP consists of N-terminal domain (orange box) essential domain for chaperone interaction, core domain (blue box), catalytic site (neon boxes) for peptide cleavage, oligomerization sensor (purple box), and handle domain (red box) responsible for formation of complex ClpP structure. The QXT motif (green box) is responsible for stabilizing complex ClpP (Mabanglo and Houry, 2022). Image was generated in BioRender.

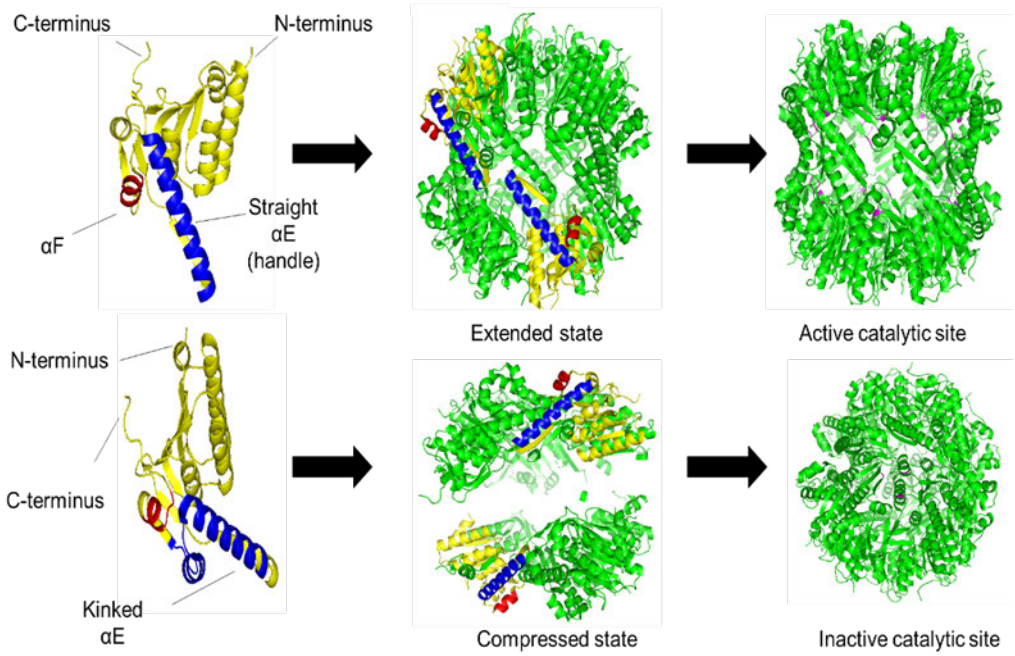

Figure 7: Different proteolytic conformations of ClpP. Crystal structure of ClpP isolated from *S. aureus* showing extended as well as compressed conformation. AlphaE-helix (αE) and alphaF-helix (αF) is shown in blue and red respectively. Structures were modified using PyMOL (Malik and Brötz-Oesterhelt, 2017).

The loop in the N-terminal domain then forms an axial pore which regulates substrate access to the active site. The substrates may be short peptides (7 to 8 residues) or aggregated/ misfolded proteins. The aggregated or misfolded proteins are usually tagged with degrons such as the SsrA-tagged protein to be recognized by Clp ATPases which are molecular chaperones belonging to the heat shock protein 100 family (Illigmann *et al*., 2021, Tao and Biswas, 2015, Hoskins and Wickner, 2006). Clp ATPases binds misfolded or aggregated proteins to refold and reactivate them through energy obtained from ATP hydrolysis (Frees *et al*., 2014, Gur and Sauer, 2008, Bukau *et al*., 2006). To maintain protein homeostasis and prevent the build-up of aggregated proteins in the cell, Clp ATPases associate with ClpP via its N-terminal domain, this association is important for the alignment of the catalytic triad. Therefore, proteins that cannot be rescued or unfolded are translocated into the ClpP proteolytic chamber for degradation (Figure 8). In contrast, shorter peptides can be degraded independently of Clp ATPases by ClpP.

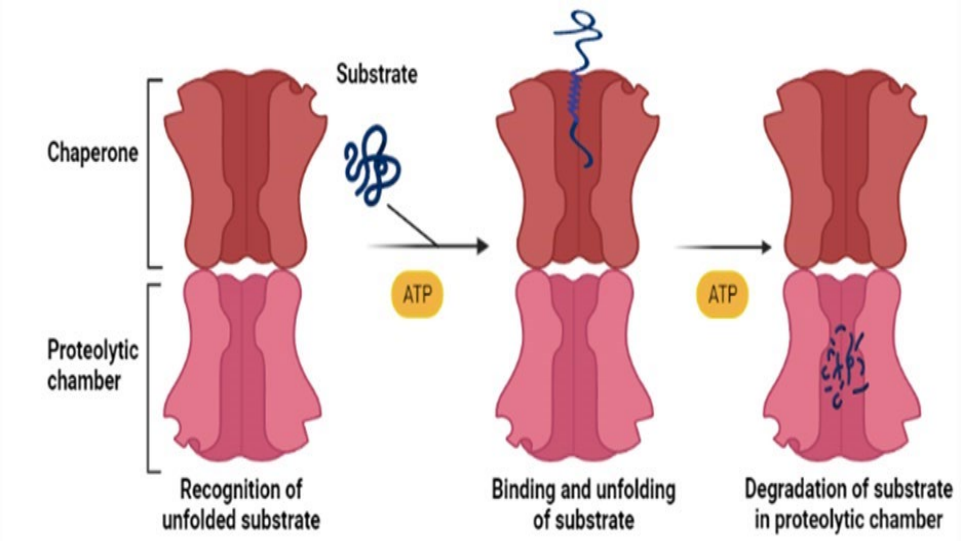

Figure 8: Hsp100 unfolding and degradation mechanism. Clp ATPase that act as a molecular chaperone are able to unfold damage proteins which act as substrate to proteolytic compartment through the use of energy generated from ATP hydrolysis in which they are degraded to small polypeptides (Doyle *et al*., 2013). Image was generated in BioRender.

1.7. Drugs targeting ClpP

Seeing the importance of ClpP for survival in bacterial cells (Table 3), it becomes increasingly important to develop novel strategies to target this protein for drug development. Consequently, there are different ClpP inhibitors that are being developed to target the catalytic site of ClpP (Table 4) (Moreno-Cinos *et al*., 2019).

Currently, there are different ClpP inhibitors that have been identified (Table 5) and in the pipeline of investigation. These inhibitors target the catalytic site of ClpP resulting in conformational changes in the tetradecameric structure, thus rendering the enzyme complex inactive (Moreno-Cinos *et al*., 2019). The instability of these compounds in plasma limits their potential clinical applications.

Table 5: Inhibitors of the catalytic site of ClpP

Name of Inhibitor	Compound	Structure	Mechanism of action	References
β-lactone	D3	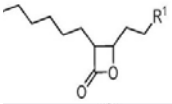	Suicide inhibitor responsible for disrupting O-acyl-enzyme product by which active ClpP attack carbonyl of β-lactone ring.	(Moreno-Cinos *et al*., 2019, Compton *et al*., 2013, Chastanet *et al*., 2001)
Boronates	Bortezomib (BTZ)	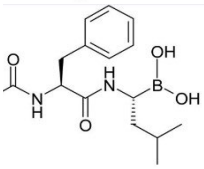	Bind to ClpP via threonine via hydroxyl group leading enzyme dysfunction	(Moreira *et al*., 2017a)((Moreira *et al*., 2017b, Chen *et al*., 2011)
Phenyl ester	AV170	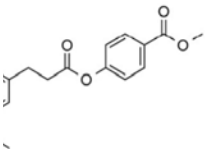	Binds to the catalytic site of ClpP, triggering conformational changes that result in the deoligomirisation of the ClpP tetradecamer.	(Schwarz *et al*., 2022, Hackl *et al*., 2015)
Chloromethyl ketones	Benzyloxycarbonyl leucyltyrosine chloromethyl ketone (ZLY-CMK)	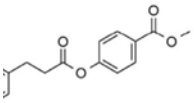	Forms two covalent bonds with serine and histidine of ClpP leading to covalent modification.	(Szyk and Maurizi, 2006)
β-sultams	RSKO7	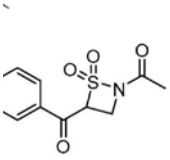	Attacks active site serine residue and converts it into dehydroalanine. This results in the disassembly of the active ClpP complex.	(Queraltó *et al*., 2023, Moreno-Cinos *et al*., 2019)

1.8. Objectives

K. pneumoniae is a member of the *Enterobacteria* family, and a Gram-negative pathogen which poses a major health concern in nosocomial settings. Attempts to control *K. pneumoniae* infections have been hampered by the emergence of multidrug resistant strains which use various biochemical mechanisms to evade the actions of antibiotics. Therefore, there is an urgent need to design novel strategies and preventative measures to eliminate infections associated with *K. pneumoniae*. One such strategy is to design drugs to target enzymes such as ClpP which play an essential role in protein homeostasis.

It is known that ClpP associates with Clp ATPases is response to stressful environmental conditions which may be induced by factors such as antibiotic treatment, heat or osmotic stress (Lemos and Burne, 2002). Studies performed with knockout mutants of these proteins have highlighted their importance in pathogenicity virulence and viability (Aljghami *et al*., 2022). Currently, studies focusing on *K. pneumoniae* have mainly focused on Clp ATPases. Not much is known about the structure and diversity of ClpP in *K. pneumoniae*. Taking into account that other studies in pathogens such as *S. aureus*, and *E. coli* have demonstrated that targeting

ClpP results in conformational changes that prohibits the formation of the tetradecameric complex and ClpP-Clp ATPase interaction (Moreno-Cinos *et al*., 2019). This results in the build-up of aggregated proteins and eventually leads to cell death.

Prior to designing inhibitors targeting *K. pneumoniae* ClpP it is important to investigate the diversity of *clpp* genes in the *Klebsiella* species. Currently no studies were identified which focused on the diversity of *clpp* genes in the *Klebsiella* species. This information is important given that it is known some pathogens such as *M. tuberculosis* contain multiple isoforms of ClpP. Furthermore, no studies reporting the expression and purification of soluble *K. pneumoniae* ClpP were found. To address this knowledge, gap this study aimed to investigate the diversity of *clpp* genes in the *Klebsiella* species and recombinantly express and purify the ClpP protein. To achieve these aims, the study objectives were as follows:

- Genome wide analysis of the *clpp* gene in the *Klebsiella* species
- Homology modelling of the hypothetical structure of *K. pneumoniae* ClpP
- Assessing the dynamic nature of ClpP using molecular dynamic simulations
- Optimizing the overexpression and purification of soluble recombinant ClpP.

Chapter 2: Methodology

2.1. *In silico* analysis

2.1.1. Genome data mining

National Centre for Biotechnology Information (NCBI) genome database was used to find *Klebsiella* strains. From the complete genomes, the protein files for the 100 published strains were downloaded and searched for the ClpP protein using the key words “ClpP” or “Clp protease”. The resulting FASTA sequences were copied into a separate file and further analysed using InterPro and Pfam to verify the presence of ClpP protein features. The 100 strains selected for analysis included 4 species, namely: *Klebsiella aerogenes*, *Klebsiella michiganensis*, *K. pneumoniae* and *Klebsiella pneumoniae subsp. pneumoniae* (Table A1). The analysed protein sequences were then labelled according to their species names and strain codes.

2.1.2. Homology Analysis

The percentage identity of the mined sequences of *Kp* ClpP were analysed using Clustal Omega. Additionally, the sequences were aligned using MAFFT sequence alignment through the Ugene software.

2.1.3. Phylogenetic tree construction

The selected protein sequences were aligned using the MAFFT v6.864 embedded on the Trex server. The file for the best tree from Trex server was visualized and coloured using the interactive Tree of Life (iTOL) server.

2.1.4. Homology modelling of *Kp* ClpP

The sequence of *Kp* ClpP (accession number. WP_004144676.1) was submitted to ITASSER, PHYRE2, and Swiss-model servers. The results on these servers were compared and the best template was chosen based on sequence similarity (greater than 30%), crystallization method, and resolution of protein structure (resolution value less than 1Å). The sequence of the best template (PDB 6nb1.1) was aligned with the sequence of *Kp* ClpP using the TCOFFEE server, Version_11.00. Thereafter, the target protein was modelled and downloaded using the Swiss-Model server. The modelled protein structure was visualized using Pymol and superimposed to the template structure. The secondary stereo chemical quality of the modelled *Kp* ClpP protein was analysed using the Ramachandran plot. Molegro molecular viewer, version 7.0 was then used to remove any ligands bound to modelled *Kp* ClpP and the structure was further assessed using the MolProbity, PROCHECK, Qualitative Model Energy Analysis (QMEAN), IUPred**,** and the ProSA-web servers.

2.1.5. Molecular dynamic simulations

Molecular dynamic (MD) simulations were performed using Maestro v13.0.317 using the Desmond molecular dynamics simulation engine. The modelled *Kp* ClpP monomeric and the template proteins were submitted to the Linux (Ubuntu) desktop server for simulation studies. The modelled *Kp* ClpP protein and the template protein were placed in an orthorhombic box (distance from the box face to the outermost protein atom was set at 7 Å, the box angle was α = β = γ = 90°). The orthorhombic box was then minimized, and the system was neutralised using counter ions. Additionally, 0.15 M NaCl was added to the orthorhombic box for physiological conditioning. The prepared system was then submitted for MD simulations. MD simulation is divided into eight distinct stages; stages 1-7 are equilibration, which is made up of short simulation steps, and stage 8 is the final long range 100 ns simulation stage.

2.1.6. Post dynamic analysis

MD simulation studies performed using Schrodinger Maestro v13.0.317 was used for post dynamic analysis. Firstly, Simulation Quality Analysis was used to analyse the quality of simulations using average energy, pressure, temperature, and volume. Secondly, the Simulation Interaction Diagram algorithm was used to analyse the root mean square deviation (RMSD) of the alpha carbon (Cα) atoms, the root mean square fluctuation (RMSF) of the residues, and secondary structure element analysis. Lastly, the Simulation Events Analysis algorithm was used to calculate the radius of gyration (Rg) and atomic distance.

2.1.7. Possible binding pockets and protein disorder

Modelled *Kp* ClpP and the template protein was submitted to the DoGSiteScorer to analyse its druggability. The 3D (three dimensional) structure of both protein pockets were visualized and the size, shape, depth, volume, and chemical features of the predicted (sub) pockets were calculated. The *Kp* ClpP sequence was then used to predict disorder regions within the protein as this is an effective method to identify whether proteins can be expressed, purified, or crystallized. The sequence of *Kp* ClpP was subjected to IUPRED2 which contains two systems used to estimate protein disorder. The IUPred2 system is used to estimate disordered protein regions while ANCHOR2 system is used to estimate disordered binding regions.

2.2. In vitro analysis

Following *in silico* analysis of *Kp* ClpP *in vitro* analysis was investigated to gain insight of *K. pneumoniae* ClpP due to lack of characterization studies. *Kp* ClpP was cloned and transformed in *E. coli* transformed cells for expression and purification of recombinant *Kp* ClpP in order to characterize it.

2.2.1. Theoretical analysis of *Kp* ClpP

The amino acid sequence of *Kp* ClpP (accession number WP_ 004144676.1) was submitted to the Expert Protein Analysis System (EXPASY) ProtParam server (https://www.expasy.org/) for the analysis of physicochemical properties such as amino acid residues, theoretical molecular weight, and isoelectric point. The hydrophobicity plot of *Kp* ClpP was obtained from EXPASY ProtScale tool described by Kyte and Doolittle (Kyte and Doolittle, 1982).

2.2.2. Preparation of competent cells

A vial of non-competent *E. coli* BL21 and JM109 cells previously stored in 60% (v/v) glycerol at −80ºC were thawed at room temperature and grown in sterile 2xYT broth media [1.6 % (w/v) tryptone, 0.5 % (w/v) NaCl, 1 % (w/v) yeast extract] overnight at 37ºC, 200 rpm. The cells were further grown in 1: 100 sterile 2xYT broth media at 37ºC, 200 rpm until Optical density at 600 nm (OD_{600}) reached an absorbance value ranging between 0.3 - 0.4. The cells were pelleted by centrifugation at 2700 x g, 4ºC for 10 min and the pellet was resuspended in sterile cold 0.1 M $MgCl_2$ (8 mL) and 0.1 M $CaCl_2$ (2 ml). The cells were further centrifuged at 2700 x g, 4ºC for 10 min and the pellet was resuspended in 4 mL of 0.1 M $CaCl_2$. Competent cells were preserved by the addition of 60 % (w/v) glycerol, rapidly frozen in liquid nitrogen and stored at −80ºC.

2.2.3. Bacterial transformation

Competent *E. coli* BL21 (DE3) and JM109 cells were transformed with pCold I vector (Figure 9) containing the *Kp* ClpP insert, using heat shock treatment. The DNA sequence of *Kp* ClpP was synthesized, codon-optimized and directly cloned into pCold I vector using restriction enzymes BamH1 and SalI by GenScript (Piscataway, New Jersey, United States). Briefly, previously made competent cells were thawed and 20 µL was mixed with 1 µL recombinant plasmid (4 µg) and incubated on ice for 30 min. The mixture was heat shocked for 90 sec at 42ºC and diluted 1:4 with pre-warmed sterile 2xYT media, then incubated for 1 hour at 37°C, 200 rpm. The cells were then plated on 2xYT agar [1.6 % (w/v), 0.5 % (w/v) sodium chloride, 1 % (w/v) yeast extract, 1.5% (w/v) bacteriological agar] supplemented with 100 µg/mL ampicillin and incubated overnight at 37°C. A single colony was picked from the 2xYT agar and inoculated in 20 mL 2xYT broth supplemented with 100 µg/mL ampicillin. The culture was incubated overnight at 37°C, 200 rpm. The cell culture was then cryopreserved using 60% (w/v) glycerol at -80°C.

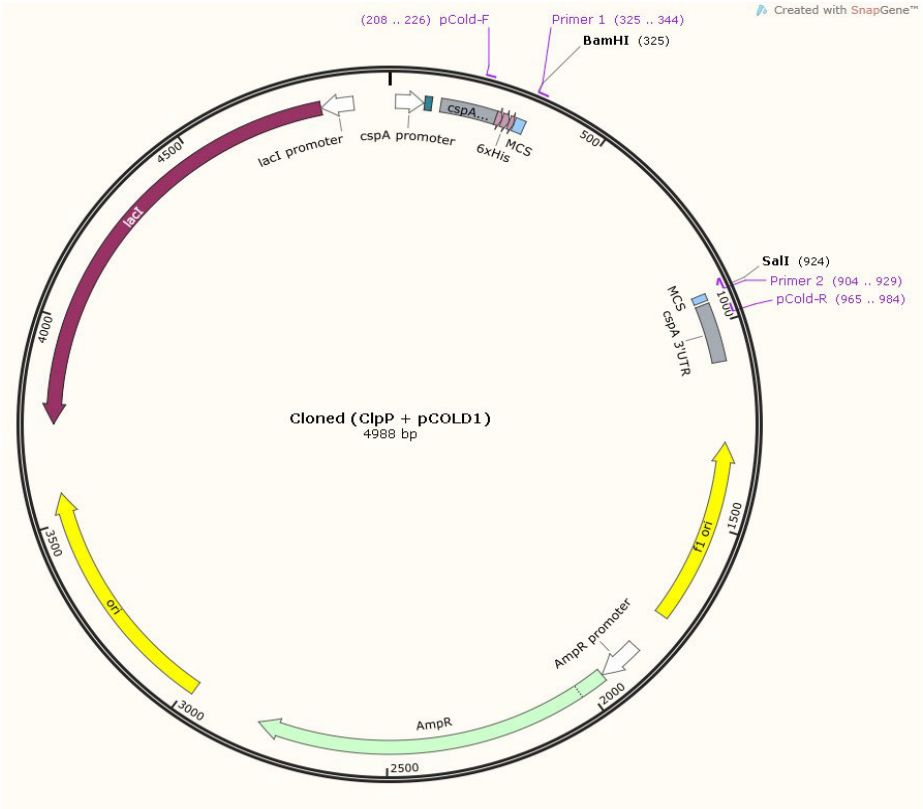

Figure 9: Vector map of pCold1 and ClpP insert. The vector map showing the ClpP insert, restriction enzymes (SalI and BamHI) and HisTag.

2.2.4. Colony Polymerase Chain Reaction (PCR)

To confirm the presence of the *Kp* ClpP gene in the BL21 cells, colony PCR was performed. Briefly, the transformed cells were grown overnight at 37°C, 200 rpm in 2xYT broth. The cells were then plated on 2xYT agar supplemented with 100 µg/mL ampicillin and incubated overnight at 37°C. Colonies were picked from the 2xYT agar and resuspended in 10 µL of sterile nuclease-free water for colony PCR. The pCold I forward and reverse primers (Table 6) were used for PCR amplification of the ClpP gene from the selected bacterial colonies.

Table 6: Primer used for DNA PCR amplification.

Primer name	Sequence (5' → 3')
pCold I forward	ACGCCATATCGCCGAAAGG
pCold I reverse	GGCAGGGATCTTAGATTCTG

PCR was performed in 25 µL reaction containing 1X Phusion HF, 200 µM dNTPs, 0.5 µM forward primer, 0.5 µM reserve primer, template DNA, 0.5 U Phusion DNA (for 25 µL reaction), and nuclease-free water. Amplification was performed with Applied Biosystems GeneAmp 9700 PCR System using conditions described in Table 7. The PCR products were diluted with purple loading dye (synthesized by New England Biolabs, United States), and analysed using a 1% agarose gel stained with ethidium bromide and visualized using the Syngene, GBox.

Table 7: Conditions for PCR

Step	Temperature (°C)	Time
Initial denaturation	98	30 sec
Denaturation	98	5 - 10 sec
Annealing	45 – 72	10 - 30 sec
Extension	72	15 - 30 sec/kb
Final extension	72	5 min

2.2.5. Optimization of *Kp* ClpP expression

Expression parameters such as modulation of induction point, time, and concentration of Isopropyl-β-D-Thiogalactopyranoside (IPTG) were optimised.

2.2.5.1. Modulation of induction point

Following *Kp* ClpP clone confirmation, the *E. coli* BL21 (DE3) cells transformed with ClpP were grown overnight in 2xYT at 37°C, 200 rpm. The cell culture was diluted 1:100 fold with fresh 2xYT media supplemented with 100 µg/mL of ampicillin and incubated at 37°C, 200 rpm and OD_{600} was monitored at 30 min intervals until static equilibrium was reached.

2.2.5.2. Expression of *Kp* ClpP at different time points and IPTG concentration

A trial expression of *Kp* ClpP was performed to test different times as well as different IPTG concentration, to find suitable expression conditions for bulk expression. Briefly, 2xYT media was inoculated with BL21 cells transformed with the *Kp* ClpP plasmid and incubated overnight at 37°C, 200 rpm. The overnight cell culture was then diluted 1:100 with sterile 2xYT media and grown at 37°C, 200 rpm supplemented with 100 µg/mL ampicillin until OD_{600} was reached with the absorbance of the culture ranging from 0.6 – 0.8. Expression was carried out at different times (4, 6, 12, 20 hours) and recombinant *Kp* ClpP was expressed with different IPTG concentrations ranging from 0.1 mM, 0.25 mM and 0.5 mM.

For all cultures, cells were harvested by centrifugation at 5000 x g, 4°C for 10 min and the resulting pellet was resuspended in PBS (10 mM sodium phosphate, 137 mM NaCl, 2.7 mM KCl, pH 7.4). Bacterial cell walls were lysed by sonication on ice for 8 min at 50% amplitude and lysed cells were centrifuged at 5000 x g, 4°C for 10 min. Protein profiles were analyzed using 15% Sodium dodecyl-sulfate polyacrylamide gel electrophoresis (SDS-PAGE) gel for both supernatant as well as resulting pellet. Protein samples were run with unstained protein ladder (ThermoFisher Scientific, USA) under reducing conditions at 80 V and stained using Coomassie brilliant R-250.

2.2.6. Western Blot

Recombinant *Kp* ClpP protein expressed at 18˚C for 6 hours, 200 rpm was harvested by centrifugation (5000 x g, 4˚C) for 10 min. Cells were disrupted by sonication and the soluble and insoluble fractions were separated by centrifugation. Proteins in the resultant soluble and insoluble fractions were separated in a 15% SDS-PAGE gel. Proteins were transferred onto a nitrocellulose paper (Pall Corporation, USA) at 20 V, 300 mA (room temperature) using Owl HEP-1 Semidry Electroblotting System (Thermo scientific, England), following manufacturers instruction. The blot was blocked for 1 hour at room temperature using blocking buffer [2% milk in Tris buffered saline (TBS), 20 mM Tris, 200 mM NaCl, pH 7.4] while shaking. Subsequently, mouse monoclonal IgG anti-His-Tag (1:5000, sc-53073) was incubated overnight shaking at 4˚C followed by three washes (5 min each) at room temperature with TBS, blots were incubated with goat anti-mouse IgG-HRP (1:10000) for 2 hours. Finally, the blot was washed three times with TBS buffer, and bands were visualized with Amersham ECL Western Blotting Detection Reagents (GE Healthcare, Chicago, IL, USA) in accordance with manufacturer's instructions. Protein bands were visualized using Syngene, GBox and estimated using the unstained protein ladder (ThermoFisher Scientific, USA).

2.2.7. Recombinant ClpP purification

Recombinant *Kp* ClpP detected in the western blot was purified based on the protocol described by Schlager *et al*. (Schlager *et al*., 2012) using a 1 mL His-Tag chelating column immobilized with Ni2+, pre-equilibrated with binding buffer [8 mM Na_2HPO4, 286 mM NaCl, 1.4 mM, KH_2PO4, 2.6 mM KCl, 5 mM imidazole and 0.1% Sarkosyl (w/v), pH 7.4.] connected to an AKTA system (Cytiva, Europe). Insoluble ClpP expressed at 18ºC, for 6 hours, 200 rpm was resuspended in lysis buffer [8 mM Na_2HPO4, 286 mM, NaCl, 1.4 mM KH_2PO4, 2.6 mM KCl and 1% SDS (w/v), pH 7.4.] supplemented with 1 mM Dithiothreitol (DTT) and sonicated on ice for 4 min at 50% amplitude. The solution was placed in ice water bath for 30 min for precipitation of SDS and centrifuged at 10 000 x g, for 30 min, 4ºC. The supernatant was filtered and loaded on a 5 mL His-Tag chelating column at a flow rate of 5 min/mL and contaminating proteins were washed with 5 column volumes of binding buffer. Weakly bound contaminating protein was washed with two wash buffers [8 mM Na_2HPO4, 286 mM, NaCl, 1.4 mM KH_2PO4, 2.6 mM KCl and 0.1% Sarkosyl (w/v), pH 7.4] one containing 20 mM imidazole and the other 50 mM imidazole respectively. Bound *Kp* ClpP was eluted and collected in 1 mL fractions using elution buffer [8 mM Na_2HPO4, 286 mM, NaCl, 1.4 mM KH_2PO4, 2.6 mM KCl and 0.1% Sarkosyl (w/v), 150 mM imidazole, pH 7.4]. All collected samples were run a 15% SDS-PAGE gel for analysis.

2.2.8. *In silico* circular dichroism

Secondary elements of modelled *Kp* ClpP were analyzed using *in silico* cd, briefly the modelled *Kp* ClpP was submitted to PDBMD2CD and CD spectra was obtained to analyse the protein secondary structure. The acquired cd spectra was compared to characteristic CD spectra to classify secondary elements.

2.2.9. Mass spectrometry

2.2.9.1. Sample in-gel digestion

Kp ClpP recombinant expression of the insoluble fraction was sequenced to identify the protein using Liquid chromatography-mass spectrometry (LC-MS). Protein band analysed by SDS-PAGE was cleaved from the gel then transferred into a sample tube containing distilled water. Protein was digested following protocol of Shevchenko et al (Özbek *et al*., 2019) briefly the protein was degraded with 25 mM NH_4HCO_3 containing 10 mM DTT for 1 hour at 60ºC then cooled at room temperature. The gel pieces from protein were incubated with 100% (v/v) acetonitrile for 10 min and supernatant was discarded. Gel peptides were further incubated with 55 mM iodoacetamide (IAA) for 20 min at room temperature in the dark and supernatant was discarded. Remaining gel peptides were dehydrated with 25 mM NH_4HCO_3 diluted in 5% (v/v) acetonitrile and dried completely. Trypsin was then added to gel peptides and placed overnight at 37ºC for digestion thereafter 0.1% (v/v) formic acid was added, and samples were dried under vacuum.

2.2.9.2. LC-MS analysis

Peptides obtained from trypsin digestion were analysed using an Evosep One LC system coupled to an AB Sciex 5600 Triple TOF mass spectrometer operated in positive ion mode. Peptides were eluted and separated using 60 SPD method on a Evosep C18 performance (150 µm × 8 cm, 1.5 µm particle size) with a gradient of 0-30% B over 21 min (A: 0.1% FA; B: 100% ACN/0.1% FA). An accumulation time of 250 ms followed by 50 fragment ion (MS/MS) scans, acquired from m/z 100-1800 with 35 ms accumulation time each was employed and precursor (MS) scans were acquired from m/z 400-1500 (2+-5+ charge states).

2.2.9.3. Data analysis

Sequences from *E. coli* were downloaded using UniProt (Swiss-Prot on 24 May 2023) and sequence of recombinant proteins as well as common contaminants were used to search raw data for each protein peptide utilizing Protein Pilot V5.0 software (SCIEX). Fixed modification and biological modification were allowed in search parameters as Trypsin (digestion enzyme) and cysteine alkylation (iodoacetamide). Protein confirmation was evaluated and only a minimum of 2 peptides identified.

Chapter 3: Results

3.1. *In silico* analysis

3.1.1. Phylogenetic analysis

Phylogenetic analysis was conducted to investigate the diversity of ClpP within the *Klebsiella* species. The phylogenetic tree showed three branches and these branches indicate that there are three common types of ClpP found in the *Klebsiella* species (Figure 10). Furthermore, branch 3 diverges more in comparison to branch 1 and branch 2, this indicates that the ClpPs of this branch are the most diverse (Figure 10). Interestingly, the *K. pneumoniae* ClpP are dispersed throughout the phylogenetic tree and are positioned on branches 1, 2 and 3, indicating the variation of the sequences. Clustal omega analysis showed that there was between 12.06 to 100% sequence similarities amongst the investigated *K. pneumoniae* strains, thus indicating the variation of the ClpP sequences.

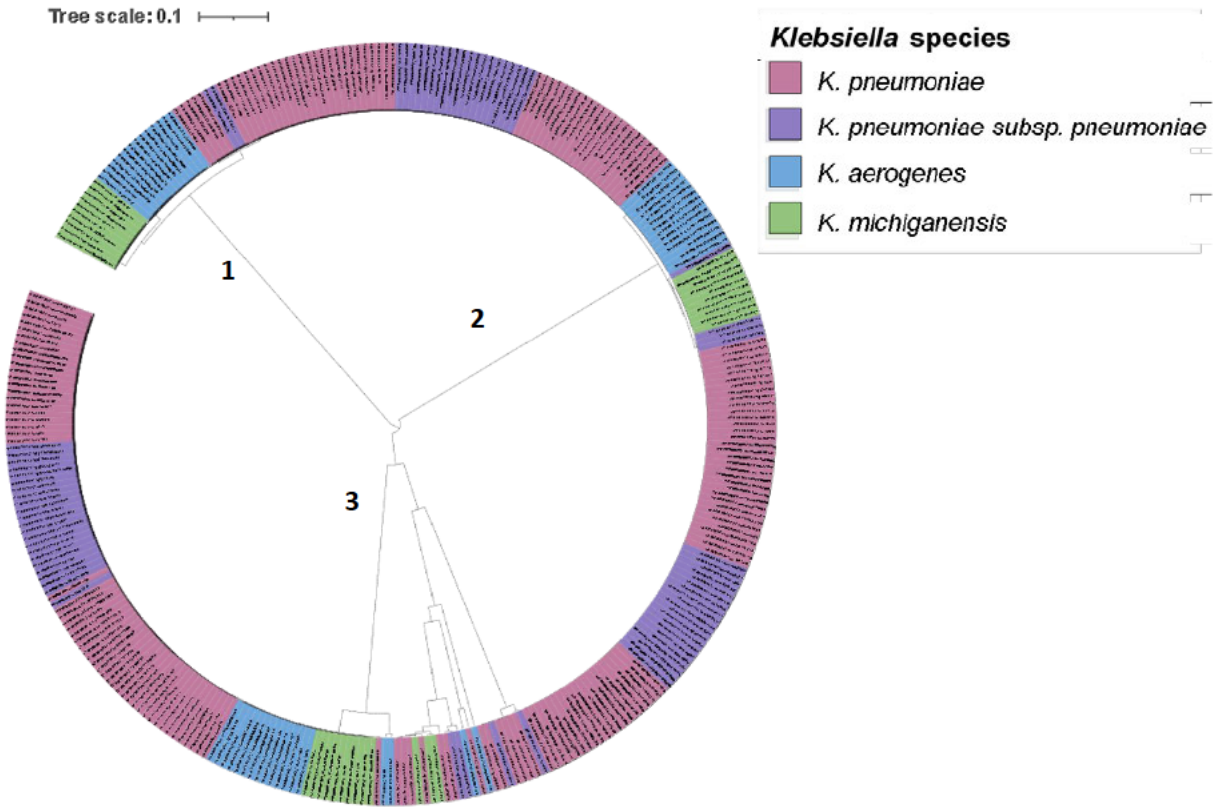

Figure 10: Phylogenetic analysis of ClpP proteins mined from four *Klebsiella* species. ClpP sequences were aligned using the Trex server and the tree was visualised using the iTOL server. The four different species of *Klebsiella* were represented in different species of *Klebsiella* were represented in different colors as denoted in the figure key. Tree distance scale: 0.1.

All the investigated *Klebsiella* strains contained two or more ClpPs (Figure 11). *K. pneumoniae* strains contain 3, 4 and 5 ClpP proteins per strain. Clustal omega analysis showed that the strains containing 3, 4 and 5 ClpPs had between 9.52 to 100%, 15.82 to 100%, 17.10 to 100% sequence similarity, respectively (Figure 12). This further confirms the variation of the ClpP sequences. There were 4, 8 and 5 isomers on ClpP amongst the *Klebsiella* strains containing 3, 4 and 5 ClpP proteins per strain, respectively. Therefore, there are a total of 17 isomeric forms of the ClpP protein amongst the *Klebsiella* species.

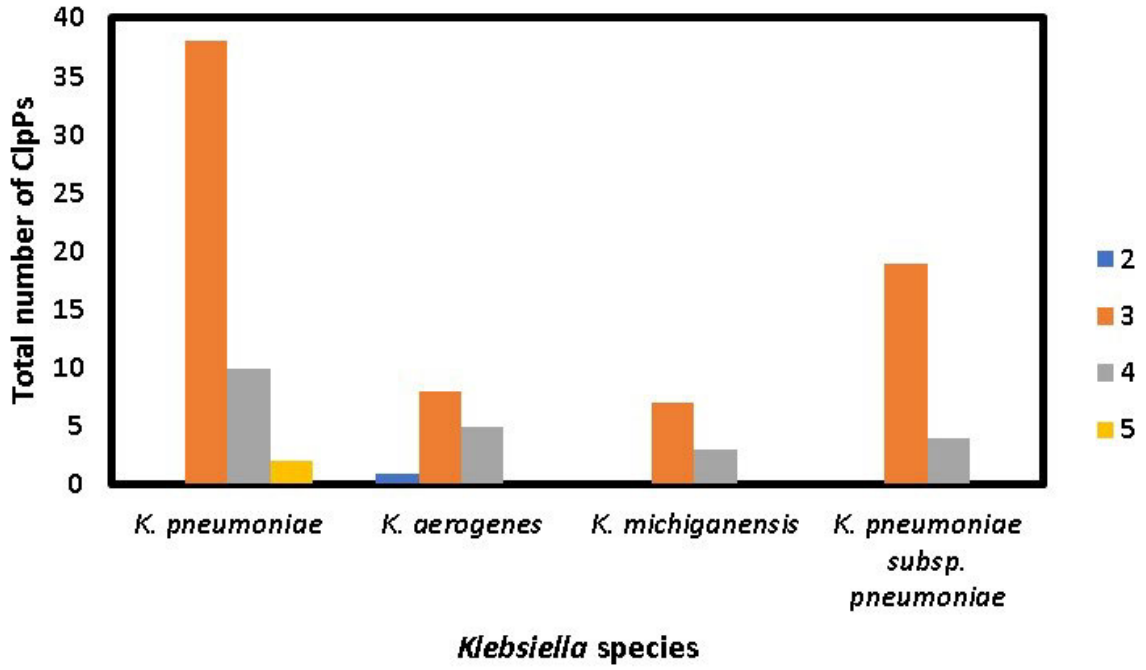

Figure 11: Total number of ClpPs in Klebsiella strains. Different *Klebsiella* species along with their different ClpPs, *K. pneumoniae* having the most ClpPs

A

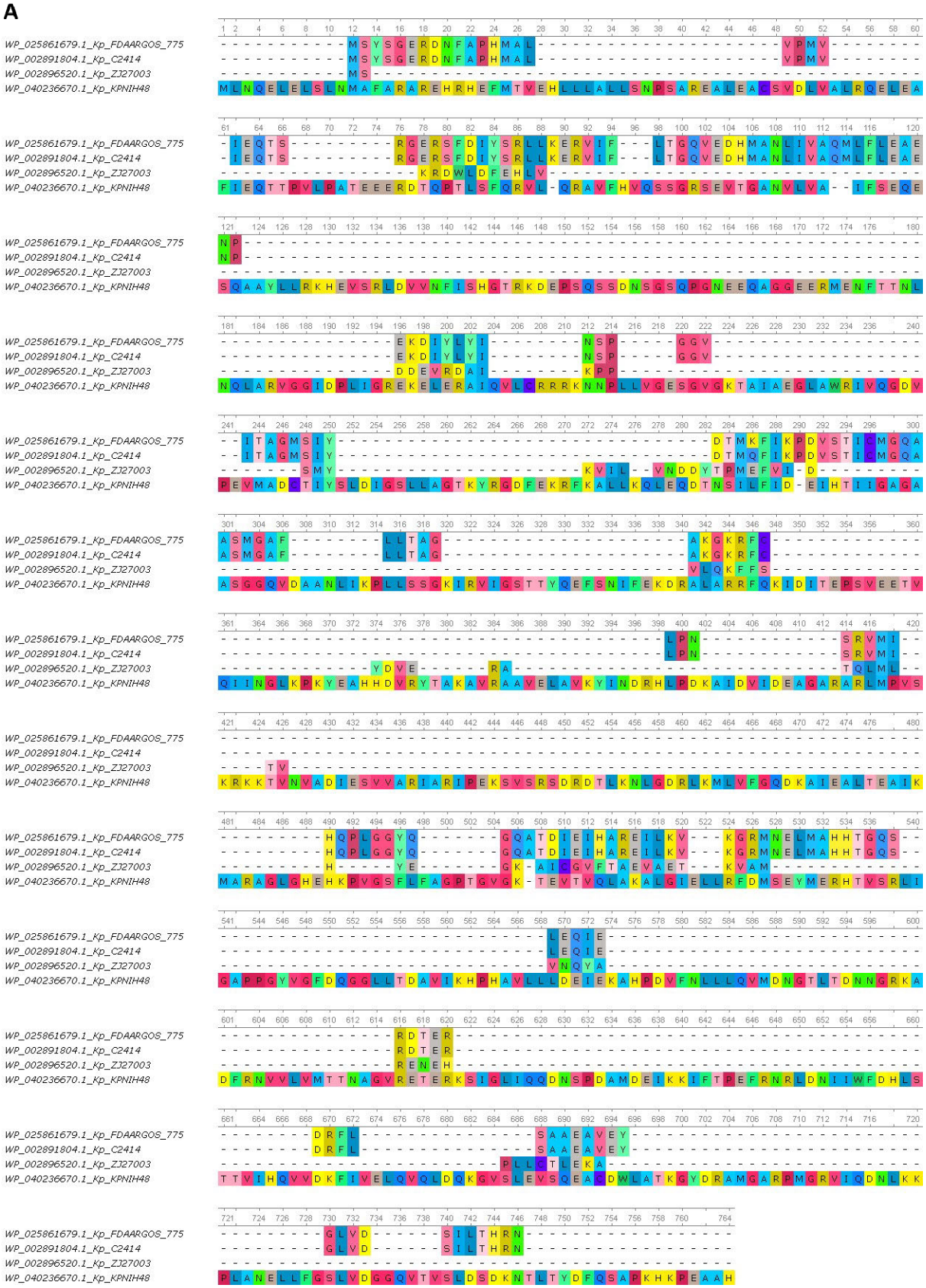
WP_025861679.1_Kp_FDAARGOS_775
WP_002891804.1_Kp_C2414
WP_002896520.1_Kp_ZJ27003
WP_040236670.1_Kp_KPNIH48

B

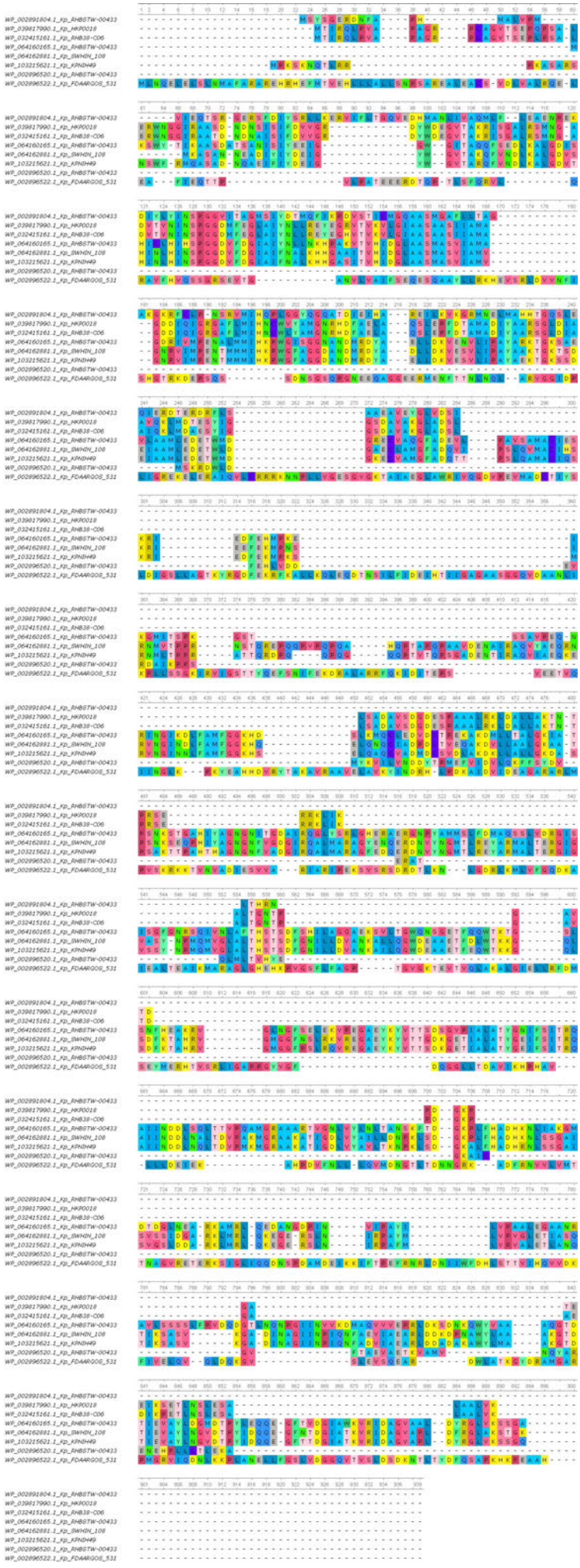
WP_002891804.1_Kp_RHBSTW-00433
WP_039817990.1_Kp_HKP0018
WP_032415161.1_Kp_RHB38-C06
WP_064160165.1_Kp_RHBSTW-00433
WP_064162881.1_Kp_SWHIN_108
WP_103215621.1_Kp_KPNIH49
WP_002896520.1_Kp_RHBSTW-00433
WP_002896522.1_Kp_FDAARGOS_531

C

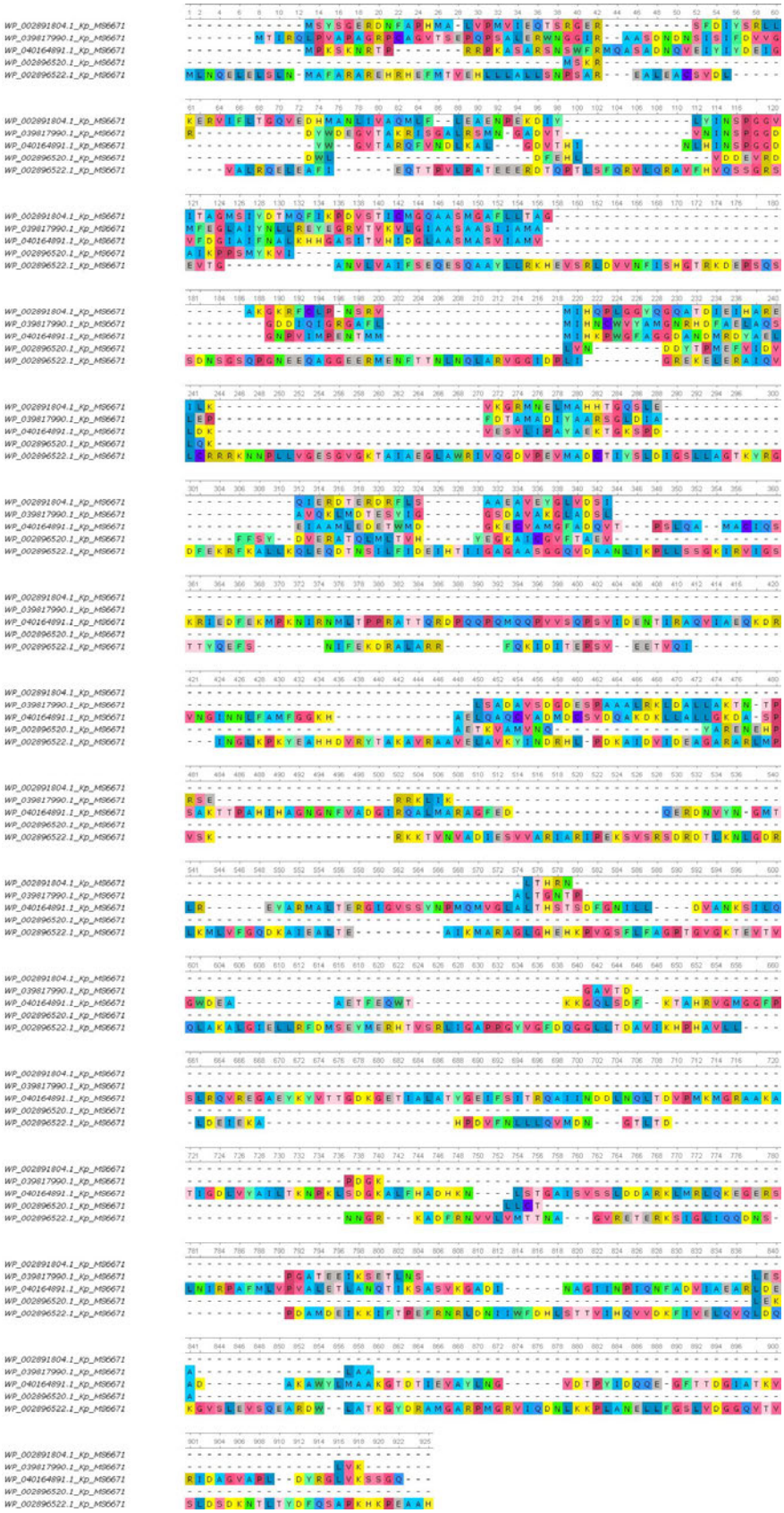

Figure 12: Protein sequence alignment of the ClpP isomers identified from the mined strains. A) Isomers identified across the strains containing 3 ClpPs. B) Isomers identified across the strains containing 4 ClpPs. C) Isomers identified across the strains containing 5 ClpPs. Alignments done using UGENE.

The hypothetical structure of *Kp* ClpP was modelled by performing a template search using various databases (Table 8). *E. coli* ClpP protease (6nb1,) had the highest identity (99%) when aligned with the *Kp* ClpP sequence indicating that both protein sequences are similar. Additionally, the target and template proteins had a 100% coverage and this suggests that both sequences are homologous (Waterhouse *et al*., 2018). The template was crystallised using X-ray diffraction and had a resolution of 1.90 Å. This high resolution indicates that the crystallised structure is highly ordered and atoms in the electron density maps clearly visible.

Table 8: Different template obtained from different databases along with PDB code, percentage identity, percentage coverage, resolution, R-free and R-work values.

Database	PDB code	Identity (%)	Coverage (%)	Resolution (Å)	R-Free	R-Work
i-Tasser	1yg6A	99	99	1.90	0.251	0.221
	7ekoL	33	96	3.30	0	0
	1yg6	99	99	1.90	0.251	0.221
	5dzk	49	99	3.07	0.232	0.198
	1yg6A	99	99	1.90	0.251	0.221
	5dzk	49	98	3.07	0.232	0.198
	6hwnA	58	95	1.95	0.211	0.186
	1yg6A	99	99	1.90	0.251	0.221
	7mk5A	98	94	2.95	0.248	0.221
	4ryfA	42	92	2.80	0.216	0.180
Phyre2	d1yg6a.1	99	93	1.90	0.251	0.221
	c6sflx	66	99	4.00	0	0
	c3q7hM	67	97	2.50	0.208	0.170
	c3kthD	69	90	2.50	0.208	0.170
	c3p2lD	65	98	2.29	0.226	0186
	c6hwmC	57	92	2.70	0.236	0.205
	c7ekqB	57	91	3.60	0	0
	c1tg6G	55	91	2.10	0.262	0.224
	c6x60A	53	98	2.81	0.235	0.198
	c1tg6a1	55	90	2.10	0.262	0.224
SWISS-MODEL	5dkp.1.D	72	99	2.38	0.239	0.196
	5dkp.1.A	72	99	2.38	0.239	0.196
	6nb1.1.C	99	100	1.90	0.244	0.209
	6nb1.1.A	99	100	1.90	0.244	0.209
	6nb.1.G	99	100	1.90	0.244	0.209
	6na1.1.A	72	99	1.90	0.244	0.209
	1tyf.1.A	99	99	2.30	0.292	0.219

3mt6.1.A	99	100	1.90	0.204	0.178
6w9t.1.F	72	99	1.65	0.282	0.237
6w9t.1.A	72	99	1.64	0.237	0.237

The alignment of template and *Kp* ClpP showed difference in three positions. The first difference was in the N-terminal domain, where the template has an extended N- terminal domain of 13 residues. Secondly, in position 156, a non-charged leucine residue in the template is replaced by charged histidine in *Kp* ClpP. Lastly, in position 178, the proline residues in the template are replaced by alanine (Figure 13). The effects on the changes on structure of *Kp* ClpP are not known hence it was important to model *Kp* ClpP despite it having a strikingly high similarity to *E. coli* ClpP protein. Furthermore, changes on the amino acid sequence of proteins (even one amino acid change) could dramatically change the structure of proteins (Figure 14). This structural change may impact function and stability of the protein (Schaefer and Rost, 2012).

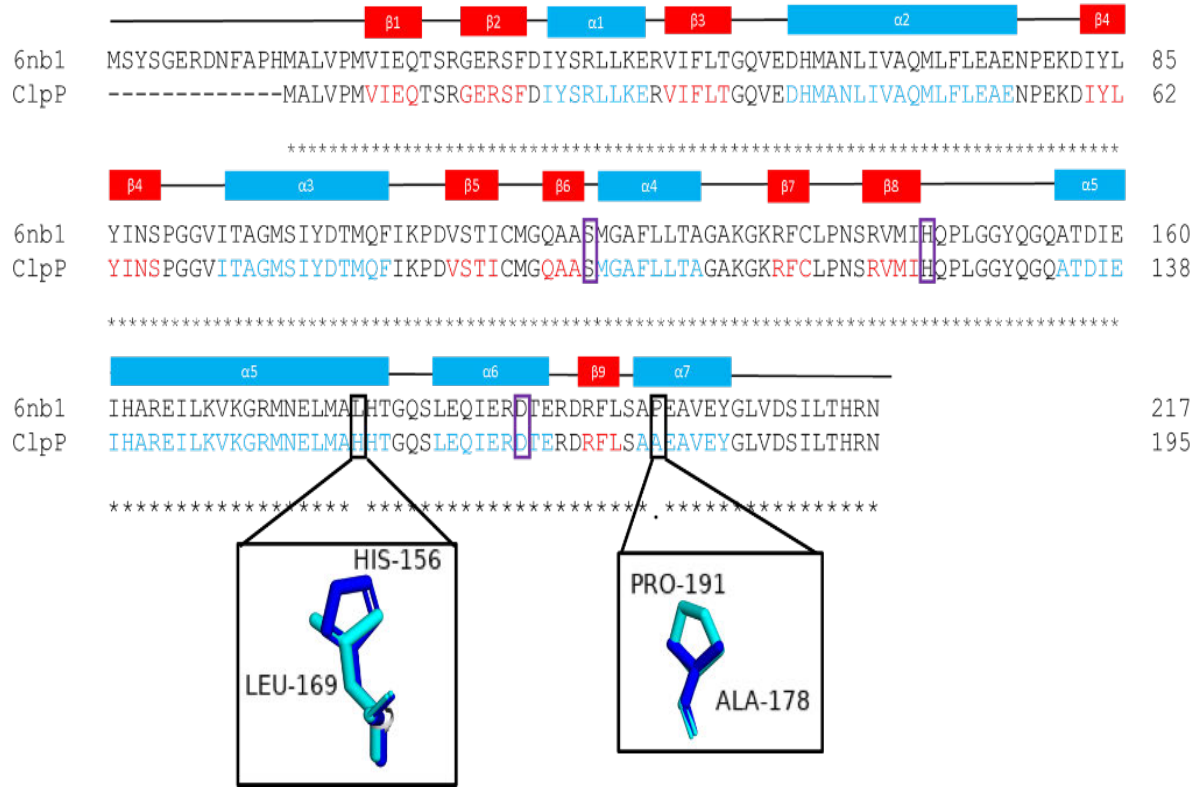

Figure 13: Sequence alignment of template (6nb1) and target (ClpP) performed using T-COFFEE. Sequence alignment showing secondary structure features, red boxes represent beta sheets (β), blue boxes representing alpha helices (α), purple boxes represent the Ser-His-Asp catalytic site. The boxed figures represent the mutated residues on the model and template. The circles show the structural differences between the model and template proteins.

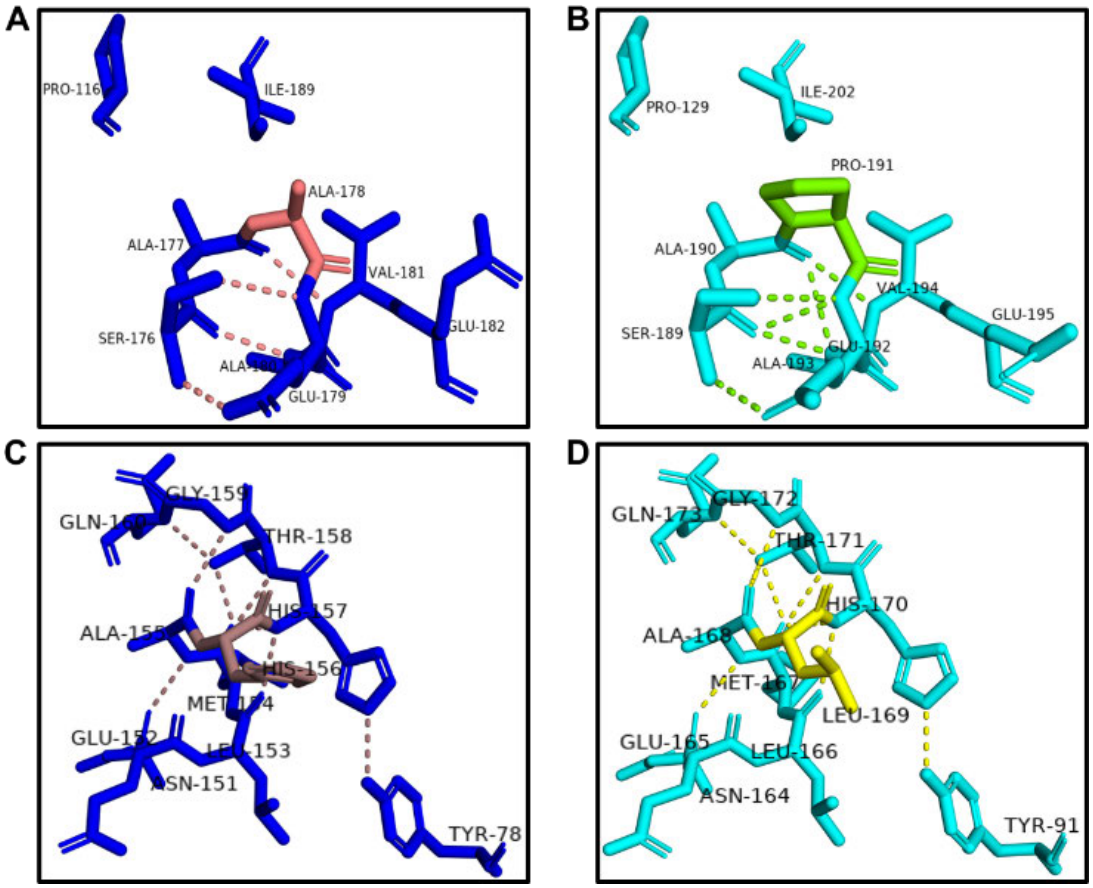

Figure 14: Effect of mutations on modelled *Kp* ClpP at position 156 and 178. A and B) effect of the Ala178 mutation on bonding within the *Kp* ClpP protein. C and D) effect of the Ala178 mutation on bonding within the ClpP protein. The dotted lines represent the bonds within 5 Å of the Ala178 and His156 residues of the modelled and template proteins.

Superimposing the structures of the template and modelled ClpP structure gave a RMSD of 0.180 Å (Figure 15). This further demonstrates that the template and target proteins are structurally homologous. Figure 7 also shows the quaternary structure of *Kp* ClpP which is a tetradecamer comprising a dimer of heptamers arranged such that they form a cylindrical shape. The *Kp* ClpP conformation shown in Figure 15 resembles that of compressed or closed ClpP where substrates cannot gain access to the active site (Díaz-Sáez *et al*., 2017).

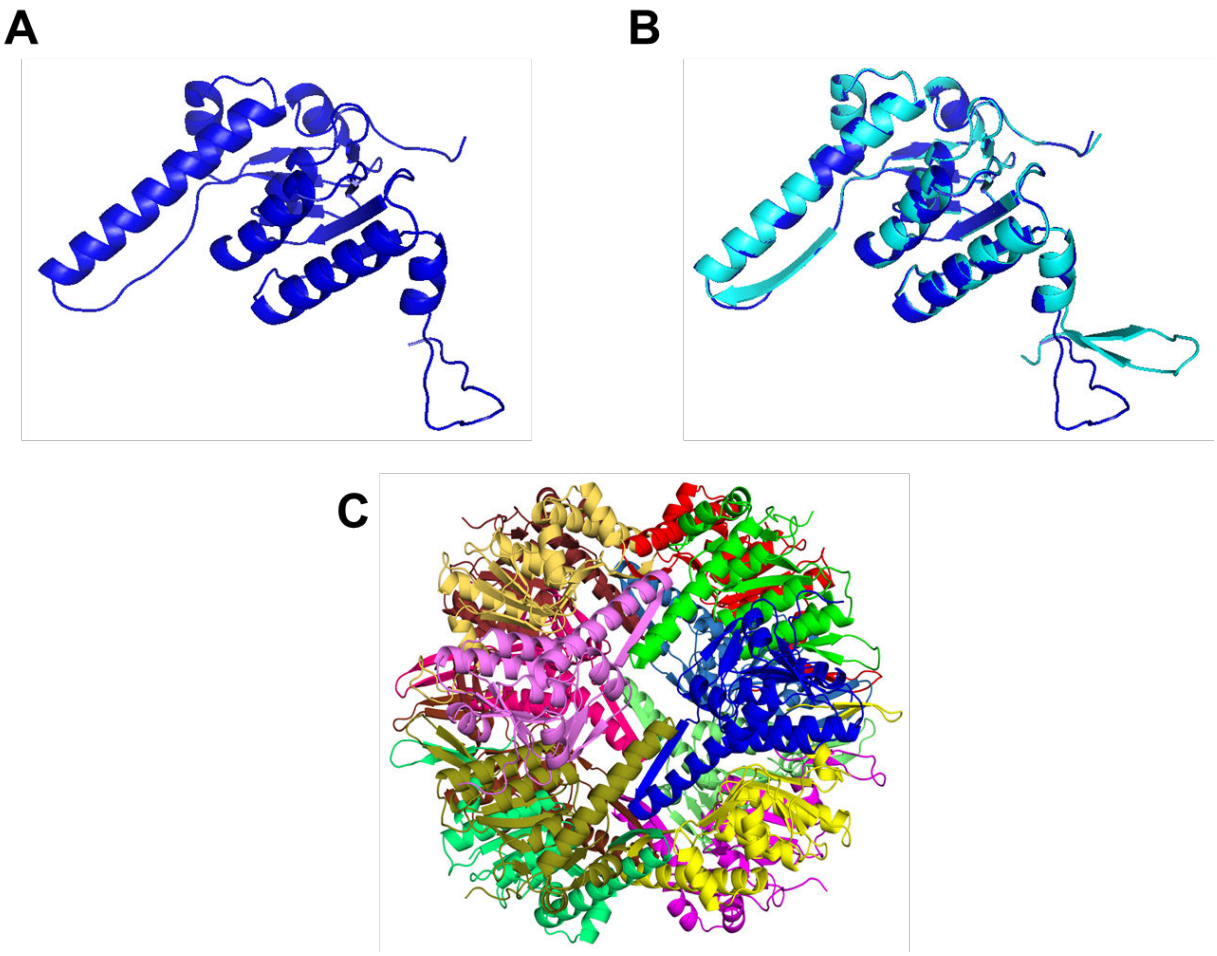

Figure 15: Structure of *K. pneumoniae* ClpP modelled using *E. coli* ClpP(6nb1) as a template. (A) Monomeric structure of *Kp* ClpP. (B) superimposed monomeric structure of *Kp* ClpP and template ClpP (6nb1) coloured in blue and cyan respectively. (C) Multimeric structure of *Kp* ClpP with chains coloured individually.

The quality of the modelled ClpP structure was examined using MolProbity, PROCHECK, QMEAN, IUPred2A, and PROSA servers. A Rama distribution Z-score of 0.63 ± 0.15 was obtained from MolProbity, this score was less than 2 and is within the acceptable range. This score indicated that the modelled *Kp* ClpP structure was of good quality. Furthermore, the Ramachandran plots of the modelled *Kp* ClpP and template proteins show a uniform distribution of most residues within favoured regions (Figure 16). According to PROCHECK, 94.1% of the modelled ClpP residues are within the most favoured regions as shown in Figure 4. This stipulates that the modelled structure and the template used for modelling are of good quality and have a stable conformation.

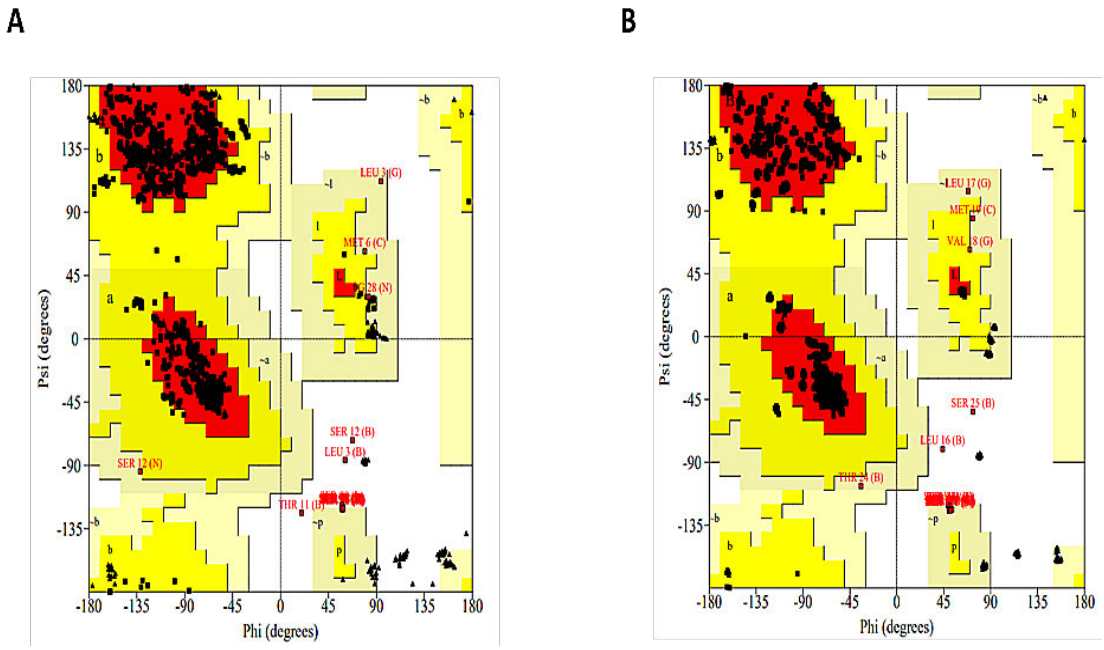

Figure 16: Ramachandran plot of modelled *Kp* ClpP protein and 6nb1 (template) obtained using the PROCHECK server. (A) Hypothetical structure of *Kp* ClpP and (B) the template (6nb1). The black dots represent amino acid residues, red zone represents favoured regions, yellow region represents allowed regions, light yellow represents generously allowed regions and white regions represent disallowed regions.

The *Kp* ClpP structure was passed through QMEAN, a web-based tool to provide the quality of the predicted protein structure (Benkert *et al.,* 2009, Benkert *et al.,* 2008). It scores predicted structure by measuring the agreement of predicted and calculated secondary structure and solvent accessibility. Figure 17 shows the evaluation of both the entire structure and individual residues of *Kp* ClpP and it can be seen that *Kp* ClpP model was allocated in the dark grey zone indicating that the modelled structure is of good quality. And this consistent with QMEAN4 value of 0.89 which lies in the high QMEAN score range.

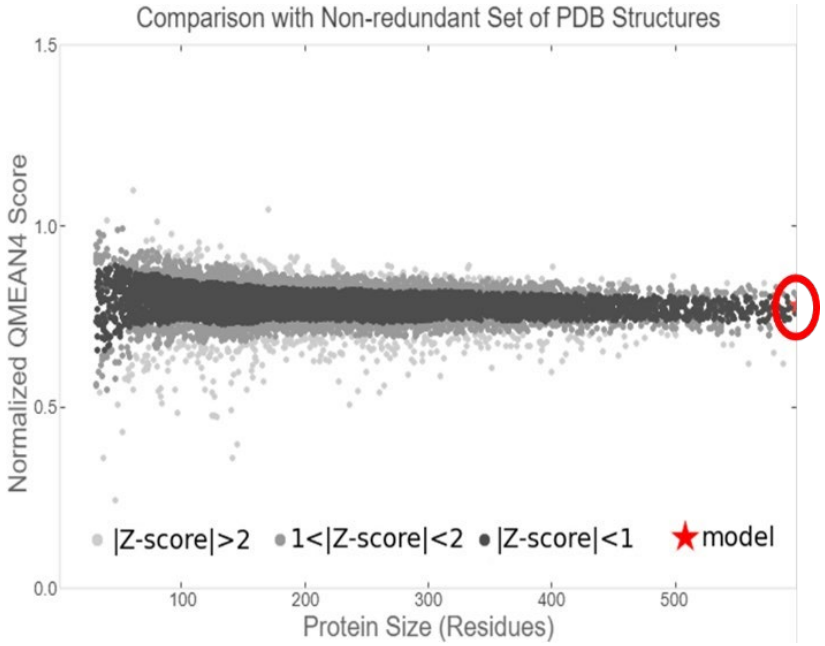

Figure 17: QMEAN score of modelled *Kp* ClpP composed of four statistical potential terms (QMEAN4). Graphical representation of QMEAN scores based on amino acid residues of modelled ClpP. The dark zone indicates good models, the red oval indicates the positioning of the modelled ClpP structure.

3.1.2. Circular Dichroism

The secondary structural elements of modelled *Kp* ClpP were assessed using cd. The spectrum obtained resembles the cd spectra of α-helical proteins which are characterized by two peaks, one positive peak at approximately 195 nm and one negative peak at approximately at 220 nm (Figure 18).

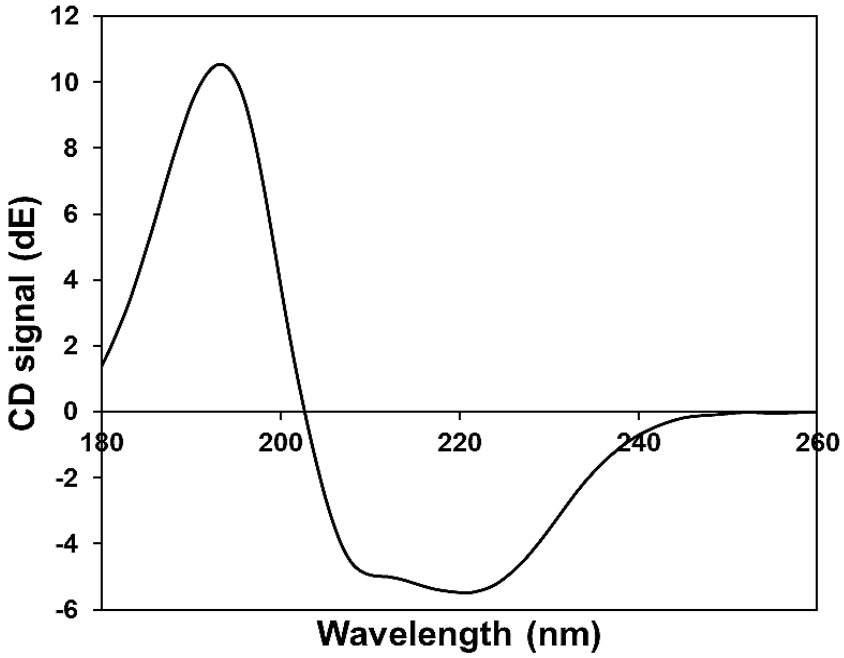

Figure 18: Circular dichroism of modelled *Kp* ClpP. In silico cd spectrum analysis of secondary structure of modelled ClpP obtained from PDBMD2CD.

3.1.3. Molecular dynamic simulations

Following structural assessments, the stability of the modelled and template proteins was investigated using molecular dynamic simulations. The average potential energy for modelled *Kp* ClpP and template protein was -90517.556 ± 61.04 kcal/mol and -74280.309 ± 55.47 kcal/mol, respectively. There is a slight, insignificant shift in the potential energy profiles of both these proteins, therefore suggesting that the *Kp* ClpP model was of adequate quality. Figure 19 shows the potential energy profiles to compare the alpha carbons of both the proteins over 100 000 ps.

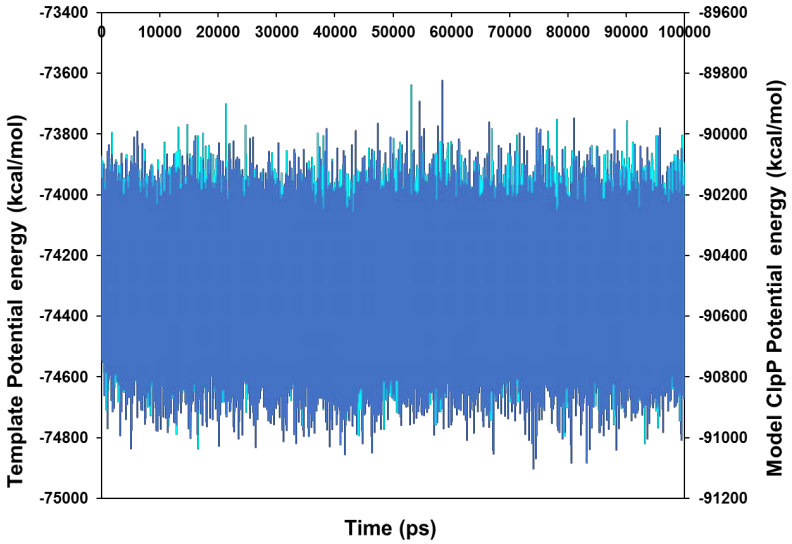

Figure 19: Potential energy profiles of the alpha carbons of the modelled and template ClpP proteins. Potential energy of modelled *Kp* ClpP (blue) and template (cyan).

The RMSD and RMSF values were calculated to assess the dynamic nature of proteins. Figure 20 shows the RMSD values of modelled *Kp* ClpP increases from 2.559 to 4.171 Å, while the RMSD values of template ClpP increases from 3.571 to 8.719 Å. The increasing RMSD values correlate with the expected dynamic nature of proteins and indicate significant conformational changes. Additionally, the template stabilises at approximately 20 ns while the RMSD of the model stabilises at around 50 ns, this confirms the stability of the modelled structure.

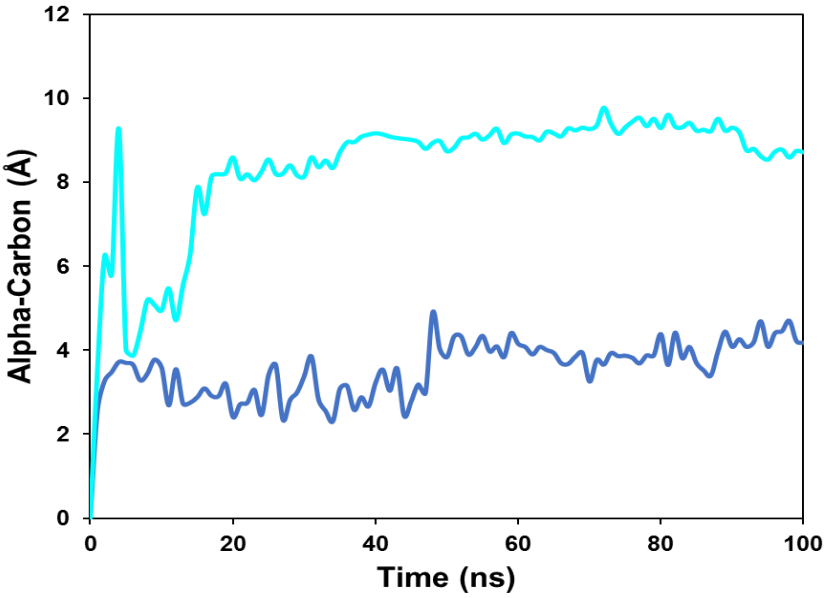

Figure 20: RMSD of the template and modelled *Kp* ClpP protein. The RMSD of template (cyan) and model *Kp* ClpP (blue) over 100 ns.

Furthermore, fluctuation of the individual amino acid residues of the proteins was evaluated using RMSF. It was observed that the pattern of residue fluctuations were very similar between template and modelled *Kp* ClpP protein. This demonstrates that similar residues contribute to the flexibility of both these proteins (Figure 21). Interestingly, the template had a high RMSF value around the N (~12.513 Å) and C-terminal (~7.519 Å) region. Furthermore, it was noted that, it was in N- and C-terminal region where, these two *Kp* ClpP proteins differ (Figure 13). Therefore, this difference seen in the RSMF values of truncation of extended N-terminal as well the mutation on C-terminus suggests that may impacts the stability of *Kp* Clp. Further studies are required to investigate the role of these regions in the stability of ClpP proteins.

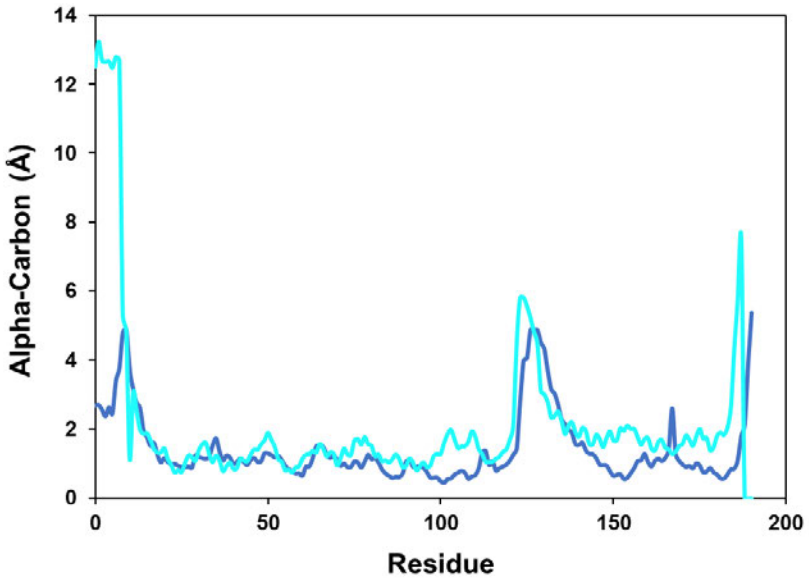

Figure 21: RMSF analysis of the template and modelled *Kp* ClpP protein. The RMSF of the template (cyan) and modelled *Kp* ClpP (blue).

Rg indicates the compactness of a protein structure and was analysed to investigate the nature of proteins through radius as well as compactness. It was observed that the modelled *Kp* ClpP structure had an average Rg value of 33 Å while the template had an average Rg of approximately 32 Å as shown in Figure 22. The Rg profile of both the proteins suggests that the proteins are constantly transforming during simulation. Additionally, this confirms that the proteins are dynamic in nature.

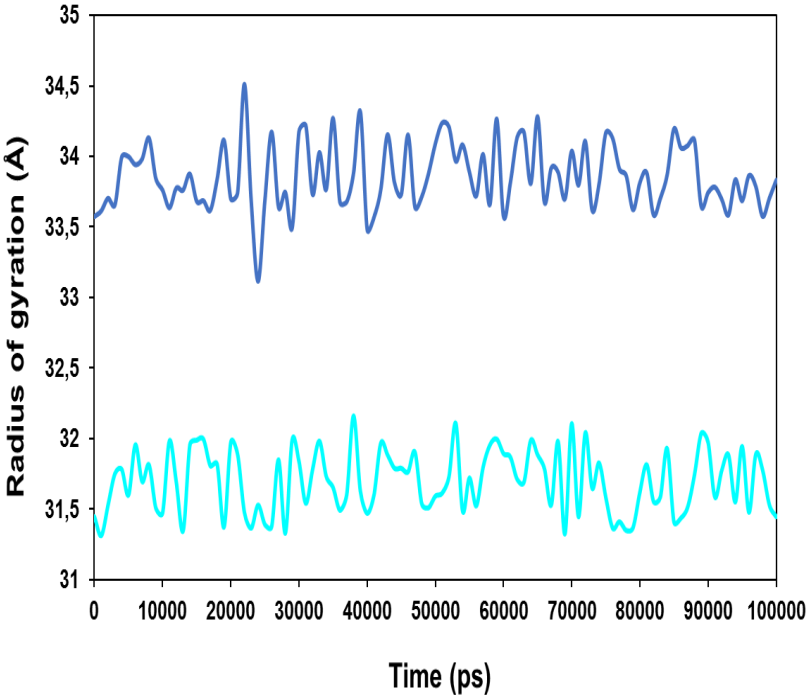

Figure 22: Trajectory analysis of the radius of gyration over 100 000 ps. Modelled *Kp* ClpP is represented as blue and template is represented as cyan.

3.1.4. Possible binding pockets

Kp ClpP interacts with proteins such as Clp ATPases to maintain protein homeostasis. To investigate the presence of binding sites in the *Kp* ClpP being analysed, the *Kp* ClpP model was assessed for the presence of potential binding sites. Additionally, the binding sites of the template were also analysed to further confirm that the modelled *Kp* ClpP and template ClpP were different despite have high sequence similarity. The DogSiteScorer server identified potential binding pockets for each protein around the same area, however the best binding pocket of each protein varied with the model having a drug score of 0.84 and the template having a drug score of 0.81 (Figure 23C). A score close to 1 indicated that the binding pocket is accessible. The surface area and volume are different from each other, further confirming that the proteins are unique. Additionally, the presence of binding sites on the protein surface indicates that there are potential binding sites on both these proteins that could be targeted to decrease protein homeostasis and cell survival.

A

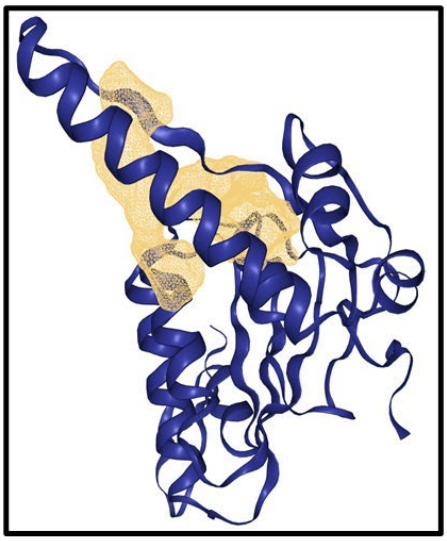

B

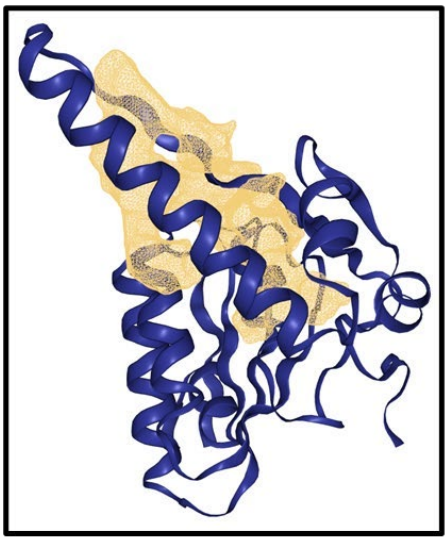

C

	Model	Template
Drug score	0.84	0.81
Surface area (Å2)	1218.5	1309.38
Volume (Å3)	875.9	1074.11
Depth (Å)	23.11	19.82

Figure 23: Prediction of detected binding sites for model and template ClpP using DoGSiteScorer. A) Binding site of the modelled *Kp* ClpP. B) binding site of the template ClpP. C) comparison of the binding site parameters of the modelled and template ClpP.

3.1.5. Protein disorder

The *K. pneumoniae* ClpP protein has not been previously expressed and purified. However, the structure of *E. coli* ClpP has been crystallised. Therefore, this indicates that *Kp* ClpP can be expressed and analysed further through *in-vitro* analysis. To further confirm this observation the hypothetical modelled *Kp* ClpP was screened for protein disorder using IUPred to gain insights of disordered regions which allows for expression and purification of proteins. It was found that the structure comprises of an ordered N-terminal domain and a disordered C-terminal domain. Approximately 15% of *Kp* ClpP residues are disordered shown in Figure 24 (indicated as a red line) thus due to a reduced amount of disordered residues this promote protein expression, purification and crystallization. Consequently, this allows for further characterization of *Kp* ClpP, while prediction of disordered binding regions by ANCHOR2 represented as a blue line shows that both the N and C-terminal domain are ordered. In spite of the fact that *Kp* ClpP contains disordered regions which often difficult to purify or crystallize, the modelled *Kp* ClpP contained less disordered regions which primarily may be responsible for variety of functions including post translation modification, cell signalling, molecular recognition and protein-protein interaction.

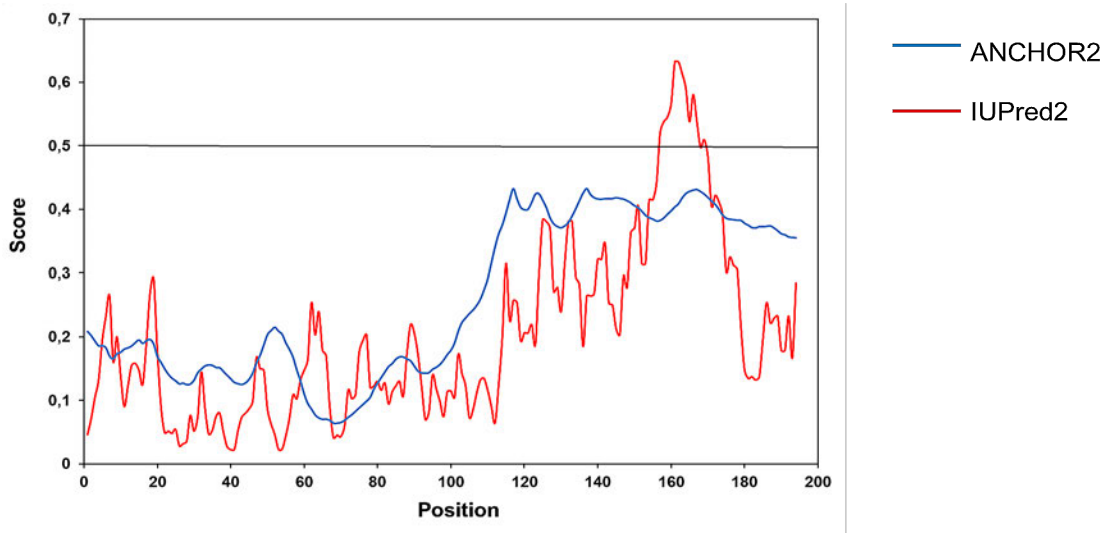

Figure 24: Graphical representation of protein disorder using the IUPred web server for ClpP. IUPred2 prediction of the ClpP using the IUPred2 long disorder, ClpP was found to be ordered using ANCHOR2 and 20% disorder in the C-terminal region using IUPred2.

3.1.6. Theoretical analysis of ClpP

Following *in silico* analysis of *Kp* ClpP *in vitro* analysis was investigated to gain insight of *K. pneumoniae* ClpP due to lack of characterization studies. Theoretical analysis was conducted and resulting physicochemical properties of ClpP are in (Table 9). It important to for the properties to be known prior expression and purification studies.

Table 9: Theoretical characterization of *Kp* ClpP. Physicochemical properties obtained from the (A) ExPASY ProtParam server.

Physicochemical properties	*Kp* ClpP
Molecular weight (Da)	21692
Amino acid residues	194
Isoelectric point	5,15

3.2. In vitro analysis

3.2.1. Clone confirmation

Gene encoding for *Kp* ClpP was synthesized and cloned into the pCold 1 vector by Genscript. Therefore prior to ClpP expression studies, the *Kp* ClpP construct was transformed into *E. coli* BL21 (DE3) cells. The transformants were screened for the presence of ClpP insert using colony PCR. Figure 25 shows that the screened colonies contained a band extrapolated to be 773 bp (Appendix Figure 1A). This band size was higher than size of ClpP which is 585 bp. This was expected since primers used in PCR are not gene specific, and they anneal in the region flanking the multiple cloning site. Therefore, the additional bases were added during the amplification of the insert.

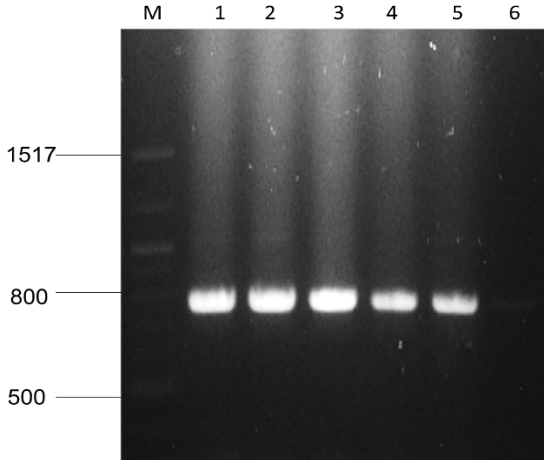

Figure 25: Colony PCR of *E. coli* BL21 (DE3) cells transformed with ClpP construct. Lane 1-5 randomly picked colonies screened for the ClpP construct and Lane 6 is the negative control. The PCR products were ran on a 1% (w/v) agarose gel using a TAE buffer ran at 80V.

3.2.2. Optimization of *Kp* ClpP expression

For expression of *Kp* ClpP, several conditions were tested to identify optimal expression conditions for ClpP. The expression studies began by first determining the ideal time to induce expression of *Kp* ClpP. Bacterial growth was monitored spectrophotometrically every 30 min intervals over 16 hours at 600 nm. Figure 26 shows the characteristic bacterial growth curve with constant growth in the lag phase in the first hour of inoculation. This was followed by exponential growth phase, where the cultured cells reached an optical density (OD) of 0.6 –

0.8 at an absorbance of 600 after 150 minutes of incubation. The OD of 0.6- 0.8 is the recommended as suitable point of protein induction due to that cells are at the log stage (growing phase) and a high protein expression is expected (Sivashanmugam *et al*., 2009). It was at this OD point were some cells were induced with of with 0.5 mM IPTG to promote recombinant expression and protein production in the cells. Both the induced and uninduced were further monitored for bacterial growth. These cells show similar growth profiles and entered the stationary phase at approximately 600 min.

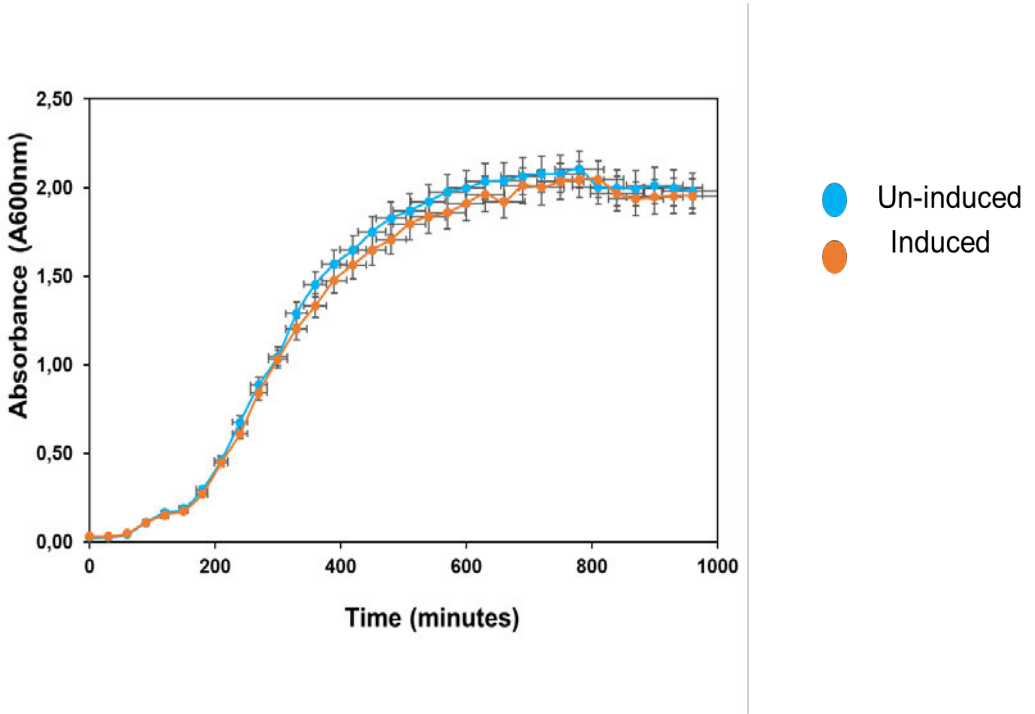

Figure 26: Quantitative monitoring of *E. coli* bacterial cell growth. Bacterial growth curve of uninduced and induced E. coli cells were grown at 37ºC and optical density was measured every 30 min. The error bars represent standard deviation of the mean from three independent experiments.

To optimise expression of *Kp* ClpP, different IPTG concentrations and post induction temperatures were tested at 18 ºC. Figure 27 shows that soluble and insoluble fraction expressed 21 and 25 kDa protein respectively. *Kp* ClpP is approximately 21 kDa, therefore it was intriguing to see a highly expressed band at 25 kDa in the insoluble fraction. On closer inspection, the 25 kDa protein is also present in the soluble fraction however in smaller quantity compare to the 21 kDa protein. It was also observed from Figure 26 is that increasing the IPTG concentration to more than 0.5 mM did not significantly result in greater yields of expressed proteins. However, the incubating the induced cell culture 20 hours resulted in better protein yields. Consequently, expression of *Kp* ClpP was induced with 0.5 mM IPTG and further incubated for 6 hours.

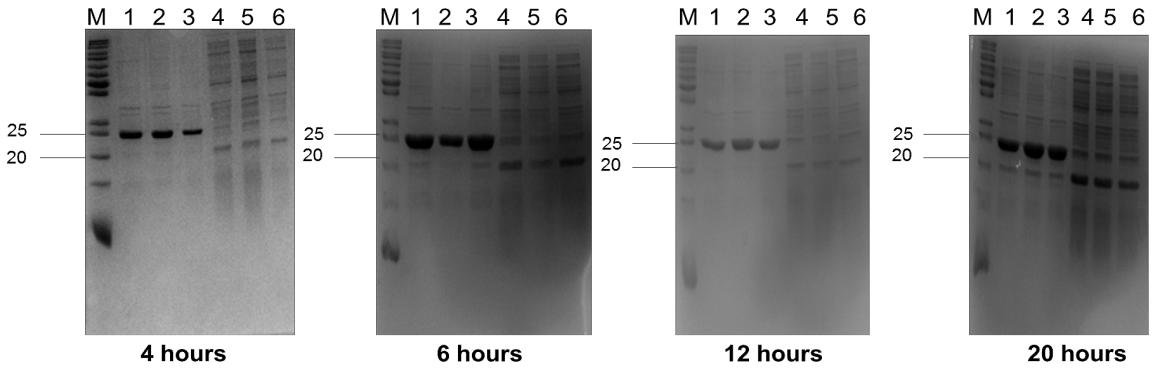

Figure 27: A reducing 15% SDS-PAGE gel of recombinant ClpP protein expressed at different times and IPTG concentrations. ClpP expression was induced with 0.1, 0,25 and 0, 5 mM IPTG and incubated for 4, 6, 12 and 20 hours at 18º C. The cells were harvested by centrifugation. For protein profile analysis, cells were lysed by sonication and centrifuged. Both the insoluble (pellet) and soluble (supernatant) were then analyzed on a 15% SDS-PAGE. All the gels were loaded as follows Lane M: molecular weight marker, Lane 1 pellet expressed with 0,1 mM IPTG, Lane 2, pellet expressed with 0.25 mM; Lane 3, pellet expressed with 0.5 mM; Lane 4 supernatant expressed with 0,1 mM IPTG, Lane 5, supernatant expressed with 0,25 mM IPTG and Lane 6, supernatant expressed with 0,5 mM IPTG.

3.2.3. 25 kDa band confirmation using Western blot and LC-MS analysis

Kp ClpP is expected contain a His-Tag based on the cloning strategy used in this study. Therefore, a western blot was performed using a primary anti-His antibody to determined which of the two bands (21 and 25 KDa) contains a His-Tag. This was deemed necessary in order to purify the correct fraction. Based on Figure 28, the 25 kDa band tested positive for His-tag, with a strong signal. This was intriguing given that the expected size of *Kp* ClpP is 21 kDa based on physiochemical property analysis. To further confirm the Western Blot results, the 25 kDa protein was sequenced using LC-MS.

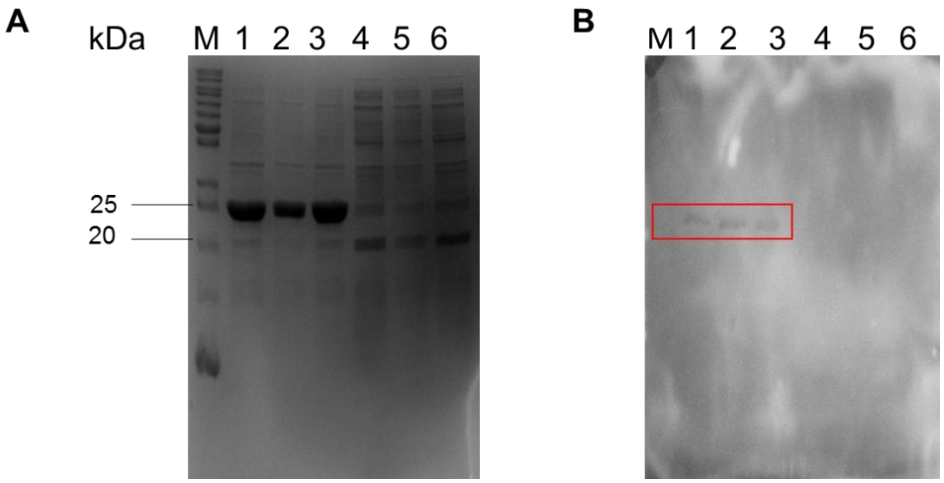

Figure 28: Confirmation of expressed *Kp* ClpP using Western blot. (A) 15% SDS-PAGE gel showing expression of *Kp* ClpP induced with different concentrations of IPTG and expressed for 6 hours post induction. (B) Western blot detection of the expressed of *Kp* ClpP induced with different concentrations of IPTG and expressed for 6 hours post induction. (B) Western blot detection of the expressed of Kp ClpP. Both gel and blot contain unstained molecular weight marker (M), Lane 1 pellet expressed with 0,1 mM IPTG, Lane 2, pellet expressed with 0.25 mM; Lane 3, pellet expressed with 0.5 mM; Lane 4 supernatant expressed with 0,1 mM IPTG, Lane 5, supernatant expressed with 0,25 mM IPTG and Lane 6, supernatant expressed with 0,5 mM IPTG.

Figure 29 shows the LC MS chromatogram of the 25 kDa band. The peptide fragments from the 25 kDa band had a high similarity of 72% *Kp* ClpP. Therefore, the mass spectrometry results are consistent with the western blot analysis.

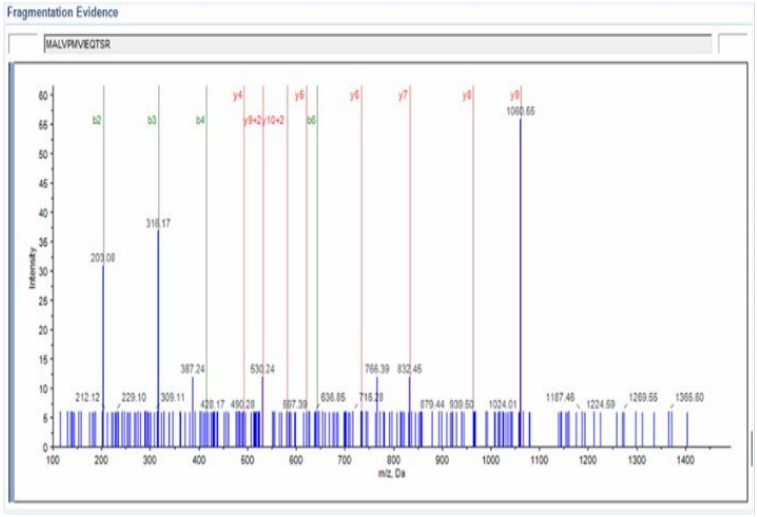

Figure 29: Mass Spectra of trypsin digestion of 25 kDa band. Mass spectrum of the different peptides identified from the insoluble fraction (25 kDa band).

3.2.4. Recombinant *Kp* ClpP purification

Following confirmation and expression of *Kp* ClpP, the insoluble fraction was solubilised and purified using affinity chromatography. The solubilized *Kp* ClpP protein was loaded onto a Ni^{+} column and it was expected to bind to the column via the histidine tag on *Kp* ClpP. Figure 30 shows that a considerable amount of protein was able to bind to the column while contaminants eluted with wash buffer. Bound *Kp* ClpP was eluted with an increased concentration of imidazole (150 mM).

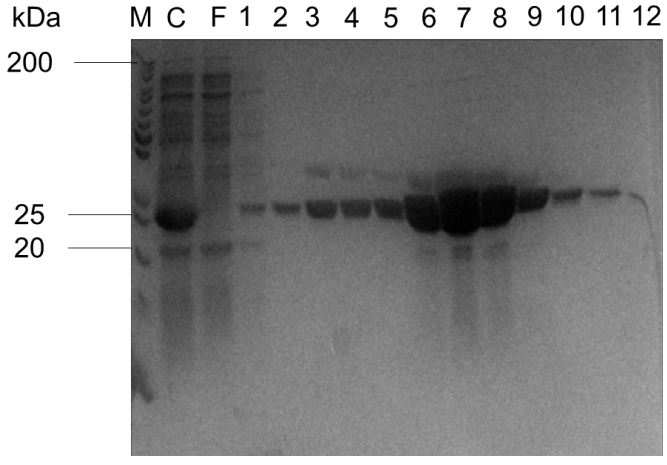

Figure 30: Recombinant *Kp* ClpP purification analysis using affinity chromatography. Recombinant *Kp* ClpP protein was overexpressed in E. coli BL21 (DE3) cells with 0.5 mM IPTG at 18°C, for 6 hours and harvested by centrifugation. The solubilized ClpP was applied to pre-equilibrated 1 mL His-Tag column (GE Healthcare, Life Sciences). Proteins eluted in the flow through were collected (F). Unbound proteins were washed with binding buffer containing 5 mM imidazole (lane 1) and 20 mM imidazole (lane 2). Bound proteins were eluted using 150 mM imidazole (lane 3 -12).

Chapter 4: Discussion and Conclusion

K. pneumoniae is a nosocomial pathogen which poses a great global health concern especially in immunocompromised patients (Podschun and Ullmann, 1998). Despite antibiotics being available for the treatment of *K. pneumoniae* infections, studies have shown that this pathogen uses various mechanisms to evade the effect of antibiotics (Riwu *et al*., 2022, Navon-Venezia *et al*., 2017). Subsequently, novel therapeutic alternatives are being investigated to target *K. pneumoniae*. One such alternative is to target ClpP which are essential in maintaining protein homeostasis under stressful environmental conditions (Khodaparast *et al*., 2021b). Not much is known about the structure and diversity of ClpP in *K. pneumoniae* therefore this study aims to address this knowledge gap.

4.1. Structural characterization of *K. pneumoniae* ClpP

Phylogenetic analysis was performed to investigate the evolutionary relationship of ClpP genes within four *Klebsiella* species namely, *K. pneumoniae*, *Klebsiella aerogenes*, *Klebsiella michiganesis* and *K. pneumoniae subsp. pneumoniae*. Phylogenetic tree analysis is a tool that shows the evolutionary relationship amongst species/genes and their speculated common ancestor (Hall, 2013). The ClpP gene was observed to be highly conserved in all investigated *Klebsiella* strains and grouped into three subclasses which branched from a common ancestor (Figure 10). Additionally, it was observed that each investigated strain contained more than one ClpP and a total of 17 ClpP isomers, displaying various variations, were identified (Figure 11 and 12). Such observed diversity of ClpP in *Klebsiella* species is consistent with alternative mRNA splicing and mutations that take place in a bacterium as result of evolutionary pressure amongst others. Alternative mRNA splicing is a process during gene expression where exons from the same gene are joined in different combination resulting in different and yet related mRNA transcripts (Ward and Cooper, 2010). These different mRNA transcripts could then be translated into protein isomers. Protein isomers are defined as protein with sequence similarity and originating from the same genetic family. The sequence similarity between isomers varies in families and species, for example in this study, strains with 3 isomers of ClpP, has as low as 9.52% similarity (Figure 11, 12). Despite these isomers being part of the same genetic family, their biological function may slightly vary (Vedula *et al*., 2017, Gunning, 2001). Another possible reason for *Klebsiella* species to have more than one isomer for ClpP could be tied evolutionary pressure where a bacterium could be exposed to changing environmental conditions (Kosová *et al*., 2021). This may give rise to isomers in prokaryotic cells with diverse biological activity. These isomers could aid pathogens to evade effect of antibiotic and survive harsh environmental condition.

Homology modelling was used to model the hypothetical structure *Kp* ClpP to gain an insight into the 3D structure of the protein (Figure 15). The structure of a protein directly relates to

protein function, therefore it is important to understand protein structure (Ji and Li, 2010). Homology modelling is a quick and inexpensive alternative to protein crystallization as gives an insight into the structure of the protein (Tastan Bishop *et al*., 2008). *Kp* Clp structure was modelled based on *E. coli* protease protein (6nb1) as it met the homology modelling template criteria. The alignment of the two sequences showed good sequence coverage (Figure 13). The quality of the modelled structure was deemed to be acceptable based on the Z-score, Rama-Z score and Qmean score which were all within acceptable range. The Z-score and Rama-Z score evaluates the atom positions and the polypeptide backbone (φ and ψ torsion angles) (Sobolev *et al*., 2020). The modelled *Kp* ClpP is homo tetradecameric which is consistent with that of structure of ClpP (Illigmann *et al*., 2021). Furthermore, the model and *in silico* CD analysis of *Kp* ClpP indicated that the protein is mainly alpha helical (Figure 18).

MD simulation was used to investigate the stability of modelled ClpP and the template protein since it used to study the behaviour of a protein at an atomic level (Hollingsworth and Dror, 2018). The potential energy profile of both proteins was observed to be relatively similar (Figure 19) and stable throughout simulation. Radius of gyration (Figure 22) of both proteins show constant transformation suggesting that both the proteins constantly transform during simulation. The overall RMSD of both proteins (Figure 20) increases over time. Both the Rg and RMSD values indicate that both the modelled and template proteins are dynamic in nature. Protein flexibility is essential for protein function because it allows for molecular interactions (Teilum *et al*., 2009). Protein flexibility was assessed RMSF and high levels of fluctuation (Figure 21) was observed, however no significant difference in flexibility was observed between template and modelled *Kp* ClpP.

The disordered regions of modelled *Kp* ClpP were investigated to identify whether the protein can be expressed, purified or crystallized (Mészáros *et al*., 2018). Disordered proteins do not form a stable tertiary structure, this affects protein function and results in difficulty expressing as well as purifying the protein (Papastratis, 2022). It was observed that *Kp* ClpP is mainly an ordered protein, suggesting that this protein may be recombinantly expressed (Figure 24).

4.2. Recombinant expression and purification of *Kp* ClpP

Kp ClpP was synthesized and cloned into pColdI for protein expression. The pCold1 vector is a cold expression system which contains cpsA promoter, 5'UTR and cpsA 3' termination site (Qing *et al*., 2004). This vector was chosen because the vector contains a cold shock protein such as cspA acts as a RNA chaperone responsible for regulation of gene expression during transcription or translation and thus enables high yields of recombinant proteins at low temperatures (Bae *et al*., 2000, Vasina and Baneyx, 1996). Additionally, pCold1 contains the translation enhancing element (TEE) sequence which promotes expression of recombinant protein in prokaryotic cells (Hayashi and Kojima, 2008). The plasmid construct was

transformed into competent *E. coli* BL21 cells. The gene insert was verified using colony PCR and an intense band at a size of approximately 773 bp (Figure 25) was observed. Following successful gene verification, recombinant *Kp* ClpP expression was optimized. Recombinant protein expression is often carried out in a bacterial host cell and microorganisms such as bacteria, yeast, filamentous fungi, as well as unicellular algae (Rosano and Ceccarelli, 2014). In this study, *E. coli* was used as an expression host cell as it has fast kinetic growth, high cell density, transformation of foreign DNA is rapid and media for cell growth is easily accessible (Rosano and Ceccarelli, 2014).

The best expression was obtained at 18ºC using 0.5 mM IPTG at 200 rpm for 6 hours (Figure 27). IPTG induces the promoter to promote the expression of the recombinant protein (Briand *et al*., 2016). Two protein bands were observed to be overexpressed, the first band was 21 kDa (in the soluble fraction) and the second was 25 kDa (in the insoluble fraction) (Figure 27). The expected size of the protein was 22 kDa. Potentially, either of the two overexpressed proteins could be the *Kp* ClpP protein. A protein may be expressed at a higher molecular weight due to post-translational modification resulting which may increase or decrease the size of protein (Wang *et al*., 2013, Larsen *et al*., 2006). However, *E. coli* host cells have not been reported to induce post-translational modifications such as glycosylation because these host cells do not have endoplasmic reticulum or Golgi body apparatus responsible for glycosylation and disulfide bridge formation (Bhatwa *et al*., 2021, Amann *et al*., 2019, McCormick *et al*., 2014).

The construct was expected to express *Kp* ClpP tagged with His-tag based on the cloning strategy (Figure 9). To confirm which of the two overexpressed proteins could be *Kp* ClpP, a western blot using anti-His Tag antibody was performed. The 25 kDa protein expressed in the insoluble fraction was then subsequently identified as *Kp* ClpP based on the western blot analysis (Figure 28). Expression in the insoluble fraction is often avoided due to protein being in an inactive state (De Marco *et al*., 2019). However, proteins in inclusion bodies can be purified from the bacterial cell by solubilizing with mild-to-harsh reducing agents (Mohammadian *et al*., 2018).

Following successful expression of *Kp* ClpP in the insoluble fraction and solubilization, the protein was purified. Protein purification is important as it allows for the study of protein function, to determine protein structure, and for protein application in an industrial or pharmaceutical environment (Smith, 2005). The *Kp* ClpP protein was purified using affinity chromatography which is a technique that isolates and purifies specific proteins by selective binding (Carter and Outten, 2021, Rodriguez *et al*., 2020, Singh *et al*., 2015). Purification of recombinant proteins can be accomplished through a histidine tag allows for fast and easy affinity purification of the recombinant protein (Köppl *et al*., 2022). In the present study *Kp* ClpP

tagged with histidine was solubilized using sakorsyl, which is a mild detergent. The advantage of using sarkosyl in comparison to stronger solubilization agents such as urea is the ability of sarkosyl to solubilize inclusion bodies without having an effect on the native structure of the protein (Massiah *et al*., 2016, Singh *et al*., 2015). The protein was then purified using nickel-ion affinity chromatography to obtain a pure *Kp* ClpP protein (Figure 30).

Western blot and LC-MS confirmed the 25 kDa band as being *Kp* ClpP. However, this was unexpected as the physicochemical analysis of this protein shows that it is 21 kDa. Possible explanation for a discrepancy in size could be due to *Kp* ClpP being bound to a small protein or insufficient denaturation of the protein through SDS addition or sample heating. The actual size of the protein needs to be validated using sensitive techniques such as high-performance liquid chromatography (HPLC), or static light scattering based methods (Gaspards., 2019, Foltda 1999).

4.3. Concluding Remarks

The overall aims and objectives of the study were achieved. ClpP was identified to be present in four different *Klebsiella* species with sequence variation. Based the model structure, *Kp* ClpP is mainly alpha helical. Molecular dynamic studies showed that this is protein is stable, and highly dynamic in nature which is consistent with its function. Considering that this protein has not been previously expressed and purified, this study provides a baseline for future studies. Future studies could focus on using alternative vectors to express the *Kp* ClpP protein in the soluble fraction. Expression of the protein in the soluble fraction would allow for protein characterization studies which are essential for drug development.

Chapter 5: References

ABUOUN, M., JONES, H., STUBBERFIELD, E., GILSON, D., SHAW, L. P., HUBBARD, A. T., CHAU, K. K., SEBRA, R., PETO, T. E. & CROOK, D. W. 2021. A genomic epidemiological study shows that prevalence of antimicrobial resistance in *Enterobacterales* is associated with the livestock host, as well as antimicrobial usage. *Microbial genomics,* 7.

AKOPIAN, T., KANDROR, O., RAJU, R. M., UNNIKRISHNAN, M., RUBIN, E. J. & GOLDBERG, A. L. 2012. The active ClpP protease from *M. tuberculosis* is a complex composed of a heptameric ClpP1 and a ClpP2 ring. *The EMBO journal,* 31**,** 15291541.

ALGHORIBI, M. F., ALQURASHI, M., OKDAH, L., ALALWAN, B., ALHEBAISHI, Y. S., ALMALKI, A., ALZAYER, M. A., ALSWAJI, A. A., DOUMITH, M. & BARRY, M. 2021. Successful treatment of infective endocarditis due to pandrug-resistant *Klebsiella pneumoniae* with ceftazidime-avibactam and aztreonam. *Scientific Reports,* 11**,** 1-9.

ALJGHAMI, M. E., BARGHASH, M. M., MAJAESIC, E., BHANDARI, V. & HOURY, W. A. 2022. Cellular functions of the ClpP protease impacting bacterial virulence. *Frontiers in Molecular Biosciences,* 9.

AMANN, T., SCHMIEDER, V., FAUSTRUP KILDEGAARD, H., BORTH, N. & ANDERSEN, M. R. 2019. Genetic engineering approaches to improve posttranslational modification of biopharmaceuticals in different production platforms. *Biotechnology and Bioengineering,* 116**,** 2778-2796.

ANTUNES, N. T. & FISHER, J. F. 2014. Acquired class D β-lactamases. *Antibiotics,* 3**,** 398434.

ARGIMÓN, S., DAVID, S., UNDERWOOD, A., ABRUDAN, M., WHEELER, N. E., KEKRE, M., ABUDAHAB, K., YEATS, C. A., GOATER, R. & TAYLOR, B. 2021. Rapid genomic characterization and global surveillance of *Klebsiella* using pathogen watch. *Clinical Infectious Diseases,* 73**,** S325-S335.

AURILIO, C., SANSONE, P., BARBARISI, M., POTA, V., GIACCARI, L. G., COPPOLINO, F., BARBARISI, A., PASSAVANTI, M. B. & PACE, M. C. 2022. Mechanisms of action of carbapenem resistance. *Antibiotics,* 11**,** 421.

BACHMAN, M. A., LENIO, S., SCHMIDT, L., OYLER, J. E. & WEISER, J. N. 2012. Interaction of lipocalin 2, transferrin, and siderophores determines the replicative niche of *Klebsiella pneumoniae* during pneumonia. *MBio,* 3**,** e00224-11.

BAE, W., XIA, B., INOUYE, M. & SEVERINOV, K. 2000. *Escherichia coli* CspA-family RNA chaperones are transcription antiterminators. *Proceedings of the National Academy of Sciences,* 97**,** 7784-7789.

BARAWI, S., HAMZAH, H., HAMASALIH, R., MOHAMMED, A., ABDALRAHMAN, B. & ABDALAZIZ, S. 2021. Antibacterial mode of action of grapefruit seed extract against local isolates of beta-lactamases-resistant Klebsiella pneumoniae and its potential application. *Intl. J. Agric. Biol.,* 26**,** 499-508.

BEHNSEN, J. & RAFFATELLU, M. 2016. Siderophores: more than stealing iron. *MBio,* 7**,** e01906-16.

BELETE, T. M. 2019. Novel targets to develop new antibacterial agents and novel alternatives to antibacterial agents. *Human Microbiome Journal,* 11**,** 100052.

BENKERT, P., KÜNZLI, M. & SCHWEDE, T. 2009. QMEAN server for protein model quality estimation. *Nucleic acids research,* 37**,** W510-W514.

BENKERT, P., TOSATTO, S. C. & SCHOMBURG, D. 2008. QMEAN: A comprehensive scoring function for model quality assessment. *Proteins: Structure, Function, and Bioinformatics,* 71**,** 261-277.

BHANDARI, V., WONG, K. S., ZHOU, J. L., MABANGLO, M. F., BATEY, R. A. & HOURY, W. A. 2018. The role of ClpP protease in bacterial pathogenesis and human diseases. *ACS chemical biology,* 13**,** 1413-1425.

BHATWA, A., WANG, W., HASSAN, Y. I., ABRAHAM, N., LI, X.-Z. & ZHOU, T. 2021. Challenges associated with the formation of recombinant protein inclusion bodies in *Escherichia coli* and strategies to address them for industrial applications. *Frontiers in Bioengineering and Biotechnology,* 9**,** 630551.

BLOCK, M. & BLANCHARD, D. L. 2022. Aminoglycosides. *StatPearls [Internet].* StatPearls Publishing.

BÖTTCHER, T. & SIEBER, S. A. 2008. β-lactones as specific inhibitors of ClpP attenuate the production of extracellular virulence factors of *Staphylococcus aureus*. *Journal of the American Chemical Society,* 130**,** 14400-14401.

BOUASSIDA, K., JAIDANE, M., BOUALLEGUE, O., TLILI, G., NAIJA, H. & MOSBAH, A. T. 2016. Nosocomial urinary tract infections caused by extended-spectrum beta lactamase uro pathogens: prevalence, pathogens, risk factors, and strategies for infection control. *Canadian Urological Association Journal,* 10**,** E87.

BRIAND, L., MARCION, G., KRIZNIK, A., HEYDEL, J.-M., ARTUR, Y., GARRIDO, C., SEIGNEURIC, R. & NEIERS, F. 2016. A self-inducible heterologous protein expression system in *Escherichia coli*. *Scientific reports,* 6**,** 33037.

BROBERG, C. A., WU, W., CAVALCOLI, J. D., MILLER, V. L. & BACHMAN, M. A. 2014. Complete genome sequence of *Klebsiella pneumoniae* strain ATCC 43816 KPPR1, a rifampin-resistant mutant commonly used in animal, genetic, and molecular biology studies. *Genome announcements,* 2**,** e00924-14.

BUKAU, B., WEISSMAN, J. & HORWICH, A. 2006. Molecular chaperones and protein quality control. *Cell,* 125**,** 443-451.

BULATI, M., BUSÀ, R., CARCIONE, C., IANNOLO, G., DI MENTO, G., CUSCINO, N., DI GESÙ, R., PICCIONELLO, A. P., BUSCEMI, S. & CARRECA, A. P. 2021. *Klebsiella pneumoniae* lipopolysaccharides serotype O2afg induce poor inflammatory immune responses ex vivo. *Microorganisms,* 9**,** 1317.

BUSH, K. & BRADFORD, P. A. 2019. Interplay between β-lactamases and new β-lactamase inhibitors. *Nature Reviews Microbiology,* 17**,** 295-306.

BUSH, N. G., DIEZ-SANTOS, I., ABBOTT, L. R. & MAXWELL, A. 2020. Quinolones: mechanism, lethality and their contributions to antibiotic resistance. *Molecules,* 25**,** 5662.

CAMPOS-MADUENO, E. I., MOSER, A. I., JOST, G., MAFFIOLI, C., BODMER, T., PERRETEN, V. & ENDIMIANI, A. 2022. Carbapenemase-producing *Klebsiella pneumoniae* strains in Switzerland: human and non-human settings may share high risk clones. *Journal of global antimicrobial resistance,* 28**,** 206-215.

CAMPOS-MADUENO, E. I., SIGRIST, T., FLÜCKIGER, U. M., RISCH, L., BODMER, T. & ENDIMIANI, A. 2021. First report of a blaVIM-1 metallo-β-lactamase-possessing *Klebsiella michiganensis*. *Journal of global antimicrobial resistance,* 25**,** 310-314.

CAMPOS, M. A., VARGAS, M. A., REGUEIRO, V., LLOMPART, C. M., ALBERTÍ, S. & BENGOECHEA, J. A. 2004. Capsule polysaccharide mediates bacterial resistance to antimicrobial peptides. *Infection and immunity,* 72**,** 7107-7114.

CAPRANICO, G., MARINELLO, J. & CHILLEMI, G. 2017. Type i DNA topoisomerases. *Journal of medicinal chemistry,* 60**,** 2169-2192.

CARTER, T. D. & OUTTEN, F. W. 2021. Ni-NTA Affinity Chromatography to Characterize Protein–Protein Interactions During Fe-S Cluster Biogenesis. *Fe-S Proteins: Methods and Protocols.* Springer.

CASSINI, A., HÖGBERG, L. D., PLACHOURAS, D., QUATTROCCHI, A., HOXHA, A., SIMONSEN, G. S., COLOMB-COTINAT, M., KRETZSCHMAR, M. E., DEVLEESSCHAUWER, B. & CECCHINI, M. 2019. Attributable deaths and disability adjusted life-years caused by infections with antibiotic-resistant bacteria in the EU and the European Economic Area in 2015: a population-level modelling analysis. *The Lancet infectious diseases,* 19**,** 56-66.

CHAI, H., ALLEN, W. E. & HICKS, R. P. 2014. Synthetic antimicrobial peptides exhibit two different binding mechanisms to the lipopolysaccharides isolated from *Pseudomonas aeruginosa* and *Klebsiella pneumoniae*. *International Journal of Medicinal Chemistry,* 2014.

CHAKRADHAR, S. 2017. Breaking through. *Nature Medicine,* 23**,** 907.

CHANUMOLU, S. K., ROUT, C. & CHAUHAN, R. S. 2012. UniDrug-target: a computational tool to identify unique drug targets in pathogenic bacteria. *PloS one,* 7**,** e32833.

CHASTANET, A., PRUDHOMME, M., CLAVERYS, J.-P. & MSADEK, T. 2001. Regulation of *Streptococcus pneumoniae* clp genes and their role in competence development and stress survival. J Bacteriol. 183(24):7295-307.

CHE, Y., XU, X., YANG, Y., BŘINDA, K., HANAGE, W., YANG, C. & ZHANG, T. 2022. High resolution genomic surveillance elucidates a multilayered hierarchical transfer of resistance between WWTP-and human/animal-associated bacteria. *Microbiome,* 10**,** 1-16.

CHEN, D., FREZZA, M., SCHMITT, S., KANWAR, J. & P DOU, Q. 2011. Bortezomib as the first proteasome inhibitor anticancer drug: current status and future perspectives. *Current cancer drug targets,* 11**,** 239-253.

CHENG, F., LI, Z., LAN, S., LIU, W., LI, X., ZHOU, Z., SONG, Z., WU, J., ZHANG, M. & SHAN, W. 2018. Characterization of *Klebsiella pneumoniae* associated with cattle infections in southwest China using multi-locus sequence typing (MLST), antibiotic resistance and virulence-associated gene profile analysis. *brazilian journal of microbiology,* 49**,** 93-100.

CHINEMEREM NWOBODO, D., UGWU, M. C., OLISELOKE ANIE, C., AL-OUQAILI, M. T., CHINEDU IKEM, J., VICTOR CHIGOZIE, U. & SAKI, M. 2022. Antibiotic resistance: The challenges and some emerging strategies for tackling a global menace. *Journal of Clinical Laboratory Analysis,* 36**,** e24655.

CHOBY, J., HOWARD-ANDERSON, J. & WEISS, D. 2020. Hypervirulent *Klebsiella pneumoniae*–clinical and molecular perspectives. *Journal of internal medicine,* 287**,** 283-300.

CHOI, K. Y., SWIERCZEWSKA, M., LEE, S. & CHEN, X. 2012. Protease-activated drug development. *Theranostics,* 2**,** 156.

CHUDEJOVA, K., KRAFTOVA, L., MATTIONI MARCHETTI, V., HRABAK, J., PAPAGIANNITSIS, C. C. & BITAR, I. 2021. Genetic plurality of OXA/NDM-encoding features characterized from *Enterobacterales* recovered from Czech hospitals. *Frontiers in microbiology,* 12**,** 641415.

CLEMENTS, A., TULL, D., JENNEY, A. W., FARN, J. L., KIM, S.-H., BISHOP, R. E., MCPHEE, J. B., HANCOCK, R. E., HARTLAND, E. L. & PEARSE, M. J. 2007. Secondary acylation of *Klebsiella pneumoniae* lipopolysaccharide contributes to sensitivity to antibacterial peptides. *Journal of Biological Chemistry,* 282**,** 1556915577.

COMPTON, C. L., SCHMITZ, K. R., SAUER, R. T. & SELLO, J. K. 2013. Antibacterial activity of and resistance to small molecule inhibitors of the ClpP peptidase. *ACS chemical biology,* 8**,** 2669-2677.

CONLAN, S., PARK, M., DEMING, C., THOMAS, P. J., YOUNG, A. C., COLEMAN, H., SISON, C., PROGRAM, N. C. S., WEINGARTEN, R. A. & LAU, A. F. 2016. Plasmid dynamics in KPC-positive *Klebsiella pneumoniae* during long-term patient colonization. *MBio,* 7**,** e00742-16.

CONLAN, S., THOMAS, P., DEMING, C., PARK, M., LAU, A., DEKKER, J., SNITKIN, E., CLARK, T., LUONG, K. & SONG, Y. 2014. Program NCS, Mullikin JC, Korlach J, Henderson DK, Frank KM, Palmore TN, Segre JA. 2014. *Single-molecule sequencing to track plasmid diversity of hospital-associated carbapenemase producing Enterobacteriaceae. Sci Transl Med,* 6**,** 254.

CRAMARIUC, O., ROG, T., JAVANAINEN, M., MONTICELLI, L., POLISHCHUK, A. V. & VATTULAINEN, I. 2012. Mechanism for translocation of fluoroquinolones across lipid membranes. *Biochimica et Biophysica Acta (BBA)-Biomembranes,* 1818**,** 2563-2571.

CULP, E. & WRIGHT, G. D. 2017. Bacterial proteases, untapped antimicrobial drug targets. *The Journal of antibiotics,* 70**,** 366-377.

DARBY, E. M., TRAMPARI, E., SIASAT, P., GAYA, M. S., ALAV, I., WEBBER, M. A. & BLAIR, J. M. 2022. Molecular mechanisms of antibiotic resistance revisited. *Nature Reviews Microbiology***,** 1-16.

DE JESUS, M. B., EHLERS, M. M., DOS SANTOS, R. F. & KOCK, M. M. 2015. Understanding β-lactamase producing *Klebsiella pneumoniae*. *InTechOpen: Rijeka, Croatia***,** 51-83.

DE KRAKER, M. E., STEWARDSON, A. J. & HARBARTH, S. 2016. Will 10 million people die a year due to antimicrobial resistance by 2050? *PLoS medicine,* 13**,** e1002184.

DE MARCO, A., FERRER-MIRALLES, N., GARCIA-FRUITÓS, E., MITRAKI, A., PETERNEL, S., RINAS, U., TRUJILLO-ROLDÁN, M. A., VALDEZ-CRUZ, N. A., VÁZQUEZ, E. & VILLAVERDE, A. 2019. Bacterial inclusion bodies are industrially exploitable amyloids. *FEMS microbiology reviews,* 43**,** 53-72.

DEHNAMAKI, M., GHANE, M. & BABAEEKHOU, L. 2020. Detection of OqxAB and QepA efflux pumps and their association with antibiotic resistance in *Klebsiella pneumoniae* isolated from urinary tract infection. *International Journal of Infection,* 7.

DÍAZ-SÁEZ, L., PANKOV, G. & HUNTER, W. N. 2017. Open and compressed conformations of *Francisella tularensis* ClpP. *Proteins: Structure, Function, and Bioinformatics,* 85**,** 188-194.

DIENE, S. M., MERHEJ, V., HENRY, M., EL FILALI, A., ROUX, V., ROBERT, C., AZZA, S., GAVORY, F., BARBE, V. & LA SCOLA, B. 2013. The rhizome of the multidrugresistant *Enterobacter aerogenes* genome reveals how new “killer bugs” are created because of a sympatric lifestyle. *Molecular biology and evolution,* 30**,** 369-383.

DOI, Y., HAZEN, T. H., BOITANO, M., TSAI, Y.-C., CLARK, T. A., KORLACH, J. & RASKO, D. A. 2014. Whole-genome assembly of *Klebsiella pneumoniae* coproducing NDM-1 and OXA-232 carbapenemases using single-molecule, real-time sequencing. *Antimicrobial agents and chemotherapy,* 58**,** 5947-5953.

DOORDUIJN, D. J., ROOIJAKKERS, S. H., VAN SCHAIK, W. & BARDOEL, B. W. 2016. Complement resistance mechanisms of *Klebsiella pneumoniae*. *Immunobiology,* 221**,** 1102-1109.

DOWLING, A. J., HILL, G. E. & BONNEAUD, C. 2020. Multiple differences in pathogen-host cell interactions following a bacterial host shift. *Scientific Reports,* 10**,** 1-12.

DOYLE, S. M., GENEST, O. & WICKNER, S. 2013. Protein rescue from aggregates by powerful molecular chaperone machines. *Nature reviews Molecular cell biology,* 14**,** 617-629.

EFFAH, C. Y., SUN, T., LIU, S. & WU, Y. 2020. *Klebsiella pneumoniae*: an increasing threat to public health. *Annals of clinical microbiology and antimicrobials,* 19**,** 1-9.

EIAMPHUNGPORN, W., SCHADUANGRAT, N., MALIK, A. A. & NANTASENAMAT, C. 2018. Tackling the antibiotic resistance caused by class A β-lactamases through the use of β-lactamase inhibitory protein. *International Journal of Molecular Sciences,* 19**,** 2222.

ELLIOTT, A. G., GANESAMOORTHY, D., COIN, L., COOPER, M. A. & CAO, M. D. 2016. Complete genome sequence of *Klebsiella quasipneumoniae* subsp. *Similipneumoniae* strain ATCC 700603. *Genome announcements,* 4**,** e00438-16.

FARRAND, A. J., RENIERE, M. L., INGMER, H., FREES, D. & SKAAR, E. P. 2013. Regulation of host hemoglobin binding by the *Staphylococcus aureus* Clp proteolytic system. *Journal of bacteriology,* 195**,** 5041-5050.

FELIX, J., WEINHÄUPL, K., CHIPOT, C., DEHEZ, F., HESSEL, A., GAUTO, D. F., MORLOT, C., ABIAN, O., GUTSCHE, I. & VELAZQUEZ-CAMPOY, A. 2019. Mechanism of the allosteric activation of the ClpP protease machinery by substrates and active-site inhibitors. *Science advances,* 5**,** eaaw3818.

FENG, Y., WEI, L., ZHU, S., QIAO, F., ZHANG, X., KANG, Y., CAI, L., KANG, M., MCNALLY, A. & ZONG, Z. 2020. Handwashing sinks as the source of transmission of ST16 carbapenem-resistant *Klebsiella pneumoniae*, an international high-risk clone, in an intensive care unit. *Journal of Hospital Infection,* 104**,** 492-496.

FERNÁNDEZ, L., BREIDENSTEIN, E. B., SONG, D. & HANCOCK, R. E. 2012. Role of intracellular proteases in the antibiotic resistance, motility, and biofilm formation of *Pseudomonas aeruginosa*. *Antimicrobial agents and chemotherapy,* 56**,** 1128-1132.

FINLAY, B. B. & MCFADDEN, G. 2006. Anti-immunology: evasion of the host immune system by bacterial and viral pathogens. *Cell,* 124**,** 767-782.

FORTERRE, P. & GADELLE, D. 2009. Phylogenomics of DNA topoisomerases: their origin and putative roles in the emergence of modern organisms. *Nucleic Acids Research,* 37**,** 679-692.

FREES, D., GERTH, U. & INGMER, H. 2014. Clp chaperones and proteases are central in stress survival, virulence and antibiotic resistance of *Staphylococcus aureus*. *International Journal of Medical Microbiology,* 304**,** 142-149.

FREES, D., QAZI, S. N., HILL, P. J. & INGMER, H. 2003. Alternative roles of ClpX and ClpP in *Staphylococcus aureus* stress tolerance and virulence. *Molecular microbiology,* 48**,** 1565-1578.

GAO, H., LIU, Y., WANG, R., WANG, Q., JIN, L. & WANG, H. 2020. The transferability and evolution of NDM-1 and KPC-2 co-producing *Klebsiella pneumoniae* from clinical settings. *EBioMedicine,* 51**,** 102599.

GNIADKOWSKI, M. 2001. Evolution and epidemiology of extended-spectrum β-lactamases (ESBLs) and ESBL-producing microorganisms. *Clinical Microbiology and Infection,* 7**,** 597-608.

GONZALEZ-FERRER, S., PEÑALOZA, H. F., BUDNICK, J. A., BAIN, W. G., NORDSTROM, H. R., LEE, J. S. & VAN TYNE, D. 2021. Finding Order in the Chaos: Outstanding questions in *Klebsiella pneumoniae* pathogenesis. *Infection and Immunity,* 89**,** e00693-20.

GUERINA, N., KESSLER, T. W., GUERINA, V., NEUTRA, M., CLEGG, H., LANGERMANN, S., SCANNAPIECO, F. & GOLDMANN, D. 1983. The role of pili and capsule in the pathogenesis of neonatal infection with *Escherichia coli* Kl. *Journal of Infectious Diseases,* 148**,** 395-405.

GUNNING, P. W. 2001. Protein isoforms and isozymes. *e LS*. GUR, E. & SAUER, R. T. 2008. Recognition of misfolded proteins by Lon, a AAA+ protease. *Genes & development,* 22**,** 2267-2277.

GURLEY, E. S., ZAMAN, R. U., SULTANA, R., BELL, M., FRY, A. M., SRINIVASAN, A., RAHMAN, M., RAHMAN, M. W., HOSSAIN, M. J. & LUBY, S. P. 2010. Rates of hospital-acquired respiratory illness in Bangladeshi tertiary care hospitals: results from a low-cost pilot surveillance strategy. *Clinical infectious diseases,* 50**,** 10841090.

HACKL, M. W., LAKEMEYER, M., DAHMEN, M., GLASER, M., PAHL, A., LORENZ-BAATH, K., MENZEL, T., SIEVERS, S., BÖTTCHER, T. & ANTES, I. 2015. Phenyl esters are potent inhibitors of caseinolytic protease P and reveal a stereogenic switch for deoligomerization. *Journal of the American Chemical Society,* 137**,** 8475-8483.

HALL, B. G. 2013. Building phylogenetic trees from molecular data with MEGA. *Molecular biology and evolution,* 30**,** 1229-1235.

HAYASHI, K. & KOJIMA, C. 2008. pCold-GST vector: a novel cold-shock vector containing GST tag for soluble protein production. *Protein expression and purification,* 62**,** 120127.

HELGESEN, E., SÆTRE, F. & SKARSTAD, K. 2021. Topoisomerase IV tracks behind the replication fork and the SeqA complex during DNA replication in *Escherichia coli*. *Scientific Reports,* 11**,** 474.

HIRVONEN, V. H., HAMMOND, K., CHUDYK, E. I., LIMB, M. A., SPENCER, J., MULHOLLAND, A. J. & VAN DER KAMP, M. W. 2019. An efficient computational assay for β-lactam antibiotic breakdown by class a β-lactamases. *Journal of chemical information and modelling,* 59**,** 3365-3369.

HOLDEN, V. I. & BACHMAN, M. A. 2015. Diverging roles of bacterial siderophores during infection. *Metallomics,* 7**,** 986-995.

HOLDEN, V. I., BREEN, P., HOULE, S., DOZOIS, C. M. & BACHMAN, M. A. 2016. *Klebsiella pneumoniae* siderophores induce inflammation, bacterial dissemination, and HIF-1α stabilization during pneumonia. *MBio,* 7**,** e01397-16.

HOLLINGSWORTH, S. A. & DROR, R. O. 2018. Molecular dynamics simulation for all. *Neuron,* 99**,** 1129-1143.

HOSKINS, J. R. & WICKNER, S. 2006. Two peptide sequences can function cooperatively to facilitate binding and unfolding by ClpA and degradation by ClpAP. *Proceedings of the National Academy of Sciences,* 103**,** 909-914.

HSIEH, P.-F., LIN, T.-L., YANG, F.-L., WU, M.-C., PAN, Y.-J., WU, S.-H. & WANG, J.-T. 2012. Lipopolysaccharide O1 antigen contributes to the virulence in *Klebsiella pneumoniae* causing pyogenic liver abscess. *PloS one,* 7**,** e33155.

HU, Y., WEI, L., FENG, Y., XIE, Y. & ZONG, Z. 2018. *Klebsiella huaxiensis* sp. nov., recovered from human urine. *bioRxiv***,** 335075.

HUANG, L., WU, C., GAO, H., XU, C., DAI, M., HUANG, L., HAO, H., WANG, X. & CHENG, G. 2022. Bacterial multidrug efflux pumps at the frontline of antimicrobial resistance: An overview. *Antibiotics,* 11**,** 520.

HUANG, T.-W., WANG, J.-T., LAUDERDALE, T.-L., LIAO, T.-L., LAI, J.-F., TAN, M.-C., LIN, A.-C., CHEN, Y.-T., TSAI, S.-F. & CHANG, S.-C. 2013. Complete sequences of two plasmids in a bla NDM-1-positive *Klebsiella oxytoca* isolate from Taiwan. *Antimicrobial agents and chemotherapy,* 57**,** 4072-4076.

HUDSON, C. M., BENT, Z. W., MEAGHER, R. J. & WILLIAMS, K. P. 2014. Resistance determinants and mobile genetic elements of an NDM-1-encoding *Klebsiella pneumoniae* strain. *PloS one,* 9**,** e99209.

HUEMER, M., MAIRPADY SHAMBAT, S., BRUGGER, S. D. & ZINKERNAGEL, A. S. 2020. Antibiotic resistance and persistence—Implications for human health and treatment perspectives. *EMBO reports,* 21**,** e51034.

HWANG, B. J., PARK, W. J., CHUNG, C. H. & GOLDBERG, A. L. 1987. *Escherichia coli* contains a soluble ATP-dependent protease (Ti) distinct from protease La. *Proceedings of the National Academy of Sciences,* 84**,** 5550-5554.

ILLIGMANN, A., THOMA, Y., PAN, S., REINHARDT, L. & BRÖTZ-OESTERHELT, H. 2021. Contribution of the Clp protease to bacterial survival and mitochondrial homoeostasis. *Microbial Physiology,* 31**,** 260-279.

ITO, R., SHINDO, Y., KOBAYASHI, D., ANDO, M., JIN, W., WACHINO, J.-I., YAMADA, K., KIMURA, K., YAGI, T. & HASEGAWA, Y. 2015. Molecular epidemiological characteristics of *Klebsiella pneumoniae* associated with bacteremia among patients with pneumonia. *Journal of clinical microbiology,* 53**,** 879-886.

JACOBY, G. A. 2005. Mechanisms of resistance to quinolones. *Clinical infectious diseases,* 41**,** S120-S126.

JI, Y.-Y. & LI, Y.-Q. 2010. The role of secondary structure in protein structure selection. *The European Physical Journal E,* 32**,** 103-107.

JIANG, W., YANG, W., ZHAO, X., WANG, N. & REN, H. 2020. *Klebsiella pneumoniae* presents antimicrobial drug resistance for β-lactam through the ESBL/PBP signaling pathway. *Experimental and therapeutic medicine,* 19**,** 2449-2456.

KAHNE, S. C. & DARWIN, K. H. 2021. Structural determinants of regulated proteolysis in pathogenic bacteria by ClpP and the proteasome. *Current Opinion in Structural Biology,* 67**,** 120-126.

KAPOOR, G., SAIGAL, S. & ELONGAVAN, A. 2017. Action and resistance mechanisms of antibiotics: A guide for clinicians. *Journal of anaesthesiology, clinical pharmacology,* 33**,** 300.

KAREEM, S. M., AL-KADMY, I. M., KAZAAL, S. S., MOHAMMED ALI, A. N., AZIZ, S. N., MAKHARITA, R. R., ALGAMMAL, A. M., AL-REJAIE, S., BEHL, T. & BATIHA, G. E.S. 2021. Detection of gyrA and parC mutations and prevalence of plasmid-mediated quinolone resistance genes in Klebsiella pneumoniae. *Infection and Drug Resistance***,** 555-563.

KATAYAMA-FUJIMURA, Y., GOTTESMAN, S. & MAURIZI, M. 1987. A multiple-component, ATP-dependent protease from *Escherichia coli*. *Journal of Biological Chemistry,* 262**,** 4477-4485.

KHAN, A. R. & JAMES, M. N. 1998. Molecular mechanisms for the conversion of zymogens to active proteolytic enzymes. *Protein Science,* 7**,** 815-836.

KHANNA, N. R. & GERRIETS, V. 2021. Beta lactamase inhibitors. *StatPearls [Internet].* StatPearls Publishing.

KHODAPARAST, L., WU, G., KHODAPARAST, L., SCHMIDT, B. Z., ROUSSEAU, F. & SCHYMKOWITZ, J. 2021a. Bacterial Protein Homeostasis Disruption as a Therapeutic Intervention. *Frontiers in Molecular Biosciences,* 8**,** 434.

KHODAPARAST, L., WU, G., KHODAPARAST, L., SCHMIDT, B. Z., ROUSSEAU, F. & SCHYMKOWITZ, J. 2021b. Bacterial protein homeostasis disruption as a therapeutic intervention. *Frontiers in Molecular Biosciences,* 8**,** 681855.

KIM, H. B., WANG, M., PARK, C. H., KIM, E.-C., JACOBY, G. A. & HOOPER, D. C. 2009. oqxAB encoding a multidrug efflux pump in human clinical isolates of *Enterobacteriaceae*. *Antimicrobial agents and chemotherapy,* 53**,** 3582-3584.

KIMBER, M. S., YU, A. Y. H., BORG, M., LEUNG, E., CHAN, H. S. & HOURY, W. A. 2010. Structural and theoretical studies indicate that the cylindrical protease ClpP samples extended and compact conformations. *Structure,* 18**,** 798-808.

KLENOTIC, P. A., MOSENG, M. A., MORGAN, C. E. & YU, E. W. 2020. Structural and functional diversity of resistance–nodulation–cell division transporters. *Chemical Reviews,* 121**,** 5378-5416.

KÖPPL, C., LINGG, N., FISCHER, A., KRÖß, C., LOIBL, J., BUCHINGER, W., SCHNEIDER, R., JUNGBAUER, A., STRIEDNER, G. & CSERJAN-PUSCHMANN, M. 2022. Fusion tag design influences soluble recombinant protein production in *Escherichia coli*. *International Journal of Molecular Sciences,* 23**,** 7678.

KOSOVÁ, K., VÍTÁMVÁS, P., PRÁŠIL, I. T., KLÍMA, M. & RENAUT, J. 2021. Plant proteoforms under environmental stress: Functional proteins arising from a single gene. *Frontiers in Plant Science***,** 2887.

KRAUSE, K. M., SERIO, A. W., KANE, T. R. & CONNOLLY, L. E. 2016. Aminoglycosides: an overview. *Cold Spring Harbor perspectives in medicine,* 6**,** a027029.

KUEHN, B. M. 2013. “Nightmare” bacteria on the rise in US hospitals, long-term care facilities. *Jama,* 309**,** 1573-1574.

KWON, T., YANG, J. W., LEE, S., YUN, M.-R., YOO, W. G., KIM, H. S., CHA, J.-O. & KIM, D.-W. 2016. Complete genome sequence of *Klebsiella pneumoniae* subsp. *pneumoniae* KP617, coproducing OXA-232 and NDM-1 carbapenemases, isolated in South Korea. *Genome Announcements,* 4**,** e01550-15.

KYTE, J. & DOOLITTLE, R. F. 1982. A simple method for displaying the hydropathic character of a protein. *Journal of molecular biology,* 157**,** 105-132.

LABBY, K. J. & GARNEAU-TSODIKOVA, S. 2013. Strategies to overcome the action of aminoglycoside-modifying enzymes for treating resistant bacterial infections. *Future medicinal chemistry,* 5**,** 1285-1309.

LAI, C.-C., LIN, T.-L., TSENG, S.-P., HUANG, Y.-T., WANG, J.-T., CHANG, S.-C., TENG, L.-J. & HSUEH, P.-R. 2011. Pelvic abscess caused by New Delhi metallo-βlactamase-1-producing *Klebsiella oxytoca* in Taiwan in a patient who underwent renal transplantation in China. *Diagnostic microbiology and infectious disease,* 71**,** 474475.

LANTZ, M. 1997. Are bacterial proteases important virulence factors? *Journal of periodontal research,* 32**,** 126-132.

LARSEN, M. R., TRELLE, M. B., THINGHOLM, T. E. & JENSEN, O. N. 2006. Analysis of posttranslational modifications of proteins by tandem mass spectrometry: Mass Spectrometry For Proteomics Analysis. *Biotechniques,* 40**,** 790-798.

LAWLOR, M. S., HSU, J., RICK, P. D. & MILLER, V. L. 2005. Identification of *Klebsiella pneumoniae* virulence determinants using an intranasal infection model. *Molecular microbiology,* 58**,** 1054-1073.

LAWS, M., SHAABAN, A. & RAHMAN, K. M. 2019. Antibiotic resistance breakers: current approaches and future directions. *FEMS Microbiology Reviews,* 43**,** 490-516.

LEE, C.-R., LEE, J. H., PARK, K. S., JEON, J. H., KIM, Y. B., CHA, C.-J., JEONG, B. C. & LEE, S. H. 2017. Antimicrobial resistance of hypervirulent *Klebsiella pneumoniae*: epidemiology, hypervirulence-associated determinants, and resistance mechanisms. *Frontiers in cellular and infection microbiology,* 7**,** 483.

LEMOS, J. A. & BURNE, R. A. 2002. Regulation and physiological significance of ClpC and ClpP *in Streptococcus mutans*. *J Bacteriol*. 184(22):6357-66.

LI, B., ZHAO, Y., LIU, C., CHEN, Z. & ZHOU, D. 2014. Molecular pathogenesis of *Klebsiella pneumoniae*. *Future microbiology,* 9**,** 1071-1081.

LIAO, T.-L., LIN, A.-C., CHEN, E., HUANG, T.-W., LIU, Y.-M., CHANG, Y.-H., LAI, J.-F., LAUDERDALE, T.-L., WANG, J.-T. & CHANG, S.-C. 2012. Complete genome sequence of *Klebsiella oxytoca* E718, a New Delhi metallo-β-lactamase-1-producing nosocomial strain. Bacteriol. 194(19):5454.

LIN, A.-C., LIAO, T.-L., LIN, Y.-C., LAI, Y.-C., LU, M.-C. & CHEN, Y.-T. 2012. Complete genome sequence of *Klebsiella pneumoniae* 1084, a hypermucoviscosity-negative K1 clinical strain. Bacteriol. 194(22):6316.

LIN, Y.-C., LU, M.-C., TANG, H.-L., LIU, H.-C., CHEN, C.-H., LIU, K.-S., LIN, C., CHIOU, C.S., CHIANG, M.-K. & CHEN, C.-M. 2011. Assessment of hypermucoviscosity as a virulence factor for experimental *Klebsiella pneumoniae* infections: comparative virulence analysis with hypermucoviscosity-negative strain. *BMC microbiology,* 11**,** 18.

LIU, P.-P., LIU, Y., WANG, L.-H., WEI, D.-D. & WAN, L.-G. 2016. Draft genome sequence of an NDM-5-producing *Klebsiella pneumoniae* sequence type 14 strain of serotype K2. *Genome announcements,* 4**,** e01610-15.

MA, Y., WU, X., LI, S., TANG, L., CHEN, M. & AN, Q. 2021. Proposal for reunification of the genus Raoultella with the genus Klebsiella and reclassification of *Raoultella electrica* as *Klebsiella electrica* comb. nov. *Research in Microbiology,* 172**,** 103851.

MABANGLO, M. F. & HOURY, W. A. 2022. Recent structural insights into the mechanism of ClpP protease regulation by AAA+ chaperones and small molecules. *Journal of Biological Chemistry***,** 101781.

MABANGLO, M. F., LEUNG, E., VAHIDI, S., SERAPHIM, T. V., EGER, B. T., BRYSON, S., BHANDARI, V., ZHOU, J. L., MAO, Y.-Q. & RIZZOLO, K. 2019. ClpP protease activation results from the reorganization of the electrostatic interaction networks at the entrance pores. *Communications Biology,* 2**,** 410.

MAKI, G. & ZERVOS, M. 2021. Health care–acquired infections in low-and middle-income countries and the role of infection prevention and control. *Infectious Disease Clinics,* 35**,** 827-839.

MALIK, I. & BRÖTZ-OESTERHELT, H. 2017. Conformational control of the bacterial Clp protease by natural product antibiotics. *Natural product reports,* 34**,** 815-831.

MARTIN, R. M. & BACHMAN, M. A. 2018. Colonization, infection, and the accessory genome of *Klebsiella pneumoniae*. *Frontiers in cellular and infection microbiology,* 8**,** 4.

MASSIAH, M. A., WRIGHT, K. M. & DU, H. 2016. Obtaining soluble folded proteins from inclusion bodies using sarkosyl, triton X-100, and CHAPS: application to LB and M9 minimal media. *Current protocols in protein science,* 84**,** 6.13. 1-6.13. 24.

MATHERS, A. J., STOESSER, N., SHEPPARD, A. E., PANKHURST, L., GIESS, A., YEH, A. J., DIDELOT, X., TURNER, S. D., SEBRA, R. & KASARSKIS, A. 2015. *Klebsiella pneumoniae* carbapenemase (KPC)-producing *K. pneumoniae* at a single institution: insights into endemicity from whole-genome sequencing. *Antimicrobial agents and chemotherapy,* 59**,** 1656-1663.

MATSUURA, M. 2013. Structural modifications of bacterial lipopolysaccharide that facilitate gram-negative bacteria evasion of host innate immunity. *Frontiers in immunology,* 4**,** 109.

MAURIZI, M., CLARK, W. P., KIM, S.-H. & GOTTESMAN, S. 1990. Clp P represents a unique family of serine proteases. *Journal of Biological Chemistry,* 265**,** 1254612552.

MAURYA, N., JANGRA, M., TAMBAT, R. & NANDANWAR, H. 2019. Alliance of efflux pumps with β-lactamases in multidrug-resistant *Klebsiella pneumoniae* isolates. *Microbial Drug Resistance,* 25**,** 1155-1163.

MCCORMICK, A. M., JARMUSIK, N. A., ENDRIZZI, E. J. & LEIPZIG, N. D. 2014. Expression, isolation, and purification of soluble and insoluble biotinylated proteins for nerve tissue regeneration. *JoVE (Journal of Visualized Experiments)***,** e51295.

MÉSZÁROS, B., ERDŐS, G. & DOSZTÁNYI, Z. 2018. IUPred2A: context-dependent prediction of protein disorder as a function of redox state and protein binding. *Nucleic acids research,* 46**,** W329-W337.

MOHAMMADIAN, A., KAGHAZIAN, H., KAVIANPOUR, A. & JALALIRAD, R. 2018. Solubilization of inclusion body proteins using low and very low concentrations of chemicals: implications of novel combined chemical treatment designs in enhancement of post-solubilization target protein purity and biological activity. *Journal of Chemical Technology & Biotechnology,* 93**,** 1579-1587.

MORA-OCHOMOGO, M. & LOHANS, C. T. 2021. β-Lactam antibiotic targets and resistance mechanisms: from covalent inhibitors to substrates. *RSC Medicinal Chemistry,* 12**,** 1623-1639.

MOREIRA, W., SANTHANAKRISHNAN, S., DYMOCK, B. W. & DICK, T. 2017a. Bortezomib warhead-switch confers dual activity against mycobacterial caseinolytic protease and proteasome and selectivity against human proteasome. *Frontiers in Microbiology,* 8**,** 746.

MOREIRA, W., SANTHANAKRISHNAN, S., NGAN, G. J., LOW, C. B., SANGTHONGPITAG, K., POULSEN, A., DYMOCK, B. W. & DICK, T. 2017b. Towards selective mycobacterial ClpP1P2 inhibitors with reduced activity against the human proteasome. *Antimicrobial agents and chemotherapy,* 61**,** e02307-16.

MORENO-CINOS, C., GOOSSENS, K., SALADO, I. G., VAN DER VEKEN, P., DE WINTER, H. & AUGUSTYNS, K. 2019. ClpP protease, a promising antimicrobial target. *International journal of molecular sciences,* 20**,** 2232.

MOYA, C. & MAICAS, S. 2020. Antimicrobial resistance in *Klebsiella pneumoniae* strains: mechanisms and outbreaks. *Proceedings*, 66, 11.

MULANI, M. S., KAMBLE, E. E., KUMKAR, S. N., TAWRE, M. S. & PARDESI, K. R. 2019. Emerging strategies to combat ESKAPE pathogens in the era of antimicrobial resistance: a review. *Frontiers in microbiology,* 10**,** 539.

MÜLLER, A. L., HRYSHKO, L. V. & DHALLA, N. S. 2013. Extracellular and intracellular proteases in cardiac dysfunction due to ischemia–reperfusion injury. *International journal of cardiology,* 164**,** 39-47.

MUNITA, J. M. & ARIAS, C. A. 2016. Mechanisms of antibiotic resistance. *Virulence mechanisms of bacterial pathogens***,** 481-511.

MURPHY, C. N., MORTENSEN, M. S., KROGFELT, K. A. & CLEGG, S. 2013. Role of *Klebsiella pneumoniae* type 1 and type 3 fimbriae in colonizing silicone tubes implanted into the bladders of mice as a model of catheter-associated urinary tract infections. *Infection and immunity,* 81**,** 3009-3017.

NAMIKAWA, H., NIKI, M., NIKI, M., OINUMA, K.-I., YAMADA, K., NAKAIE, K., TSUBOUCHI, T., TOCHINO, Y., TAKEMOTO, Y. & KANEKO, Y. 2022. Siderophore production as a biomarker for *Klebsiella pneumoniae* strains that cause sepsis: A pilot study. *Journal of the Formosan Medical Association,* 121**,** 848-855.

NAMIKAWA, H., YAMADA, K., SAKIYAMA, A., IMOTO, W., YAMAIRI, K., SHIBATA, W., YOSHII, N., NIKI, M., NAKAIE, K. & OINUMA, K.-I. 2019. Clinical characteristics of bacteremia caused by hyper mucoviscous *Klebsiella pneumoniae* at a tertiary hospital. *Diagnostic Microbiology and Infectious Disease,* 95**,** 84-88.

NASIRI, G., PEYMANI, A., FARIVAR, T. N. & HOSSEINI, P. 2018. Molecular epidemiology of aminoglycoside resistance in clinical isolates of *Klebsiella pneumoniae* collected from Qazvin and Tehran provinces, Iran. *Infection, Genetics and Evolution,* 64**,** 219224.

NAUTA, K. M., HO, T. D. & ELLERMEIER, C. D. 2021. The penicillin-binding protein PbpP is a sensor of β-lactams and is required for activation of the extracytoplasmic function σ factor σP in *Bacillus thuringiensis*. *Mbio,* 12**,** e00179-21.

NAVON-VENEZIA, S., KONDRATYEVA, K. & CARATTOLI, A. 2017. Klebsiella pneumoniae: a major worldwide source and shuttle for antibiotic resistance. *FEMS microbiology reviews,* 41**,** 252-275.

NEILANDS, J. 1995. Siderophores: structure and function of microbial iron transport compounds. *Journal of Biological Chemistry,* 270**,** 26723-26726.

NEITZEL, J. J. 2010. Enzyme catalysis: the serine proteases. *Nature Education,* 3**,** 21.

NEURATH, H. 1986. The versatility of proteolytic enzymes. *Journal of cellular biochemistry,* 32**,** 35-49.

NOURI, K., FENG, Y. & SCHIMMER, A. D. 2020. Mitochondrial ClpP serine protease biological function and emerging target for cancer therapy. *Cell death & disease,* 11**,** 841.

OCHOŃSKA, D., ŚCIBIK, Ł. & BRZYCHCZY-WŁOCH, M. 2021. Biofilm formation of clinical *Klebsiella pneumoniae* strains isolated from tracheostomy tubes and their association with antimicrobial resistance, virulence and genetic diversity. *Pathogens,* 10**,** 1345.

OELSCHLAEGER, P. 2021. β-Lactamases: Sequence, structure, function, and inhibition. *Biomolecules*. 11(7):986.

OLIVEIRA, R., CASTRO, J., SILVA, S., OLIVEIRA, H., SAAVEDRA, M. J., AZEVEDO, N. F. & ALMEIDA, C. 2022. Exploring the antibiotic resistance profile of clinical *Klebsiella pneumoniae* isolates in Portugal. *Antibiotics,* 11**,** 1613.

OPOKU-TEMENG, C., KOBAYASHI, S. D. & DELEO, F. R. 2019. *Klebsiella pneumoniae* capsule polysaccharide as a target for therapeutics and vaccines. *Computational and structural biotechnology journal,* 17**,** 1360-1366.

ÖZBEK, R., WIELSCH, N., VOGEL, H., LOCHNIT, G., FOERSTER, F., VILCINSKAS, A. & VON REUMONT, B. M. 2019. Proteo-transcriptomic characterization of the venom from the *endoparasitoid* wasp *Pimpla turionellae* with aspects on its biology and evolution. *Toxins,* 11**,** 721.

PACZOSA, M. K. & MECSAS, J. 2016. *Klebsiella pneumoniae*: going on the offense with a strong defense. *Microbiology and Molecular Biology Reviews,* 80**,** 629-661.

PAKZAD, I., KARIN, M. Z., TAHERIKALANI, M., BOUSTANSHENAS, M. & LARI, A. R. 2013. Contribution of AcrAB efflux pump to ciprofloxacin resistance *in Klebsiella pneumoniae* isolated from burn patients. *GMS hygiene and infection control,* 8.

PANJAITAN, N. S. D., HORNG, Y.-T., CHIEN, C.-C., YANG, H.-C., YOU, R.-I. & SOO, P.-C. 2021. The PTS components in *Klebsiella pneumoniae* affect bacterial capsular polysaccharide production and macrophage phagocytosis resistance. *Microorganisms,* 9**,** 335.

PAPASTRATIS, I. 2022. Intrinsically disordered protein prediction for genomes and metagenomes. Msc dissertation. Aristotle University of Thessaloniki. https://ikee.lib.auth.gr/record/337693/files/GRI-2022-33999.pdf

PARK, C.-Y., KIM, E.-H., CHOI, S.-Y., TRAN, T. D.-H., KIM, I.-H., KIM, S.-N., PYO, S. & RHEE, D.-K. 2010. Virulence attenuation of *Streptococcus pneumoniae* clpP mutant by sensitivity to oxidative stress in macrophages via an NO-mediated pathway. *The Journal of Microbiology,* 48**,** 229-235.

PATERSON, D. L. 2006. Resistance in gram-negative bacteria: *Enterobacteriaceae*. *American journal of infection control,* 34**,** S20-S28.

PETERSSON, A. K. M. 2017. Comprehensive mutational analysis of the efflux regulator marR. MSc dissertation. Uppsala University, Disciplinary Domain of Medicine and Pharmacy, Faculty of Medicine, Department of Medical Biochemistry and Microbiology. http://www.diva-portal.org/smash/record.jsf?pid=diva2%3A1120013&dswid=-5427#

PHILIPPE, N., MAIGRE, L., SANTINI, S., PINET, E., CLAVERIE, J.-M., DAVIN-RÉGLI, A.V., PAGES, J.-M. & MASI, M. 2015. In vivo evolution of bacterial resistance in two cases of *Enterobacter aerogenes* infections during treatment with imipenem. *PLoS One,* 10**,** e0138828.

PITOUT, J. D., NORDMANN, P. & POIREL, L. 2015. Carbapenemase-producing *Klebsiella pneumoniae*, a key pathogen set for global nosocomial dominance. *Antimicrobial agents and chemotherapy,* 59**,** 5873-5884.

PITT, M. E., ELLIOTT, A. G., CAO, M. D., GANESAMOORTHY, D., KARAISKOS, I., GIAMARELLOU, H., ABBOUD, C. S., BLASKOVICH, M. A., COOPER, M. A. & COIN, L. J. 2018. Multifactorial chromosomal variants regulate polymyxin resistance in extensively drug-resistant *Klebsiella pneumoniae*. *Microbial genomics,* 4.

PIZARRO-CERDÁ, J. & COSSART, P. 2006. Bacterial adhesion and entry into host cells. *Cell,* 124**,** 715-727.

PODSCHUN, R., PIETSCH, S., HÖLLER, C. & ULLMANN, U. 2001. Incidence of *Klebsiella* species in surface waters and their expression of virulence factors. *Applied and environmental microbiology,* 67**,** 3325-3327.

PODSCHUN, R. & ULLMANN, U. 1998. Klebsiella spp. as nosocomial pathogens: epidemiology, taxonomy, typing methods, and pathogenicity factors. *Clinical microbiology reviews,* 11**,** 589-603.

POMAKOVA, D., HSIAO, C., BEANAN, J., OLSON, R., MACDONALD, U., KEYNAN, Y. & RUSSO, T. 2012. Clinical and phenotypic differences between classic and hypervirulent *Klebsiella pneumonia*: an emerging and under-recognized pathogenic variant. *European journal of clinical microbiology & infectious diseases,* 31**,** 981-989.

POWERS, J. C., ASGIAN, J. L., EKICI, Ö. D. & JAMES, K. E. 2002. Irreversible inhibitors of serine, cysteine, and threonine proteases. *Chemical reviews,* 102**,** 4639-4750.

PRADIER, L. & BEDHOMME, S. 2023. Ecology, more than antibiotics consumption, is the major predictor for the global distribution of aminoglycoside-modifying enzymes. *Elife,* 12**,** e77015.

PRESTINACI, F., PEZZOTTI, P. & PANTOSTI, A. 2015. Antimicrobial resistance: a global multifaceted phenomenon. *Pathogens and global health,* 109**,** 309-318.

PULZOVA, L., NAVRATILOVA, L. & COMOR, L. 2017. Alterations in outer membrane permeability favor drug-resistant phenotype of Klebsiella pneumoniae. *Microbial drug resistance,* 23**,** 413-420.

QING, G., MA, L.-C., KHORCHID, A., SWAPNA, G., MAL, T. K., TAKAYAMA, M. M., XIA, B., PHADTARE, S., KE, H. & ACTON, T. 2004. Cold-shock induced high-yield protein production in *Escherichia coli*. *Nature biotechnology,* 22**,** 877-882.

QUERALTÓ, C., ÁLVAREZ, R., ORTEGA, C., DÍAZ-YÁÑEZ, F., PAREDES-SABJA, D. & GIL, F. 2023. Role and Regulation of Clp Proteases: A Target against Gram-Positive Bacteria. *Bacteria,* 2**,** 21-36.

RAMOS, P. I. P., PICÃO, R. C., DE ALMEIDA, L. G. P., LIMA, N. C. B., GIRARDELLO, R., VIVAN, A. C. P., XAVIER, D. E., BARCELLOS, F. G., PELISSON, M. & VESPERO, E. C. 2014. Comparative analysis of the complete genome of KPC-2-producing *Klebsiella pneumoniae* Kp13 reveals remarkable genome plasticity and a wide repertoire of virulence and resistance mechanisms. *BMC genomics,* 15**,** 1-16.

RATHORE, S., SINHA, D., ASAD, M., BÖTTCHER, T., AFRIN, F., CHAUHAN, V. S., GUPTA, D., SIEBER, S. A. & MOHMMED, A. 2010. A cyanobacterial serine protease of *Plasmodium falciparum* is targeted to the apicoplast and plays an important role in its growth and development. *Molecular microbiology,* 77**,** 873-890.

RAWLINGS, N. D., BARRETT, A. J. & BATEMAN, A. 2011. Asparagine Peptide Lyases: A SEVENTH CATALYTIC TYPE OF PROTEOLYTIC ENZYMES. *Journal of Biological Chemistry,* 286**,** 38321-38328.

REDGRAVE, L. S., SUTTON, S. B., WEBBER, M. A. & PIDDOCK, L. J. 2014. Fluoroquinolone resistance: mechanisms, impact on bacteria, and role in evolutionary success. *Trends in microbiology,* 22**,** 438-445.

REECE, R. J. & MAXWELL, A. 1991. DNA gyrase: structure and function. *Critical reviews in biochemistry and molecular biology,* 26**,** 335-375.

RENDUELES, O. 2020. Deciphering the role of the capsule of *Klebsiella pneumoniae* during pathogenesis: A cautionary tale. *Molecular Microbiology,* 113**,** 883-888.

RIWU, K. H. P., EFFENDI, M. H., RANTAM, F. A., KHAIRULLAH, A. R. & WIDODO, A. 2022. A review: Virulence factors of *Klebsiella pneumonia* as emerging infection on the food chain. *Veterinary World,* 15.

RODRIGUEZ, E. L., PODDAR, S., IFTEKHAR, S., SUH, K., WOOLFORK, A. G., OVBUDE, S., PEKAREK, A., WALTERS, M., LOTT, S. & HAGE, D. S. 2020. Affinity chromatography: A review of trends and developments over the past 50 years. *Journal of Chromatography B,* 1157**,** 122332.

ROSANO, G. L. & CECCARELLI, E. A. 2014. Recombinant protein expression in *Escherichia coli*: advances and challenges. *Frontiers in microbiology,* 5**,** 172.

SABIROVA, J. S., XAVIER, B. B., COPPENS, J., ZARKOTOU, O., LAMMENS, C., JANSSENS, L., BURGGRAVE, R., WAGNER, T., GOOSSENS, H. & MALHOTRAKUMAR, S. 2016. Whole-genome typing and characterization of bla VIM19harbouring ST383 *Klebsiella pneumoniae* by PFGE, whole-genome mapping and WGS. *Journal of Antimicrobial Chemotherapy,* 71**,** 1501-1509.

SAKAMOTO, N., AKEDA, Y., SUGAWARA, Y., TAKEUCHI, D., MOTOOKA, D., YAMAMOTO, N., LAOLERD, W., SANTANIRAND, P. & HAMADA, S. 2018. Genomic characterization of carbapenemase-producing *Klebsiella pneumoniae* with chromosomally carried bla NDM-1. *Antimicrobial agents and chemotherapy,* 62**,** e01520-18.

SANTAJIT, S. & INDRAWATTANA, N. 2016. Mechanisms of antimicrobial resistance in ESKAPE pathogens. *BioMed research international,* 2016.

SASSETTI, E., DURANTE CRUZ, C., TAMMELA, P., WINTERHALTER, M., AUGUSTYNS, K., GRIBBON, P. & WINDSHÜGEL, B. 2019. Identification and characterization of approved drugs and drug-like compounds as covalent *Escherichia coli* ClpP inhibitors. *International journal of molecular sciences,* 20**,** 2686.

SATLIN, M. J., CHEN, L., PATEL, G., GOMEZ-SIMMONDS, A., WESTON, G., KIM, A. C., SEO, S. K., ROSENTHAL, M. E., SPERBER, S. J. & JENKINS, S. G. 2017. Multicenter clinical and molecular epidemiological analysis of bacteremia due to carbapenem-resistant *Enterobacteriaceae* (CRE) in the CRE epicenter of the United States. *Antimicrobial agents and chemotherapy,* 61**,** e02349-16.

SAXON, A., HASSNER, A., SWABB, E. A., WHEELER, B. & ADKINSON JR, N. F. 1984. Lack of cross-reactivity between aztreonam, a monobactam antibiotic, and penicillin in penicillin-allergic subjects. *Journal of Infectious Diseases,* 149**,** 16-22.

SCHAEFER, C. & ROST, B. Predict impact of single amino acid change upon protein structure. BMC genomics, 2012. BioMed Central, 1-10.

SCHLAGER, B., STRAESSLE, A. & HAFEN, E. 2012. Use of anionic denaturing detergents to purify insoluble proteins after overexpression. *BMC biotechnology,* 12**,** 1-7.

SCHRADER, S. M., VAUBOURGEIX, J. & NATHAN, C. 2020. Biology of antimicrobial resistance and approaches to combat it. *Science translational medicine,* 12**,** eaaz6992.

SCHROLL, C., BARKEN, K. B., KROGFELT, K. A. & STRUVE, C. 2010. Role of type 1 and type 3 fimbriae in *Klebsiella pneumoniae* biofilm formation. *BMC microbiology,* 10**,** 110.

SCHWARZ, M., HÜBNER, I. & SIEBER, S. A. 2022. Tailored Phenyl Esters Inhibit ClpXP and Attenuate *Staphylococcus aureus* α-Hemolysin Secretion. *ChemBioChem,* 23**,** e202200253.

SEKIZUKA, T., INAMINE, Y., SEGAWA, T., HASHINO, M., YATSU, K. & KURODA, M. 2019a. Potential KPC-2 carbapenemase reservoir of environmental Aeromonas hydrophila and Aeromonas caviae isolates from the effluent of an urban wastewater treatment plant in Japan. *Environmental microbiology reports,* 11**,** 589-597.

SEKIZUKA, T., INAMINE, Y., SEGAWA, T. & KURODA, M. 2019b. Characterization of NDM-5-and CTX-M-55-coproducing *Escherichia coli* GSH8M-2 isolated from the effluent of a wastewater treatment plant in Tokyo Bay. *Infection and Drug Resistance,* 12**,** 2243.

SEKIZUKA, T., YATSU, K., INAMINE, Y., SEGAWA, T., NISHIO, M., KISHI, N. & KURODA, M. 2018. Complete genome sequence of a bla KPC-2-positive *Klebsiella pneumoniae* strain isolated from the effluent of an urban sewage treatment plant in Japan. *Msphere,* 3**,** e00314-18.

SEQUEIRA, R. P., MCDONALD, J. A., MARCHESI, J. R. & CLARKE, T. B. 2020. Commensal Bacteroidetes protect against *Klebsiella pneumoniae* colonization and transmission through IL-36 signalling. *Nature microbiology,* 5**,** 304-313.

SERIO, A. W., KEEPERS, T., ANDREWS, L. & KRAUSE, K. M. 2018. Aminoglycoside revival: review of a historically important class of antimicrobials undergoing rejuvenation. *EcoSal Plus,* 8.

SETHUVEL, D. P. M., BAKTHAVATCHALAM, Y. D., KARTHIK, M., IRULAPPAN, M., SHRIVASTAVA, R., PERIASAMY, H. & VEERARAGHAVAN, B. 2023. β-Lactam Resistance in ESKAPE Pathogens Mediated Through Modifications in Penicillin Binding Proteins: An Overview. *Infectious Diseases and Therapy***,** 1-13.

SHANKAR, C., BASU, S., LAL, B., SHANMUGAM, S., VASUDEVAN, K., MATHUR, P., RAMAIAH, S., ANBARASU, A. & VEERARAGHAVAN, B. 2021. Aerobactin Seems To Be a Promising Marker Compared With Unstable RmpA2 for the Identification of Hypervirulent Carbapenem-Resistant *Klebsiella pneumoniae*: In *Silico* and In Vitro Evidence. *Frontiers in Cellular and Infection Microbiology,* 11.

SHANKAR, C., VASUDEVAN, K., JACOB, J. J., BAKER, S., ISAAC, B. J., NEERAVI, A. R., SETHUVEL, D. P. M., GEORGE, B. & VEERARAGHAVAN, B. 2022. Hybrid Plasmids Encoding Antimicrobial Resistance and Virulence Traits Among Hypervirulent *Klebsiella pneumoniae* ST2096 in India. *Frontiers in cellular and infection microbiology***,** 435.

SHELENKOV, A., MIKHAYLOVA, Y., YANUSHEVICH, Y., SAMOILOV, A., PETROVA, L., FOMINA, V., GUSAROV, V., ZAMYATIN, M., SHAGIN, D. & AKIMKIN, V. 2020. Molecular typing, characterization of antimicrobial resistance, virulence profiling and analysis of whole-genome sequence of clinical *Klebsiella pneumoniae* isolates. *Antibiotics,* 9**,** 261.

SHEPPARD, A. E., STOESSER, N., SEBRA, R., KASARSKIS, A., DEIKUS, G., ANSON, L., WALKER, A. S., PETO, T. E., CROOK, D. W. & MATHERS, A. J. 2016. Complete genome sequence of KPC-producing *Klebsiella pneumoniae* strain CAV1193. *Genome announcements,* 4**,** e01649-15.

SHIN, S. H., KIM, S., KIM, J. Y., LEE, S., UM, Y., OH, M.-K., KIM, Y.-R., LEE, J. & YANG, K.-S. 2012a. Complete genome sequence of *Enterobacter aerogenes* KCTC 2190. *J Bacteriol*. 194(9):2373-4.

SHIN, S. H., KIM, S., KIM, J. Y., LEE, S., UM, Y., OH, M.-K., KIM, Y.-R., LEE, J. & YANG, K.-S. 2012b. Complete genome sequence of *Klebsiella oxytoca* KCTC 1686, used in production of 2, 3-butanediol. *J Bacteriol*. 194(9):2371-2.

SHIN, S. H., KIM, S., KIM, J. Y., LEE, S., UM, Y., OH, M.-K., KIM, Y.-R., LEE, J. & YANG, K.-S. 2012c. Complete genome sequence of the 2, 3-butanediol-producing *Klebsiella pneumoniae* strain KCTC 2242. *J Bacteriol*. 194(10):2736-7.

SICHTIG, H., MINOGUE, T., YAN, Y., STEFAN, C., HALL, A., TALLON, L., SADZEWICZ, L., NADENDLA, S., KLIMKE, W. & HATCHER, E. 2019. FDA-ARGOS is a database with

public quality-controlled reference genomes for diagnostic use and regulatory science. *Nature communications,* 10**,** 1-13.

SIKARWAR, A. & BATRA, H. V. 2023. Challenge to healthcare: Multidrug resistance in *Klebsiella pneumoniae*. International Conference on Food Engineering and Biotechnology IPCBEE. Vol. 9.

SILVA, N., OLIVEIRA, M., BANDEIRA, A. C. & BRITES, C. 2006. Risk factors for infection by extended-spectrum beta-lactamase producing *Klebsiella pneumoniae* in a tertiary hospital in Salvador, Brazil. *Brazilian Journal of Infectious Diseases,* 10**,** 191-193.

SINGER, J. R., BLOSSER, E. G., ZINDL, C. L., SILBERGER, D. J., CONLAN, S., LAUFER, V. A., DITORO, D., DEMING, C., KUMAR, R. & MORROW, C. D. 2019. Preventing dysbiosis of the neonatal mouse intestinal microbiome protects against late-onset sepsis. *Nature medicine,* 25**,** 1772-1782.

SINGH, A., UPADHYAY, V., UPADHYAY, A. K., SINGH, S. M. & PANDA, A. K. 2015. Protein recovery from inclusion bodies of *Escherichia coli* using mild solubilization process. *Microbial cell factories,* 14**,** 1-10.

SIVASHANMUGAM, A., MURRAY, V., CUI, C., ZHANG, Y., WANG, J. & LI, Q. 2009. Practical protocols for production of very high yields of recombinant proteins using *Escherichia coli*. *Protein science,* 18**,** 936-948.

SMITH, C. 2005. Striving for purity: advances in protein purification. *Nature methods,* 2**,** 7177.

SNITKIN, E., ZELAZNY, A., THOMAS, P., STOCK, F., HENDERSON, D., PALMORE, T. & SEGRE, J. 2012. NISC Comparative Sequencing Program Group. Tracking a hospital outbreak of carbapenem-resistant Klebsiella pneumoniae with whole-genome sequencing. *Sci Transl Med* 4:148ra116. doi: 10.1126

SOBOLEV, O. V., AFONINE, P. V., MORIARTY, N. W., HEKKELMAN, M. L., JOOSTEN, R. P., PERRAKIS, A. & ADAMS, P. D. 2020. A global Ramachandran score identifies protein structures with unlikely stereochemistry. *Structure,* 28**,** 1249-1258. e2.

SRINIVASAN, V. B., SINGH, B. B., PRIYADARSHI, N., CHAUHAN, N. K. & RAJAMOHAN, G. 2014. Role of novel multidrug efflux pump involved in drug resistance in *Klebsiella pneumoniae*. *PloS one,* 9**,** e96288.

STEWART, J., JUDD, L. M., JENNEY, A., HOLT, K. E., WYRES, K. L. & HAWKEY, J. 2022. Epidemiology and genomic analysis of *Klebsiella oxytoca* from a single hospital network in Australia. *BMC infectious diseases,* 22**,** 1-10.

STRACY, M., WOLLMAN, A. J. M., KAJA, E., GAPINSKI, J., LEE, J.-E., LEEK, V. A., MCKIE, S. J., MITCHENALL, L. A., MAXWELL, A. & SHERRATT, D. J. 2019. Single molecule imaging of DNA gyrase activity in living *Escherichia coli*. *Nucleic acids research,* 47**,** 210-220.

SZYK, A. & MAURIZI, M. R. 2006. Crystal structure at 1.9 Å of *E. coli* ClpP with a peptide covalently bound at the active site. *Journal of structural biology,* 156**,** 165-174.

TAO, L. & BISWAS, I. 2015. Degradation of SsrA-tagged proteins in *streptococci*. *Microbiology,* 161**,** 884.

TASTAN BISHOP, A. O., DE BEER, T. A. & JOUBERT, F. 2008. Protein homology modelling and its use in South Africa: research in action. *South African Journal of Science,* 104**,** 2-6.

TEILUM, K., OLSEN, J. G. & KRAGELUND, B. B. 2009. Functional aspects of protein flexibility. *Cellular and Molecular Life Sciences,* 66**,** 2231-2247.

TOOKE, C. L., HINCHLIFFE, P., BRAGGINTON, E. C., COLENSO, C. K., HIRVONEN, V. H., TAKEBAYASHI, Y. & SPENCER, J. 2019. β-Lactamases and β-Lactamase Inhibitors in the 21st Century. *Journal of molecular biology,* 431**,** 3472-3500.

TSAKOU, F., JERSIE-CHRISTENSEN, R., JENSSEN, H. & MOJSOSKA, B. 2020. The role of proteomics in bacterial response to antibiotics. *Pharmaceuticals,* 13**,** 214.

TURNER, J., MURAOKA, A., BEDENBAUGH, M., CHILDRESS, B., PERNOT, L., WIENCEK, M. & PETERSON, Y. K. 2022. The chemical relationship among beta lactam antibiotics and potential impacts on reactivity and decomposition. *Frontiers in Microbiology,* 13.

VASINA, J. A. & BANEYX, F. 1996. Recombinant protein expression at low temperatures under the transcriptional control of the major *Escherichia coli* cold shock promoter cspA. *Applied and environmental microbiology,* 62**,** 1444-1447.

VEDULA, P., KUROSAKA, S., LEU, N., WOLF, Y., SHABALINA, S., WANG, J., STERLING, S., DONG, D. & KASHINA, A. 2017. Diverse functions of closely homologous actin isoforms are defined by their nucleotide, rather than their amino acid sequence. *bioRxiv***,** 227546.

VEZINA, B., JUDD, L. M., MCDOUGALL, F. K., BOARDMAN, W. S., POWER, M. L., HAWKEY, J., BRISSE, S., MONK, J. M., HOLT, K. E. & WYRES, K. L. 2022. Transmission of *Klebsiella strains* and plasmids within and between Grey-headed flying fox colonies. *Environmental Microbiology*.

VOGWILL, T., COMFORT, A., FURIÓ, V. & MACLEAN, R. 2016. Persistence and resistance as complementary bacterial adaptations to antibiotics. *Journal of evolutionary biology,* 29**,** 1223-1233.

VOOS, W. 2013. Chaperone–protease networks in mitochondrial protein homeostasis. *Biochimica et Biophysica Acta (BBA)-Molecular Cell Research,* 1833**,** 388-399.

VUOTTO, C., LONGO, F., BALICE, M. P., DONELLI, G. & VARALDO, P. E. 2014. Antibiotic resistance related to biofilm formation in *Klebsiella pneumoniae*. *Pathogens,* 3**,** 743758.

WANDERSMAN, C. 1989. Secretion, processing and activation of bacterial extracellular proteases. *Molecular microbiology,* 3**,** 1825-1831.

WANG, X., PATTISON, J. S. & SU, H. 2013. Posttranslational modification and quality control. *Circulation research,* 112**,** 367-381.

WARD, A. J. & COOPER, T. A. 2010. The pathobiology of splicing. *The Journal of Pathology: A Journal of the Pathological Society of Great Britain and Ireland,* 220**,** 152-163.

WARD, O., RAO, M. & KULKARNI, A. 2009. Proteases, Production, Encyclopedia of Enzymes. Editor in Chief: Moselio Schaechter. Elsevier Inc.

WARDENBURG, K. E., POTTER, R. F., D'SOUZA, A. W., HUSSAIN, T., WALLACE, M. A., ANDLEEB, S., BURNHAM, C.-A. D. & DANTAS, G. 2019. Phenotypic and genotypic characterization of linezolid-resistant Enterococcus faecium from the USA and Pakistan. *Journal of Antimicrobial Chemotherapy,* 74**,** 3445-3452.

WATERHOUSE, A., BERTONI, M., BIENERT, S., STUDER, G., TAURIELLO, G., GUMIENNY, R., HEER, F. T., DE BEER, T. A. P., REMPFER, C. & BORDOLI, L. 2018. SWISS-MODEL: homology modelling of protein structures and complexes. *Nucleic acids research,* 46**,** W296-W303.

WEINGARTEN, R. A., JOHNSON, R. C., CONLAN, S., RAMSBURG, A. M., DEKKER, J. P., LAU, A. F., KHIL, P., ODOM, R. T., DEMING, C. & PARK, M. 2018. Genomic analysis

of hospital plumbing reveals diverse reservoir of bacterial plasmids conferring carbapenem resistance. *MBio,* 9**,** e02011-17.

WEN, Z. & ZHANG, J.-R. 2015. Bacterial capsules. *Molecular medical microbiology*. Academic Press, 2015. 33-53.

WILSON, B. R., BOGDAN, A. R., MIYAZAWA, M., HASHIMOTO, K. & TSUJI, Y. 2016. Siderophores in iron metabolism: from mechanism to therapy potential. *Trends in molecular medicine,* 22**,** 1077-1090.

WRIGHT, M. S., PEREZ, F., BRINKAC, L., JACOBS, M. R., KAYE, K., COBER, E., VAN DUIN, D., MARSHALL, S. H., HUJER, A. M. & RUDIN, S. D. 2014. Population structure of KPC-producing *Klebsiella pneumoniae* isolates from midwestern US hospitals. *Antimicrobial agents and chemotherapy,* 58**,** 4961-4965.

WU, H. & FIVES-TAYLOR, P. M. 2001. Molecular strategies for fimbrial expression and assembly. *Critical Reviews in Oral Biology & Medicine,* 12**,** 101-115.

XANTHOPOULOU, K., CARATTOLI, A., WILLE, J., BIEHL, L. M., ROHDE, H., FAROWSKI, F., KRUT, O., VILLA, L., FEUDI, C. & SEIFERT, H. 2020. Antibiotic resistance and mobile genetic elements in extensively drug-resistant *Klebsiella pneumoniae* sequence type 147 recovered from Germany. *Antibiotics,* 9**,** 675.

XAVIER, B. B., LAMMENS, C., BUTAYE, P., GOOSSENS, H. & MALHOTRA-KUMAR, S. 2016. Complete sequence of an IncFII plasmid harbouring the colistin resistance gene mcr-1 isolated from Belgian pig farms. *Journal of Antimicrobial Chemotherapy,* 71**,** 2342-2344.

YAKOUT, M. A. & ALI, G. H. 2022. A novel parC mutation potentiating fluoroquinolone resistance in *Klebsiella pneumoniae* and *Escherichia coli* clinical isolates. *The Journal of Infection in Developing Countries,* 16**,** 314-319.

YAN, R., LU, Y., ZHU, Y., LAN, P., JIANG, S., LU, J., SHEN, P., YU, Y., ZHOU, J. & JIANG, Y. 2021a. A sequence type 23 hypervirulent *Klebsiella pneumoniae* strain Presenting carbapenem resistance by acquiring an IncP1 blaKPC-2 plasmid. *Frontiers in cellular and infection microbiology***,** 481.

YAN, X., YANG, J., WANG, Q. & LIN, S. 2021b. Transcriptomic analysis reveals resistance mechanisms of Klebsiella michiganensis to copper toxicity under acidic conditions. *Ecotoxicology and Environmental Safety,* 211**,** 111919.

YE, F., ZHANG, J., LIU, H., HILGENFELD, R., ZHANG, R., KONG, X., LI, L., LU, J., ZHANG, X. & LI, D. 2013. Helix unfolding/refolding characterizes the functional dynamics of *Staphylococcus aureus* Clp protease. *Journal of Biological Chemistry,* 288**,** 17643-17653.

YOON, E.-J. & JEONG, S. H. 2021. Class D β-lactamases. *Journal of Antimicrobial Chemotherapy,* 76**,** 836-864.

YU, A. Y. H. & HOURY, W. A. 2007. ClpP: a distinctive family of cylindrical energy dependent serine proteases. *FEBS letters,* 581**,** 3749-3757.

ZHANG, X., LI, Q., LIN, H., ZHOU, W., QIAN, C., SUN, Z., LIN, L., LIU, H., LU, J. & LIN, X. 2021. High-level aminoglycoside resistance in human clinical *Klebsiella pneumoniae* complex isolates and characteristics of armA-carrying IncHI5 plasmids. *Frontiers in Microbiology,* 12**,** 636396.

ZHANG, X., OUYANG, J., HE, W., ZENG, T., LIU, B., JIANG, H., ZHANG, Y., ZHOU, L., ZHOU, H. & LIU, Z. 2020. Co-occurrence of rapid gene gain and loss in an interhospital outbreak of carbapenem-resistant hypervirulent ST11-K64 *Klebsiella pneumoniae*. *Frontiers in microbiology,* 11**,** 579618.

ZHAO, X., XU, C., DOMAGALA, J. & DRLICA, K. 1997. DNA topoisomerase targets of the fluoroquinolones: a strategy for avoiding bacterial resistance. *Proceedings of the National Academy of Sciences,* 94**,** 13991-13996.

ZHOU, J., LI, S., LEUNG, K. K., O'DONOVAN, B., ZOU, J. Y., DERISI, J. L. & WELLS, J. A. 2020. Deep profiling of protease substrate specificity enabled by dual random and scanned human proteome substrate phage libraries. *Proceedings of the National Academy of Sciences,* 117**,** 25464-25475.

ZHU, J., WANG, T., CHEN, L. & DU, H. 2021. Virulence factors in hypervirulent *Klebsiella pneumoniae*. *Frontiers in microbiology,* 12**,** 642484.

ZOWAWI, H. M., FORDE, B. M., ALFARESI, M., ALZAROUNI, A., FARAHAT, Y., CHONG, T.-M., YIN, W.-F., CHAN, K.-G., LI, J. & SCHEMBRI, M. A. 2015. Stepwise evolution of pandrug-resistance in *Klebsiella pneumoniae*. *Scientific reports,* 5**,** 1-8.

Appendix

Table A1: Dataset of different *Klebsiella* strains obtain on NCBI genome.

Name of species	Strain	Reference
Klebsiella aerogenes	FDAARGOS_1442	(Sichtig *et al*., 2019)
Klebsiella aerogenes	KCTC 2190	(Shin *et al*., 2012a)
Klebsiella aerogenes	G7	(Philippe *et al*., 2015)
Klebsiella aerogenes	RHBSTW-00898	(AbuOun *et al*., 2021)
Klebsiella aerogenes	FDAARGOS_327	(Sichtig *et al*., 2019)
Klebsiella aerogenes	FDAARGOS_152	(Sichtig *et a*l., 2019)
Klebsiella aerogenes	FDAARGOS_641	(Sichtig *et al*., 2019)
Klebsiella aerogenes	FDAARGOS_513	(Sichtig *et al*., 2019)
Klebsiella aerogenes	FDAARGOS_363	(Sichtig *et al*., 2019)
Klebsiella aerogenes	FDAARGOS_139	(Sichtig *et al*., 2019)
Klebsiella aerogenes	FDAARGOS 1441	(Sichtig *et al*., 2019)
Klebsiella aerogenes	WP5-W18-CRE-01	(Sekizuka *et al*., 2019a), (Sekizuka *et al*., 2019b), (Sekizuka *et al*., 2018)
Klebsiella aerogenes	CAV1320	(Sheppard *et al*., 2016), (Mathers *et al*., 2015)
Klebsiella aerogenes	EA1509E	(Diene *et al*., 2013)
Klebsiella michiganensis	BD-50-Km	(Campos-Madueno *et al*., 2021)
Klebsiella michiganensis	RHBSTW-00167	(AbuOun *et al*., 2021)
Klebsiella michiganensis	RHB20-C02	(AbuOun *et al*., 2021)
Klebsiella michiganensis	RHBSTW-00409	(AbuOun *et al*., 2021)
Klebsiella michiganensis	Kmfe267	(Zhang *et al*., 2020)
Klebsiella michiganensis	X2-1	(Yan *et al*., 2021b)
Klebsiella michiganensis	RHBSTW-00909	(AbuOun *et al*., 2021)
Klebsiella michiganensis	E718	(Huang *et al*., 2013), (Liao *et al.,* 2012), (Lai *et al*., 2011)
Klebsiella michiganensis	KCTC 1686	(Shin *et al*., 2012b)
Klebsiella michiganensis	FDAARGOS_647	(Sichtig *et al*., 2019)
Klebsiella pneumoniae	FDAARGOS_775	(Sichtig *et al*., 2019)
Klebsiella pneumoniae	0113481141	(Campos-Madueno *et a*l., 2022)
Klebsiella pneumoniae	KPNIH48	(Weingarten *et al*., 2018)
Klebsiella pneumoniae	KPNIH50	(Weingarten *et al*., 2018)
Klebsiella pneumoniae	C2414	(Gao *et al*., 2020)
Klebsiella pneumoniae	FDAARGOS_444	(Sichtig *et al*., 2019)
Klebsiella pneumoniae	WCHKP2	(Feng et al., 2020), (Hu *et al*., 2018)
Klebsiella pneumoniae	2_GR_12	(Pitt *et al*., 2018), (Elliott *et al*., 2016)
Klebsiella pneumoniae	HKP0067	(Xanthopoulou *et al*., 2020)
Klebsiella pneumoniae	FDAARGOS_439	(Sichtig *et al*., 2019)
Klebsiella pneumoniae	RHBSTW-00433	(AbuOun *et al*., 2021)
Klebsiella pneumoniae	WCHKP095845	(Feng *et al*., 2020), (Hu *et al*., 2018)
Klebsiella pneumoniae	STIN_93	(Che *et al*., 2022)

Klebsiella pneumoniae	RHB38-C06	(AbuOun *et al*., 2021)
Klebsiella pneumoniae	SWHIN_108	(Che *et al*., 2022)
Klebsiella pneumoniae	RHBSTW-00982	(AbuOun *et al*., 2021)
Klebsiella pneumoniae	SWHEFF_62	(Che *et al*., 2022)
Klebsiella pneumoniae	fekpn2511	(Zhang *et al*., 2020)
Klebsiella pneumoniae	FF979	(Vezina *et a*l., 2022)
Klebsiella pneumoniae	HKP0018	(Xanthopoulou *et al*., 2020)
Klebsiella pneumoniae	C2414	(Gao *et al*., 2020)
Klebsiella pneumoniae	KP64	(Sakamoto *et al*., 2018)
Klebsiella pneumoniae	FF1023	(Vezina *et al*., 2022)
Klebsiella pneumonia subsp. pneumoniae	SCKP020046	(Feng et al., 2020), (Hu *et al*., 2018)
Klebsiella pneumonia subsp. pneumoniae	WCHKP020039	(Feng *et al*., 2020), (Hu *et al*., 2018)
Klebsiella pneumonia subsp. pneumoniae	NUHL24835	(Liu *et al*., 2016)
Klebsiella pneumoniae subsp. pneumoniae	SA-KpST14	(Alghoribi *et al*., 2021)
Klebsiella pneumoniae subsp. pneumoniae	ATCC 43816 KPPR1	(Broberg *et al*., 2014), (Lawlor *et al*., 2005)
Klebsiella pneumoniae subsp. pneumoniae	TGH10	(Xavier *et al*., 2016), (Sabirova *et al*., 2016), (Xavier *et al*., 2016)
Klebsiella pneumoniae subsp. pneumoniae	TGH13	(Xavier *et al*., 2016), (Sabirova *et al*., 2016), (Xavier *et al*., 2016)
Klebsiella pneumoniae subsp. pneumoniae	KPNIH30	(Conlan *et al*., 2014)
Klebsiella pneumoniae subsp. pneumoniae	KPNIH29	(Conlan *et al*., 2014)
Klebsiella pneumoniae subsp. pneumoniae	SCKP040074	(Feng *et al*., 2020), (Hu *et al*., 2018)
Klebsiella pneumoniae subsp. pneumoniae	KPNIH31	(Conlan *et al.,* 2014)
Klebsiella pneumoniae subsp. pneumoniae	WCHKP015096	(Feng *et al*., 2020), (Hu *et* al., 2018)
Klebsiella pneumoniae subsp. pneumoniae	KPNIH33	(Conlan *et al.,* 2014)
Klebsiella pneumoniae	KCTC 2242	(Shin *et a*l., 2012c)
Klebsiella pneumoniae subsp. pneumoniae	KPNIH10	(Conlan *et al*., 2014), (Snitkin *et al*., 2012)
Klebsiella pneumoniae subsp. pneumoniae	KPNIH1	(Conlan *et al*., 2014), (Conlan *et al*., 2016), (Snitkin *et a*l., 2012)
Klebsiella pneumoniae	DMC1097	(Wright *et al.,* 2014)
Klebsiella pneumoniae subsp. pneumoniae	1084	(Lin *et al*., 2012), (Lin *et al*., 2011)
Klebsiella pneumoniae subsp. pneumoniae	PittNDM01	(Doi *et al*., 2014)
Klebsiella pneumoniae	UHKPC07	(Wright *et al*., 2014)
Klebsiella pneumoniae subsp. pneumoniae	KPR0928	(Conlan *et al*., 2014)
Klebsiella pneumoniae	500_1420	(Wright *et al*., 2014)

Klebsiella pneumoniae subsp. pneumoniae	Kp13	(Ramos *et al*., 2014)
Klebsiella pneumoniae	400195-1-18	(Campos-Madueno *et al*., 2022)
Klebsiella pneumoniae	400195-2-18	(Campos-Madueno *et al*., 2022)
Klebsiella pneumoniae	FDAARGOS_1328	(Sichtig *et a*l., 2019)
Klebsiella pneumoniae	Xen39	(Singer *et a*l., 2019)
Klebsiella pneumoniae	RHB39-C09	(AbuOun *et al*., 2021)
. Klebsiella pneumoniae	ATCC BAA-2146	(Hudson *et al*., 2014)
Klebsiella pneumoniae	OCU_hvKP1	(Namikawa *et al*., 2019), (Namikawa *et al*., 2019)
Klebsiella pneumoniae	WCHKP115069	(Feng *et al*., 2020), (Hu *et al*., 2018)
Klebsiella pneumoniae	WCHKP095005	(Feng *et al*., 2020), (Hu *et al*., 2018)
Klebsiella pneumoniae	6611.48	(Campos-Madueno *et al*., 2022)
Klebsiella pneumoniae	KP_160	(Wardenburg *et al*., 2019), (Wardenburg *et al*., 2019)
Klebsiella pneumoniae	ZJ27003	(Yan *et al*., 2021a)
Klebsiella pneumoniae	6604.68	(Campos-Madueno *et al*., 2022)
Klebsiella pneumoniae	WCHKP090329	(Yan *et al*., 2021a)
Klebsiella pneumoniae	16_GR_13	(Pitt *et al*., 2018), (Elliott *et al*., 2016)
Klebsiella pneumoniae	CAV1042	(Sheppard *et al*., 2016), (Mathers *et al*., 2015)
Klebsiella pneumoniae	BA25665	(Shankar *et al.,* 2022), (Shankar *et al*., 2021)
Klebsiella pneumoniae	FDAARGOS_531	(Sichtig *et al*., 2019)
Klebsiella pneumoniae	SCKP020003	(Feng *et al*., 2020), (Hu *et al*., 2018)
Klebsiella pneumoniae	BA2105	(Shankar *et al*., 2022), (Shankar *et al*., 2021)
Klebsiella pneumoniae	KP617	(Kwon *et al*., 2016)
Klebsiella pneumoniae	39427	(Satlin *et al*., 2017)
Klebsiella pneumoniae	6709.15-I	(Campos-Madueno *et al*., 2022)
Klebsiella pneumoniae	CriePir116	(Shelenkov *et al*., 2020)
Klebsiella pneumoniae	6711.43	(Campos-Madueno *et al*., 2022)
Klebsiella pneumoniae	KPNIH49	(Weingarten *et al*., 2018)
Klebsiella pneumoniae	MS6671	(Zowawi *et al*., 2015)
Klebsiella pneumoniae	CAV1596	(Sheppard *et al*., 2016), (Mathers *et al*., 2015)
Klebsiella pneumoniae	47733	(Chudejova *et a*l., 2021)

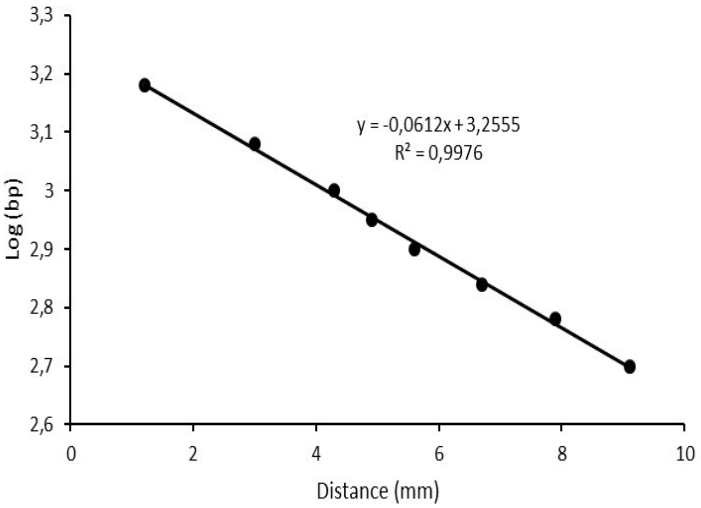

Figure A1: Standard curve showing relative distance travelled along with log bp sizes of 100 bp quick load DNA marker run on a 1% agarose gel. Recombinant pCold1-ClpP PCR products were run on a 1% agarose gel together with known Quick load 100 bp standard (New England BioLabs, United States) and stained with ethidium bromide.